universität
wien

DIPLOMARBEIT

Detachment Folding and Salt Tectonics in the Permian Haselgebirge (Hallstatt, Northern Calcareous Alps)

angestrebter akademischer Grad

Magister der Naturwissenschaften (Mag. rer.nat.)

Verfasser:	Nikolaus Schmid
Matrikel-Nummer:	9605532
Studienrichtung:	Geologie (Studienzweig A431)
Betreuer:	Univ.-Prof. Mag. Dr. Bernhard Grasemann

Wien, Oktober 2009

Table of Contents

Abstract

The Northern Calcareous Alps (NCA), which belong to the northernmost part of the Upper Austroalpine thrust complex, represent a fold and thrust belt at the frontal part of the Eastern Alps. During the Alpine orogeny the carbonate dominated successions of the NCA were deformed in a brittle style when they were decoupled along detachment horizons with relatively low shear strength. The late Permian to early Triassic evaporites of the Austroalpine Haselgebirgs-formation build up the basal detachment in large parts of the NCA. As a consequence the sedimentary succession of Thethyan and Penninic carbonates lost its depositional basement and now rests with over-thrust contact on Molasse and Flysch sediments.

The field area of this study is situated near Hallstatt around the Echerntal valley in the central part of the NCA. At that spot the prevailing lagoonal sediments of the Dachstein Nappe are tectonically juxtaposed with the pelagic sediments of the Hallstatt Nappe. The tectonic processes within the NCA and especially the structural relation between Dachstein and Hallstatt Nappe are still a point of discussion. Against the dominant tectonic model (e.g. Tollmann, 1963), which demands a top-to-north displacement, some authors suggest large scale top-to-west and northwest thrusting in the early stages of Alpine orogeny (e.g. Linzer et al., 1995). Observations in the studied area confirm thrusting towards WNW. Sedimentary surfaces and thrust faults are generally dipping to ESE and in bedding-plane parallel slickensides evidence for a top-to-WNW movement was found. Furthermore microstructures like SC-fabric and stylolites of thin-sections from Dachstein Limestone in the Echernwand support these assumptions.

Movement to WNW was observed in the Hallstatt and in the Dachstein Nappe but there are clear differences in style of deformation. Different viscosity and different thickness (with respect to the overburden thickness) of a detachment horizon are essential parameters for the structures found in the overlying beds. In the Dachstein Nappe, due to the higher basal friction, fold bend folding and foreland vergent duplexes are typical. At the border area to the Hallstatt Nappe (northern slope of the Echernwand), above the ductile evaporitic layers, additional detachment folds and hinterland vergent structures are observed.

The Hallstatt Nappe within the evaporitic Haselgebirge is located northwest of the Echerntal valley and contains the halite rich Hallstatt salt deposit that played an important role for the Hallstatt region since ancient times. 3D modeling of the salt deposit with GoCAD^{Tm} illustrated that the nearly 3km long and about 500m broad saltbody in the northern slope of the Echerntal valley strikes ESE-WNW – more or less parallel to the observed main tectonic transport direction. Within the evaporites high strain ductile deformation structures like δ- and σ-clasts or isoclinal folding are observed. Microstructural investigations of thin-sections confirm the mylonitic fabric as for example dynamic recristallisation of evaporites and fracturing of rigid clasts within a ductile reacting matrix are observed. More evidence of the intense internal deformation of the Haselgebirge is given by scratched and polished surfaces of clay clasts embedded in the weaker salty-clayey matrix.

The shape of the saltbody and structural measurements indicate a relation between the Hallstatt salt deposit and a major strike-slip movement at the northern boundary of the Hallstatt Nappe.

Kurzfassung

Die Nördlichen Kalkalpen, die zum Oberostalpinen Deckenstapel gehören, stellen einen Falten- und Überschiebungsgürtel im frontalen Abschnitt der Ostalpen dar. Als höchster tektonischer Schichtkomplex wurden die überwiegend aus Karbonaten bestehenden Gesteinsschichten während der alpinen Orogenese von ihrem ursprünglichen Sedimentationsuntergrund abgeschert. Die spät permischen bis früh triassischen Evaporite des Haselgebirges fungierten dabei aufgrund der relativ geringen Scherfestigkeit als basaler Entkopplungshorizont großer Teile der Nördlichen Kalkalpen. Die großteils aus Karbonaten der Tethys und des Penninischen Ozeans bestehenden Sedimentabfolgen kommen heute mit Überschiebungskontakt auf Molasse- und Flyschsedimenten zu liegen. Die Verkürzung verursachte in diesem Deckenstapel die Ausbildung von Überschiebungen und Falten.

Das Arbeitsgebiet befindet sich westlich von Hallstatt rund um das Echerntal, im zentralen Abschnitt der Nördlichen Kalkalpen. In diesem Bereich kommen die überwiegend lagunären Sedimente der Dachstein Decke mit tektonischem Kontakt neben tiefmarinen Sedimenten der Hallstätter Decke zu liegen. Die tektonischen Prozesse die die Nördlichen Kalkalpen in ihrer heutigen Form entstehen ließen und vor allem die strukturelle Beziehung der Dachstein und Hallstatt Decke zueinander sind immer noch ein häufig diskutiertes Thema. Gegenüber dem vorherrschenden tektonischen Modell (z.B. Tollmann, 1963), das einen nordwärtigen Versatz verlangt, bevorzugen einige Autoren großmaßstäbliche Überschiebungen nach W bis NW in den frühen Stadien der alpinen Gebirgsbildung (z.B. Linzer et al., 1995). Die vorliegende strukturgeologische Geländekartierung bestätigt im interessierenden Gebiet einen tektonischen Versatz nach WNW. Sowohl sedimentäre Schichtflächen als auch Überschiebungsbahnen fallen generell Richtung ESE ein, und auf schichtparallelen Harnischflächen wurden Lineare beobachtet, die eine Bewegungsrichtung nach WNW anzeigen. Weiters wird die Überschiebung nach WNW auch durch Mikrostrukturen wie SC-Gefüge und Stylolithe in Dünnschliffen von Dachsteinkalk-Proben aus der Echernwand bekräftigt.

Die WNW-orientierte Bewegungsrichtung kann sowohl in der Dachstein als auch Hallstätter Decke beobachtet werden, aber der Deformationsstil zeigt deutliche Unterschiede. Die unterschiedliche Viskosität und die Schichtmächtikeit des Abscherungshorizonts im Verhältnis zur überlagernden Mächtigkeit sind entscheidende Kriterien für Strukturen, die in den überlagernden Gesteinsschichten entstehen. Aufgrund des größeren Reibungswiderstands innerhalb der Dachstein Decke finden sich hier vor allem Fault-bend Folds und vorwärts vergente Stapelung. Demgegenüber sind im Grenzbereich zur Hallstatt Decke, wo der duktile salzreiche Horizont in die Überschiebung miteingebunden ist, zusätzlich Detachment Folds und rückwärts vergente Stapelung zu beobachten.

Die Hallstätter Decke mit den evaporitischen Abfolgen des Haselgebirges befindet sich nordwestlich des Echerntals. Die Hallstätter Salzlagerstätte hat seit prähistorischer Zeit eine entscheidende Bedeutung für die Region. Eine 3D Modellierung der Salzlagerstätte mit GoCAD^{Tm} veranschaulicht, dass der knapp 3km lange und 500m breite Salzkörper ESE-WNW – parallel zur tektonischen Haupttransportrichtung – verläuft. Die Evaporite zeigen duktile „high strain“ Deformation, wie δ- und σ- Klasten oder die Ausbildung von Isoklinalfalten. Mikroskopische Beobachtungen in Dünnschliffen zeigen ebenfalls mylonitische Strukturen wie „stairstepping“ und Zerbrechen rigider Klasten im duktilen Salz sowie dynamische Rekristallisation. Einen weiteren Beweis für die starke interne Deformation des Haselgebirges liefern gekritzte und polierte Oberflächen an Tonklasten, die in der duktileren salzig-tonigen Matrix "schwimmen".

Die Form des Salzkörpers, gemeinsam mit den strukturellen Messungen im Haselgebirge, weist auf einen Zusammenhang der Salzlagerstätte mit einer großen Seitenverschiebung entlang der nördlichen Begrenzung der Hallstätter Decke hin.

Acknowledgements

I would like to express my gratitude to all persons, who contributed to the success of this diploma thesis either with their professional or personal support and gave me the possibility to finish this work.

A special thank goes to Professor Dr. Bernhard Grasemann and Mag. Dr. Erich Draganits, my supervisors who initialised the thesis, for careful leading and valuable help during the development of the project. As this project was worked out by three diploma students I owe many thanks to my student colleagues Klaus Arnberger and Mario Habermüller for their active discussions about this thesis and their companionship during fieldwork.

Further I want to thank Professor Dr. Leopold Weber for contacting the Salinen Austria AG and the Salinen Austria AG itself for admittance to the Hallstatt salt mine and for handling out some geological maps of the salt deposit.

I am deeply indebted to my parents who made my enjoyable studying years possible, not at least with their financial support. They never lost their confidence in me although it took me a long time to finish my academic studies.

Finally I would like to give a very special thank to my wife Yvonne whose patient love enabled me to complete this work and to my lovely children Julian, Valentin and Marlene.

1. Introduction

This diploma work was initialised by a project within the "Hochschuljubiläumsstiftung" of Vienna (H-32/2001): "Quantifizierung von Deformation in österreichischen Salzlagerstätten". In the course of this project three diploma theses were worked out in and around the Hallstatt saltmine.

1.1 Geographical overview

The area of investigation is located west of Lake Hallstatt in the mountainous Salzkammergut in southern Upper Austria, near the border to Salzburg and Steiermark. This district belongs to the Hallstatt – Dachstein/Salzkammergut Region, which is an UNESCO world cultural heritage site since 1997. With up to 2000mm annual precipitation it is a rather humid area and shows various landscapes: A couple of lakes, like the Lake Hallstatt, are situated in valleys that were formed by glaciers in the Pleistocene. The highly elevated carbonate platforms Dachstein and Totes Gebirge build up the southern and eastern part of the Salzkammergut region. More northern wards the "Lower Calcareous Alps" within the Traunstein, Schafberg or Höllengebirge mountains take place.

The region of interest is situated about 10km north of Mt. Dachstein (2995m), directly west of Lake Hallstatt and covers an area of about 40km² around the Echerntal and Mt. Plassen (1953m) (**Fig. 1.1**).

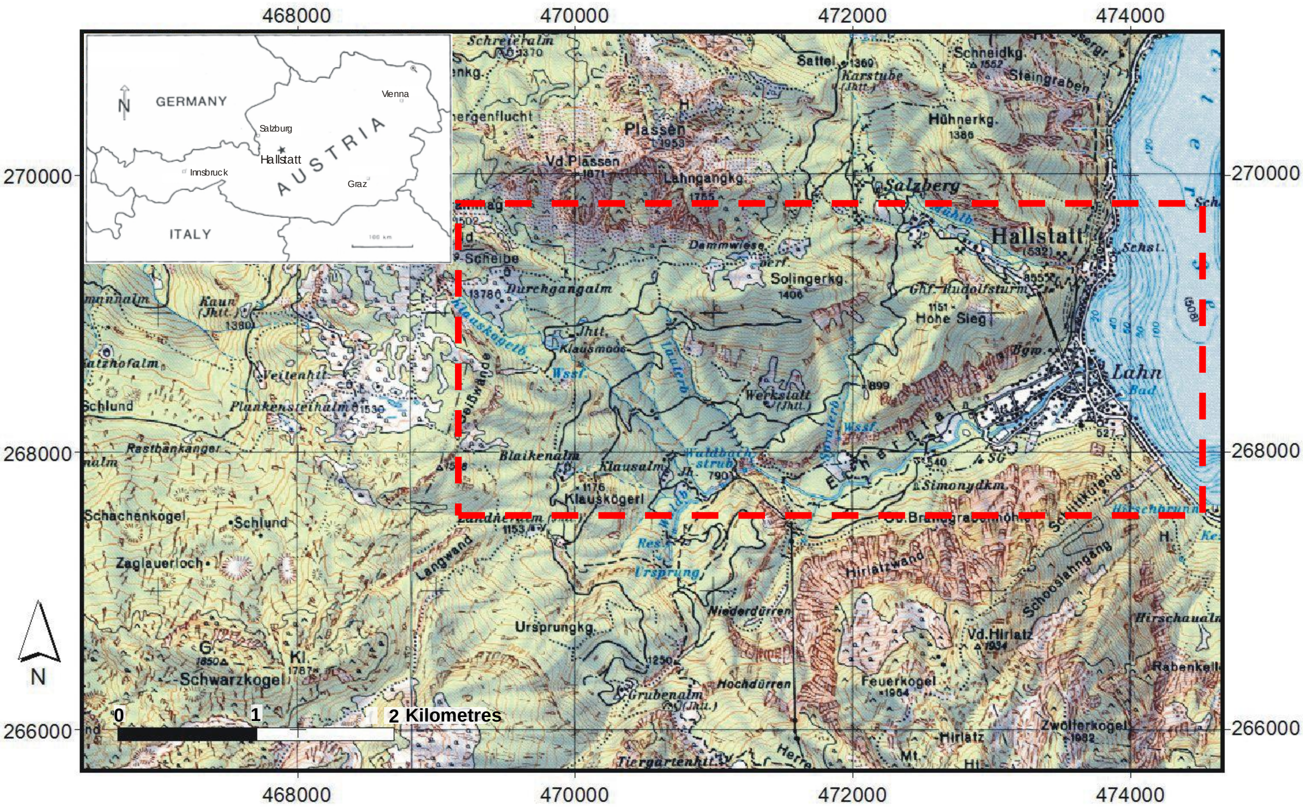

Fig. 1.1: The Area of Investigation is located around the Echerntal and Mt. Plassen, Upper Austria. This work focuses on the central part marked by the red rectangle.

As 3 diploma students were involved in the investigations, the area was split from N to S into 3 sub-areas. This work focuses on the central part, starting at the Echerntal (northern slope) and extending towards the W, south of the Mt. Plassen, until the Hohe Scheibe.

The main access to the Hallstatt salt mine is situated on the northern slope of the Echerntal. On the southern slope of the Echerntal the entry to the Hirlatzhöhle is located. With presently more than 96km investigated length and 1073m depth it is Austria`s second largest cave system (state of research march 2007). In the cause of this work, both the cave and especially the salt mine were investigated and provided interesting subsurface information.

1.2 History of salt mining in Hallstatt

Salt mining has a very old tradition in Hallstatt. Since salt mining started in Neolithic times, Hallstatt is one of the oldest industrial landscapes of the world. Even a period of the Iron Age is called the Hallstatt Age (800 – 400 B.C.).

The Hallstatt salt deposit forms a free-standing approximately 2700m long and up to 670m broad mountain crest and rises about 700m above the level of Lake Hallstatt. The deposition of the Hallstatt salt took place about 250 million years ago (Permian-Triassic-Boundary) in the shallow bays and lagoons of the pre-Mediterranean Tethys ocean. After the Alpine orogeny and the folding up of the Northern Calcareous Alps, the salt deposit consists on average of 62 % rock salt, 28 % clay and 10 % gypsum and other calcium sulphates. This evaporitic melange is called "Haselgebirge".

Neolithic beginnings**:** After the initial use of salt water from springs, mining of salt started during Neolithic times.

Stone axes and fragments of a shoe are the first proofs of a settlement at Hallstatt. At that time, picks made of antlers were the typical mining tool. The pick shown in **Fig. 1.2** was found in 1838 and a radio carbon dating in 2001 showed an age of about 7000 years.

Fig. 1.2: Pick made of antler, about 7000 years old (Barth and Lobisser, 2002)

Prehistoric salt mining**:** In the modern salt mine of Hallstatt (since 1311 A.D.), traces of prehistoric mining were discovered. Due to the preserving effect of salt, products made out of organic material like wood, fur and leather fabrics have been preserved and are precious findings for prehistoric research. These traces concentrate around three areas and define three consecutive salt mines, called Northern Group (1400-800 B.C.), Eastern Group (800-300 B.C.) and Western Group (0-400 A.D.).

The bronze aged Northern Group mines were constructed as steeply downward dipping shafts that followed "*Kernsalz*" zones with rich content of salt. The miners reached a maximum depth of 215m below the present surface. The salt was mined as fine crushed material and transported in leather baskets (**Fig.1.3**).

Fig. 1.3: A bronze aged leather basket and how the salt miners used it (Barth and Lobisser, 2002)

The Early Iron Age, also called the Hallstatt Age, was the time of the Eastern Group, which is characterized by a new mining technique. A network of tunnels followed the salt zones horizontal along the strike and instead of fine crushed material, large, typically heart-shaped blocks of salt were broken out and transported as intact pieces. Also the mining tools changed into picks of bronze. In 1734 a body of a prehistoric salt miner was discovered in this Hallstatt aged Eastern Group but it was buried and not preserved for science.

Fig. 1.4: Rich funerary assemblages (Barth and Lobisser, 2002)

A cemetery, situated at the "Salzberg Hochtal" (the foot of the salt mine used at that time) was discovered by Ramsauer in 1846. Today more than 1300 graves and their burial objects are documented and show a prospering society that based its wealth on salt mining. Even trade relations from Northern Europe to Africa are evidenced. It can be assumed that more than 4000 people had been buried there, almost half of them cremated. The cremation graves contained most of the rich funerary assemblages, reserved for a higher society. In inhumation graves, bodies were placed on their backs with a view towards the exit of the valley. The burial ground was in use from the 8th to the 4th century B.C. Therefore the cemetery can be seen as the graveyard attributed to the Eastern Group of the prehistoric mines of Hallstatt. In the 4th century B.C., a catastrophic landslide devastated the entrance of the mine, entering the shafts and tunnels of the mine, which brought an abrupt end to the prosperous culture of the valley: The end of the first high crop (Barth and Lobisser, 2002).

Fig. 1.5: A decorated scabbard of the Celts (www.hallstett.net)

The youngest prehistoric mining (Western Group) is characterized by an extended settlement at the "Dammwiese", at the southern edge of Mt. Plassen. The Celts inhabited the mine, but salt trading was controlled by the Romans. This period of mining ended with the collapse of the Western Roman Empire around 480 A.D. (Barth and Lobisser, 2002).

***Middle age and modern age*:** The subsequent Bavarian occupation was probably a peaceful settlement and was the basis of today`s folk art and customs. Around 1000 A.D., alpine salt mining slowly regained the importance it had in prehistoric and Roman times. The eldest historical documents on salt mining in Hallstatt date back to the late 13th century. The "Rudolfsturm", a watchtower, on the Salzberg was built by the Habsburg Duke Albrecht I in 1284 A.D. Few years later a "salt war" between Albrecht and the Archbishop of Salzburg broke out, sparked off by a quarrel over marketing regions for salt. Around 1311 A.D., Queen Elisabeth, King Albrecht`s widow, bestowed upon Hallstatt the rights of a market town and devoted herself to the reorganisation of the management and marketing of the salt mine in Hallstatt. Mining and the salt-works became a state-owned company and remained so until 1998. The method of salt gaining changed during the Middle Age from mining with picks into leaching the salt by water. Today the salt mine of Hallstatt is still in use, the brine processing is located in Ebensee (www.hallstatt.net).

Today only four among the halite salt mines in Austria are still active: Altaussee, Bad Ischl, Hallein and Hallstatt.

Timescale of the important stages of development at the Hallstätter Salzberg (modified after Lobisser, 2002):

Time	Period	Culture	In Hallstatt
Since ~1376 A.D.	Middle and Modern Age	Habsburg and following	Modern salt mine
0 – 400 A.D.	Roman Empire	Romans	Western Group; (settlement at the Dammwiese)
800 – 300 B.C.	Early Iron Age	Hallstatt Culture	Eastern Group
1400 – 800 B.C.	Middle/Late Bronze Age	Tumuli and urn fields	Northern Group
5600 – 4800 B.C.	Neolithic Age	First settlements	Pick made of antlers (ca. 5000 B.C.)

2. Geological setting

2.1 History of geological investigation

Due to the existing salt mine the first investigations of the Hallstatt-Dachstein region, within the Northern Calcareous Alps (NCA) date nearly back to the beginning of geology itself. Another reason of interest was the richness of fossils in the NCA. Therefore the Hallstatt-Dachstein region has been a classical area for geoscientific research of the Tethyan stratigraphy for more than 200 years. At the end of the 18^{th} century, for example, the report of Bohadsch (1782) concerning fossils in the Gosau basin was published. One of the first maps of the NCA was given in Flurl (1792) but he only differentiated the Calcareous Alps from the subalpine units. Buch (1802) reported the dominance of Limestone and the abundance of fossils in the red limestone after an exhibition through the NCA with Alexander von Humboldt. During the 19^{th} century, stratigraphy was advanced and the so called “Alpenkalk” (the whole Triassic carbonate succession) was attempted to subdivide into clearly defined rock units (Lilienbach, 1830). Lilienbach (1830) also published that the carbonates of the NCA are stratigraphically lying above the evaporitic Haselgebirge and Werfen sandstone and are covered themselves by the Gosau group in the hanging wall. One of the first sections perpendicular to the striking direction of the geological units through the Eastern Alps was drawn by Sedgwick and Murchinson (1831). Morlot (1847) and Hauer (1848) started to subdivide the so-called “Alpenkalk” due to detailed systematic investigations of the ammonite fauna of the Hallstatt limestone. In 1849 the “Geologische Reichsanstalt” was founded and in the following years the NCA were systematically mapped. In addition essential palaeontology monographs about the Tethyan stratigraphy were published by Mojsisovics (1873; 1882; 1893; 1902) and Bittner (1890).

Initial theories about the nappe structure of the NCA came up at the beginning of the 20^{th} century. A first concept of nappe structure in the central NCA was published by Haug and Lugeon (1904). In the following years Ampferer (1911, 1912a) worked on the western part, Hahn (1912; 1913b) on the middle part and Kober (1909; 1911a, b; 1912a, b) on the eastern section of the NCA. Over this period of time, the complexity of the central NCA became obvious, and in particular the complicated stratigraphy and tectonic evolution of the Hallstatt Zone was a matter of discussion by the above mentioned authors. This controversy persists even in the recent literature. In addition, Reis (1910) and Ampferer (1939) were among the first to recognize the large-scale nappe movement of the NCA towards the NW, but this model was displaced in favour of models that claimed top to north movement as a consequence of thrusting perpendicular to the European foreland (e.g. Kober, 1923).

Tollmann (1976a), Mandl (1984a) and Lein (1987) provide detailed investigations on the Triassic depositional realm, a passive continental margin of Pangea. Schäffer (1976) established the concept of Jurassic gravity gliding and Tollmann (1981) modified this theory.

The formation and structure of the salt deposits in the Permian Haselgebirge were described by Schauberger (1986), who also published detailed information about the Hallstatt salt deposit, including a cross-section through the mine (Schauberger and Medwenitsch, 1951, Schauberger, 1955). Further descriptions of Austroalpine salt mines were provided by Klaus (1953) and Medwenitsch (1958). Recent research on the thermal history and deformation of the Haselgebirge that confirmed the Permian age of the main part of the Haselgebirge was performed by Spötl (1987, 1989) and Spötl & Hasenhüttl (1998). Just a comparatively small part of the Haselgebirge indicates Early Triassic age (Spötl and Pak, 1996).

Detailed geological maps of the interesting area at a scale of 1:50 000 were published by Schäffer (1982, Blatt 96 Bad Ischl) and Plöchinger (1982, Blatt 95 St. Wolfgang).

Recent publications kept the discussion alive: Mandl (2000) reconstructed the tectono-sedimentary evolution of the eastern Alpine sector, primarily focusing on the Salzkammergut Region. Another important work concerning Eoalpine nappe movement was provided by Linzer et al. (1995), where the authors proposed NW-directed thrusting of the NCA in a right-lateral transpressional regime. Frisch and Gawlick (2003) suggested that the Hallstatt Unit – instead of a Juvavic nappe – should be regarded as the highest level of the Tirolic Units.

Habermüller (2005) and Arnberger (2006) constructed balanced cross sections that show the minimum amount of shortening in the Hallstatt area. Both suggested that the main tectonic transport direction is oriented to W up to NW. The minimum amount of shortening in the Hirlatzwand (southern slope of the Echerntal) is claimed to be 32,5% (Habermüller, 2005). Arnberger (2006) determined a minimum amount of shortening in the northern part of the Hallstatt Nappe (north of Mt. Plassen) of 42,1%.

Because of the enormous amount, the published literature was only listed in an excerpt in this chapter. A more detailed summary about the geological research of the Dachstein-Hallstatt-Region is given in Lobitzer and Mandl (2008).

2.2 Tectonic setting and palaeogeography situation of the NCA

The Northern Calcareous Alps (NCA) belong to the Austroalpine nappe complex and represent the frontal and uppermost tectonic element of the Eastern Alps. This 500km long and up to 50km wide body of Permomesozoic sediments forms a multiply deformed fold-and-thrust belt on the northern part of the Alps. The NCA extend from the Vienna basin in the east to the southern Rhine Graben in the west. An overview of the main geological units of Austria and the position of the NCA therein is given in **Fig. 2.1.**

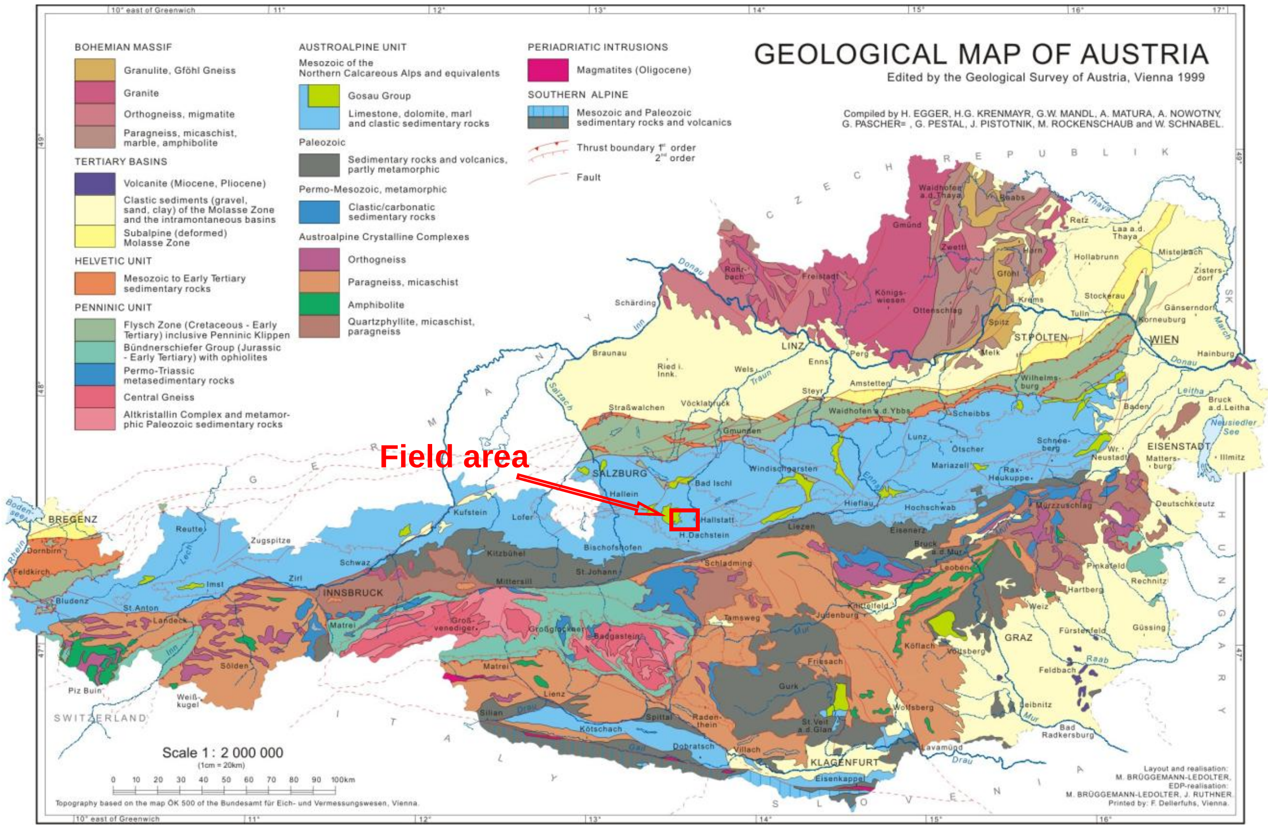

Fig. 2.1: Geological map of Austria within the NCA in the central part. Field area (Hallstatt) is marked with the red rectangle. A detailed map of the NCA is provided in Fig. 2.3 and 2.4 in this chapter (Geological Survey of Austria, 1999).

The sedimentary succession of the NCA begins in the Permian and reaches in some places up to the Eocene (Gosau Group), but the carbonate-dominated Triassic sediments are the predominant lithology. Triassic carbonates achieved respectable thicknesses of several kilometres as a result of tectonic inactivity and high subsidence rates in that period of time. The depositional realm of the NCA in Permian and Triassic times was a passive continental margin that developed on the Variscan Basement of Pangea due to rifting of the Tethys Ocean (e.g. Haas et al., 1995; Mandl, 2000). Kozur (1991) introduced the name "Hallstatt-Meliata-Ocean" for the western sector of this ocean that adjoined the NCA.

During the Jurassic a new rifting event isolated the whole Austroalpine realm, including the NCA, from its European hinterland and formed the transtensional basin of the Southern Penninic Ocean. This rifting was linked with the opening of the central Atlantic Ocean by a large scale sinistral transform fault (Faupl & Wagreich, 2000). Due to the opening of the new ocean, the Austroalpine shelf drowned completely and deep marine conditions prevailed until the Early Cretaceous. The greatest water depth was achieved in the Oxfordian, as indicated by radiolarite deposits.

Synchronous left-lateral compressional tectonics in the Tethyan Ocean caused first displacements of the tectonic uppermost Juvavic units, which palaeogeographically represented the southernmost part of the NCA. Crustal shortening continued and led to the closure of the Hallstatt-Meliata-Ocean (Faupl & Wagreich, 2000). Due to radiometric dating of metamorphism by illite crystallinity and vitrinite reflectance data of the Permian evaporitic melange at the base of the NCA, Spötl and Hasenhüttl (1998) suggest a Late Jurassic closure of the Hallstatt Meliata Ocean with subsequent thrusting. This thrusting and the uplift of the suture zone caused north directed gravitational glide movements in the southern part of the NCA (Faupl & Wagreich, 2000). As a result of this “glide tectonics” a new seafloor topography, caused by breccias, olistolithes and big gliding blocks, was generated for the Late Jurassic. Deep marine sedimentation in the basins between those sliding masses continued, while on their tops shallow marine conditions developed.

The subduction of the Tethys Ocean and the related tectonic processes in Upper Jurassic times mark the Cimmerian orogeny, the first stage of the Alpine orogeny.

During the following Eoalpine orogeny the Northern Penninic Ocean, which arose in the Lower Cretaceous, was subducted to the south, beneath the Austroalpine terrane. According to Faupl (1997) this subduction and the subsequent continent-continent collision in the Late Cretaceous were the main reasons for the Eoalpine-phase that reached its peak between Albian and Turonian. As a consequence in this period the Austroalpine nappe complex developed and the NCA were decoupled from their basement. The migration of syntectonic sedimentation towards the north indicates the displacement of the deformation front towards the north, into higher tectonic units of the NCA. The clastic material, delivered from the uplifting parts of the NCA, changed the deep water carbonate production into terrigenous facies conditions (e.g. Rossfeld Formation) in Early Cretaceous times.

As a result of the Eoalpine orogeny, the NCA were exposed to erosion until the discordant clastic sediments of the Gosau Group transgressed.

The Mesoalpine orogeny started in the Late Eocene and was characterized by ongoing northwards movement of the NCA. As a consequence the sediments of the Rhenodanubian Flysch Zone were deformed and partly overthrusted. Furthermore an asymmetric foreland basin developed that received the molasse sediments of the arising orogen.

During the final orogenic peak, the Neoalpine orogeny, Miocene uplift of the central part of the Eastern Alps caused eastward lateral extrusion along large-scale strike-slip fault systems like the Periadriatic Lineament in the south and the Mur-Mürz Line in the north (Ratschbacher, 1991). These strike slip movements also affected the NCA and led to clockwise rotations of blocks therein (e.g. Linzer et al., 1995).

2.2.1 Division of the NCA into three main structural units

In the formation of the Alpine Orogeny, the NCA were decoupled from their Palaeozoic basement. This nappe complex now, after several stages of Alpine deformation, rests on the Rhenodanubian Flysch Zone in the north and on Palaeozoic units of the Greywacke Zone in the south. The classic tectonic concept (e.g. Plöchinger, 1995) separates three main units within the NCA – from north to south, respectively from structural lower to higher units these are:

- Bajuvaric Nappe Complex
- Tyrolic Nappe Complex
- Juvavic Nappe Complex

Along rheologically weak sedimentary units, composed of clay stones, marls and evaporites three main detachment horizons of the NCA developed. According to Linzer et al. (1995) the basal detachment consists mainly of “Haselgebirge”, which is the name of the Permian melange that comprises evaporites and clay stones. Carnian black shales and evaporites build up the middle detachment level. The uppermost detachment horizon constitutes of Liassic to Lower Cretaceous thin-bedded marls and siltstones that were sedimented in deep marine conditions (**see Fig. 2.2**).

These detachment horizons are connected by two major ramps, which cut through Triassic carbonate platforms with relatively high competence. The lower one was deposited in Anisian to Ladinian times (e.g. Wettersteinkalk), the upper one is of Norian age (e.g. Dachsteinkalk).

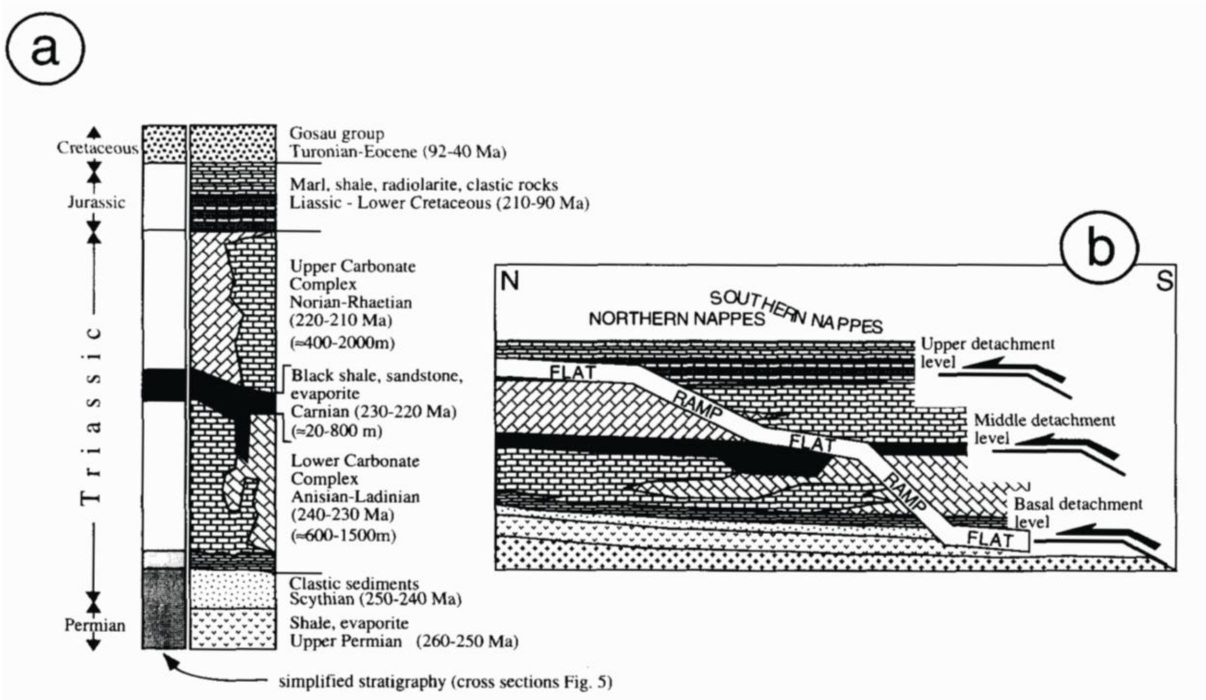

Fig. 2.2: (a) Generalized tectonostratigraphic column of the Northern Calcareous Alps. (b) Showing the three main detachment horizons of the NCA connected with a schematic flat-ramp-flat geometry (Linzer et al., 1995).

Furthermore a division into eastern, central and western NCA, as shown in **Fig. 2.3**, has become very common, as each part represents different portions of the main units and has different underlying basements (e.g. Mandl, 2000). Bajuvaric units dominate in the western part, Tyrolic is prevalent in the central section, whereas in the eastern part Juvavic, Tyrolic and Bajuvaric nappes are nearly equally distributed.

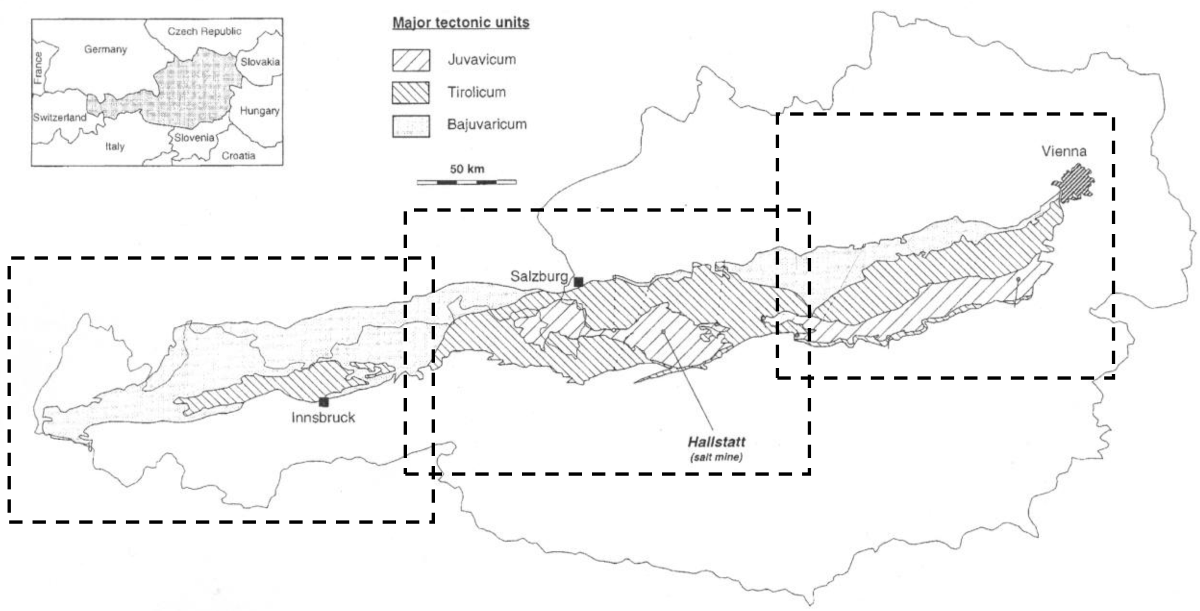

Fig. 2.3: Overview of the NCA with division into western, central and eastern part (modified after Spötl et al., 1998).

Bajuvaric Nappes

The structurally lowest unit of the NCA, the Bajuvaric Nappe Complex, is located on the northern front and overlies the North Penninic Flysch with overthrust contact. These nappes are dominated by Hauptdolomit Facies **(see chapter 2.3 Stratigraphy)** and can be further subdivided into three units:

1.) Lowest Bajuvaric; composed of Cenoman Randschuppe

2.) Lower Bajuvaric; including the Allgäu, Ternberg and Frankenfels Nappes

3.) Upper Bajuvaric; built up by the Lechtal, Reichraming, Lunz and Sulzbach Nappes.

Whereas the Bajuvaric units are well exposed in the western NCA (Cenoman Randschuppe, Allgäu Nappe, Lechtal Nappe), they are mostly overthrusted by Tyrolic nappes in the central NCA. The Bajuvaric complex of the eastern NCA is more widespread again, with the Cenoman Randschuppe and the Ternberg, Reichraming, Frankenfels, Lunz and Sulzbach Nappes (Plöchinger, 1995) (**see Fig. 2.3, 2.4 and 2.5**).

Tyrolic Nappes

The Tyrolic nappes that overrode the Bajuvaric units and got overthrusted by the Juvavic nappes during the Alpine Orogeny are either developed in Hauptdolomit Facies or, towards the southern part, in Dachstein Limestone Facies **(see chapter 2.3 Stratigraphy)**. The Tyrolic unit is subdivided into the Inntal Nappe in the western NCA, the Staufen-Höllengebirgs Nappe, Totengebirgs Nappe and Warscheneck Nappe in the central NCA and into the Reisalpen Nappe, Unterberg Nappe and Göller Nappe in the eastern NCA (Plöchinger, 1995).

Juvavic Nappes

The southernmost depositional realm of the NCA and the structurally highest unit is represented by the Juvavic Nappe Complex that is further subdivided in an Upper and Lower Juvavic. The Upper Juvavic is characterized by the Dachstein Limestone Facies whereas the Lower Juvavic is developed in Hallstatt Facies. Upper and Lower Juvavic are old terms and do not correlate with their tectonic position. In the eastern NCA the Juvavic Nappe Complex is composed of the Schneeberg, Mürzalpen and Hallstatt Nappes. The Dachstein, Hallstatt and Berchtesgarden Nappes build up this Complex in the central NCA, where it is more widespread. In the western NCA the Juvavic Nappe complex is totally absent (**Fig. 2.3, 2.4 and 2.5**, Plöchinger, 1995).

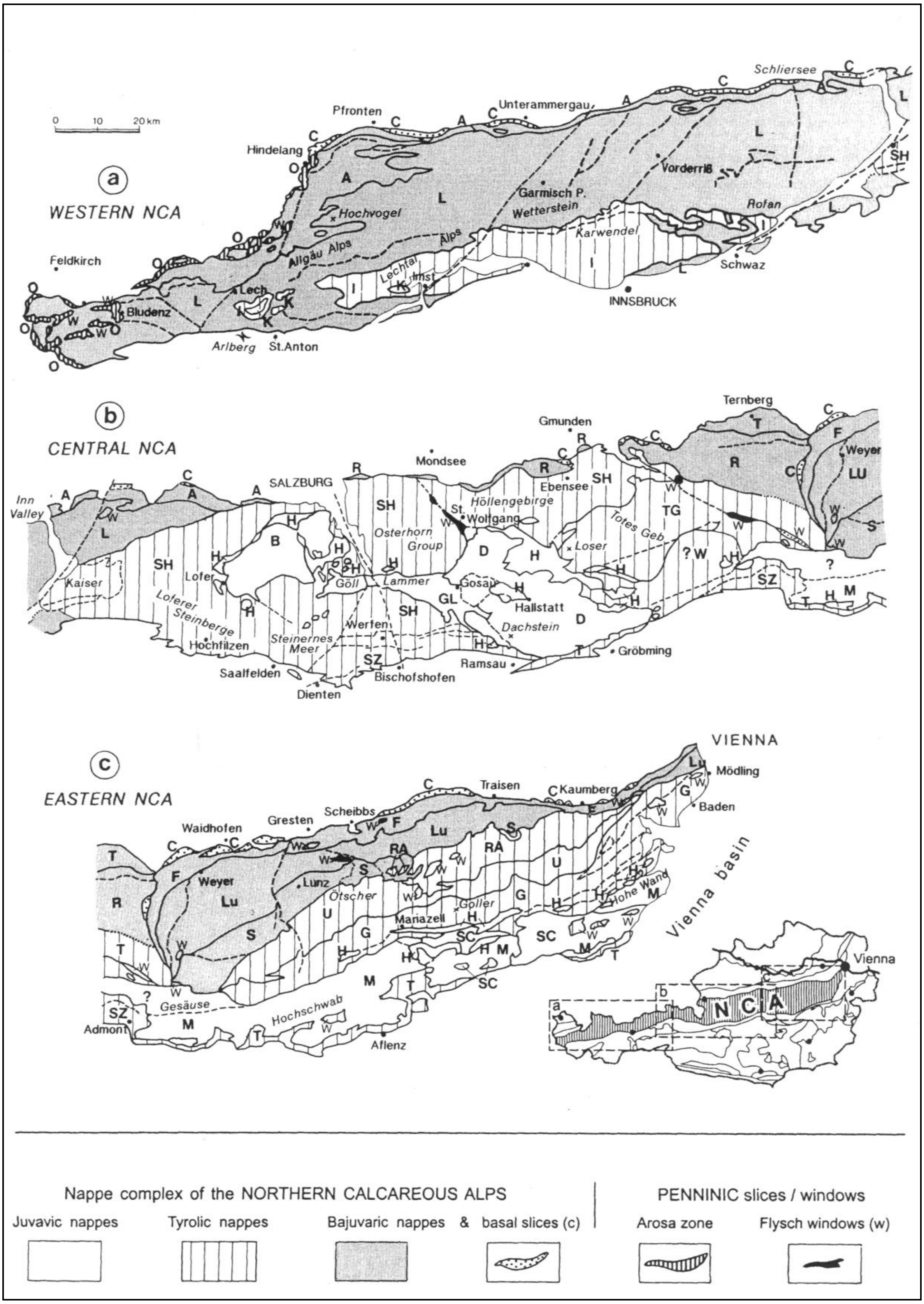

Fig. 2.4: The nappe complex of the NCA (after Mandl, 2000, modified after Plöchinger, 1995). From top to bottom: western, central and eastern section of the NCA. See next page for legend.

1. Juvavic nappe:
B = Berchtesgarden Nappe (Upper Juvavic)
D = Dachstein Nappe (Upper Juvavic)
SC = Schneeberg Nappe (Upper Juvavic)
H = Hallstatt Nappe (Lower Juvavic)
M = Mürzalpen Nappe (undifferentiated Juvavic)
GL = Göll Lammer Unit (undifferentiated Juvavic)

2. Tyrolic:
K = Krabachjoch Nappe
I = Inntal Nappe
SH = Staufen-Höllengebirge Nappe
TG = Totengebirge Nappe
W = Warscheneck Nappe
SZ = Werfen/Admont Slices (Schuppen Zone)
Ötscher Nappe: Reisalpen (RA), Göller (G) and Unterberg (U) Nappes

3. Bajuvaric:
L = Lechtal Nappe (Upper Bajuvaric)
R = Reichraming Nappe (Upper Bajuvaric)
S = Sulzbach Nappe (Upper Bajuvaric)
Lu = Lunz Nappe (Upper Bajuvaric)
A = Allgäu Nappe (Lower Bajuvaric)
T = Ternberg Nappe (Lower Bajuvaric)
F = Frankenfels Nappe (Lower Bajuvaric)

4. Lowest Bajuvaric:
C = Cenomanian Border Slice (Cenoman-Randschuppe)

5. Penninic:
O = Arosa Zone

6. Tectonic Window within the NCA:
Black = Predominating flysch windows (W)

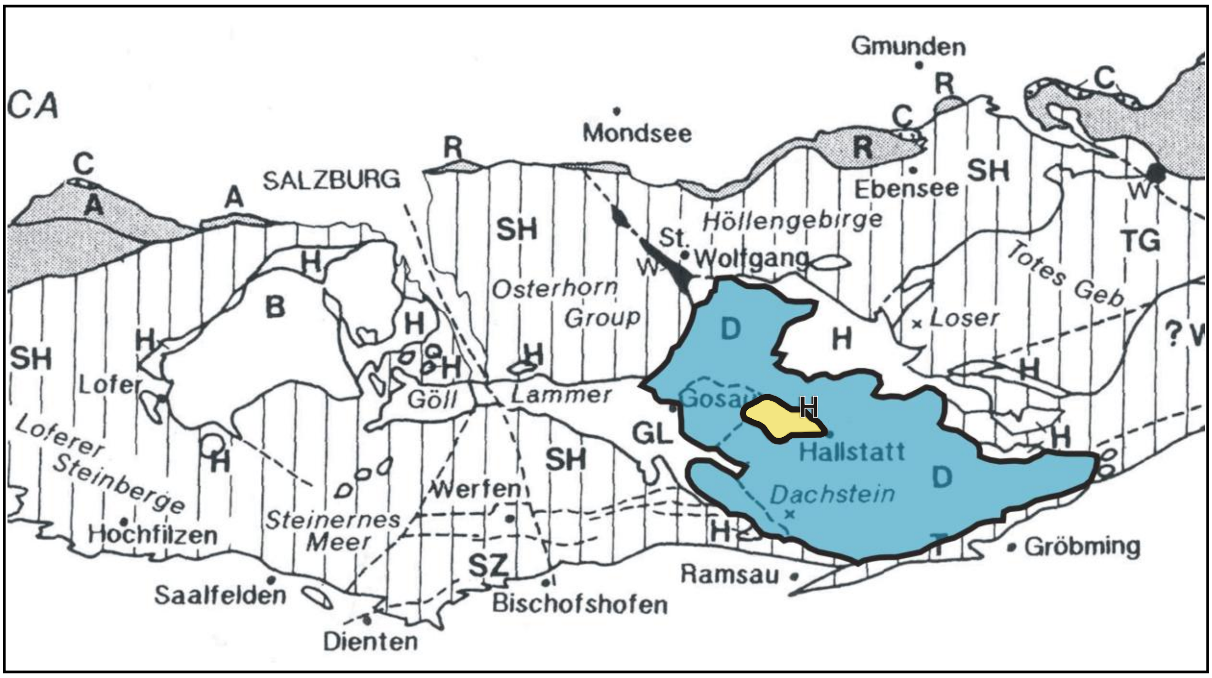

Fig.2.5: Central part of the NCA, within the area of investigation, on the southern border of the yellow marked Hallstatt Nappe (modified after Plöchinger, 1995).

2.3 Stratigraphy of the Dachstein and Hallstatt Nappes

Although this work deals mainly with structural geology, the stratigraphy of the study area is essential for understanding the tectonic evolution. In particular formations with relative low shear strength, like evaporites, influence the tectonic style significantly as they act as ductile deforming detachment horizons. As a result varying rheologies and different sediment thicknesses of the Hallstatt and Dachstein Nappes caused different deformation structures that were observed in the field.

2.3.1 Permian

Haselgebirge:

The Alpine Haselgebirge, also called East Alpine Salinar, consists of components of shales, sandstones, anhydrites, carbonates and occasional magmatic rocks within a clay-rich evaporitic matrix. The Alpine Haselgebirge is exposed in particular outcrops along a 350km long and 35km wide zone between Innsbruck and Vienna. The main components of the salt deposits consist either of halite, gypsum or anhydrite. The original depositional realm of this polyphase distorted evaporitic melange was an east-west trending continental rift setting that was periodically influenced by Thetyan sea water. Consequently a salt pan developed during dehydration stage. This salt pan covered the central deposition area and was surrounded by shabkas, mudflats and alluvial fans (**see Fig. 2.6**) (Spötl, 1989).

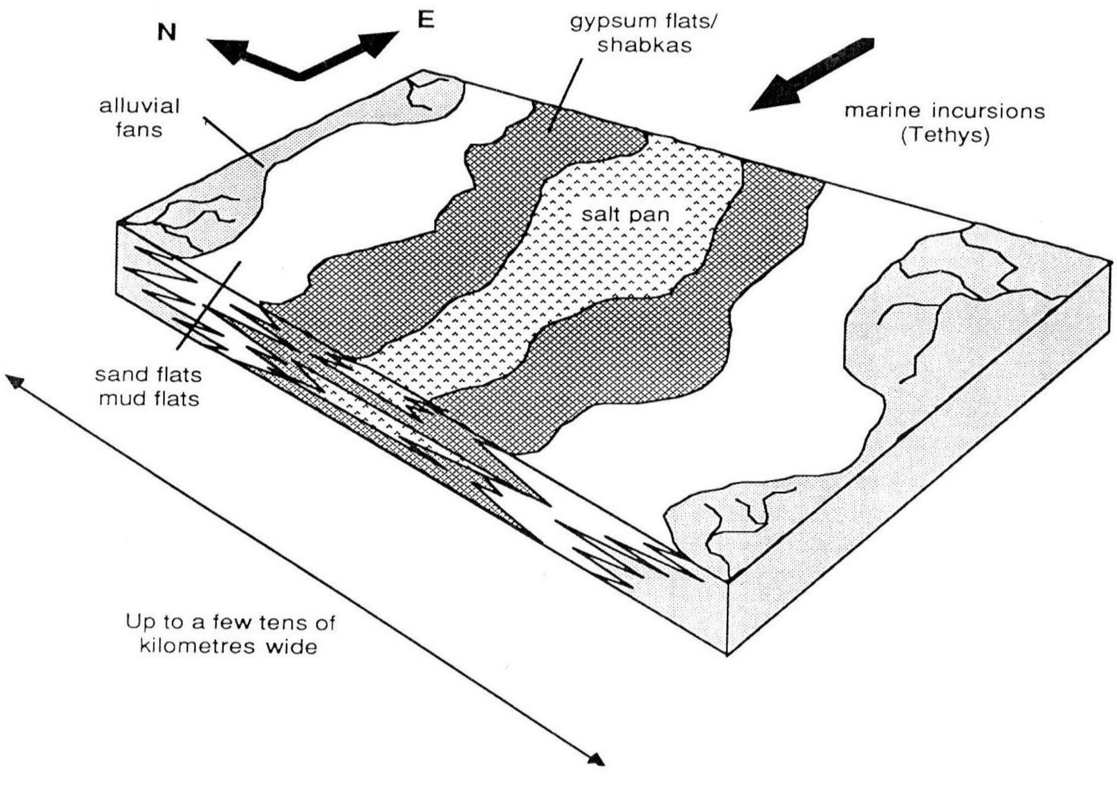

Fig. 2.6: Reconstruction of the original depositional realm of the Alpine Haselgebirge (Spötl, 1989)

Klaus (1955) used palynological investigations on intercalated shales to constrain an Upper Permian until Middle to Upper Scythian sedimentation age. These results were confirmed by S-isotope dating on anhydrites, gypsum and polyhalites by Schauberger (1986). Spötl (1989) defined the grad of evaporation by measuring the bromine content of halite. Bromine values increase with ongoing evaporation and hence with rising salinity of the environment. The East Alpine salt deposits are commonly related to the upper anhydrite facies, but intercalated salt clasts reach much higher bromine values and indicate that high saline evaporites, such as potash salt, were also deposited. Probably these high saline evaporites were mainly re-dissolved again.

Due to the intense deformation, like Alpine thrust tectonics, diapirism and gravitational gliding, an exact thickness of the primarily sediment pile of the evaporitic succession is not established. Moreover thicknesses of several hundred meters are supposed.

According to the halite concentration, salt miners categorized the following five salt rock types within the East Alpine salt deposits (Schauberger, 1986):

- *Kernsalz*
- *Kerngebirge*
- *Haselgebirge*
- *Blättersalzgebirge*
- *Tontrümmergebirge*

The *Kernsalz* comprises at least 90% halite. Fine-grained contaminants of shale or anhydrite cause a compositional banding (cb) that can either show sharp ("*Liniensalz"*) or diffuse ("*Bändersalz"*) contacts.

Kerngebirge, which contains 70-90% halite, is gray or light reddish coloured and consists of a fine crystalline salt rock without foliation. The size of the incorporated nonhalitic clasts, like shales, anhydrites and polyhalites, varies from few centimetres up to several decimetres.

Haselgebirge describes a rock salt with 10 to 70% halite. The fine grained halite matrix contains impurities mainly composed of shale, anhydrite, polyhalite and sandstone. Based on the type of shale (green, grey, black or red shale) and the colour of other intercalations, the Haselgebirge is subdivided into Green, Grey, Black or Variegated Haselgebirge. The Anhydrite-Haselgebirge, another special form, is characterized by an anhydrite matrix instead of halite. As described in the chapters above this is in contrast to the geological use of the term Alpine Haselgebirge, which is equal to the whole East Alpine Salinar.

The *Blättersalzgebirge* describes a halite content of 20-35%. Several metre sized fragments of black, green or grey shales with a very thin cover of white halite ("Blättersalz") form this type of salt rock. The big clasts of shale contain a lot of extension fissures that are filled with secondary white halite.

The *Tontrümmergebirge* is characterized by a halite content of 0-10%. This type of salt rock comprises several meter thick layers of anhydrite which are interbedded with either black shales or dolomite. Even secondary halite fillings are rare in this salt rock type that is absent in some East Alpine salt deposits.

2.3.2 Triassic

The depositional realm during Triassic times was that of a passive continental margin adjacent to the Hallstatt-Meliata Ocean. Five major facies zones developed from the continent to the open sea. These start with the terrigenous-evaporitic Keuper Facies, continued by the dolomitic Hauptdolomit Facies. The inner part of the slowly subsiding shelf is preserved by the Dachstein Limestone Facies, a carbonate platform with reefs and lagoons. The succeeding pelagic Hallstatt Facies represents the connection of the shelf with the open sea of the Tethys. The most distal section, which was already deposited on oceanic crust, is dominated by a radiolaritic facies. The area that forms the future Juvavic Nappe Complex is located in the southernmost part and involves the Dachstein Limestone and Hallstatt Facies. Today, the radiolaritic facies is not preserved in their primary stratigraphic context, but exists as redeposited Jurassic sediments (Haas et al., 1995).

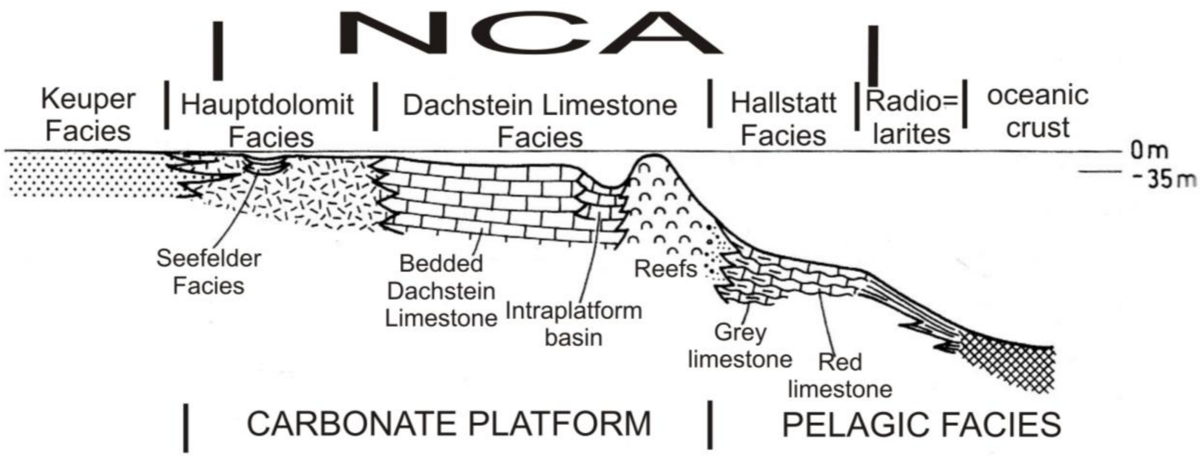

Fig. 2.7: Five major facies zones on the passive continental margin during Triassic (Haas et al., 1995)

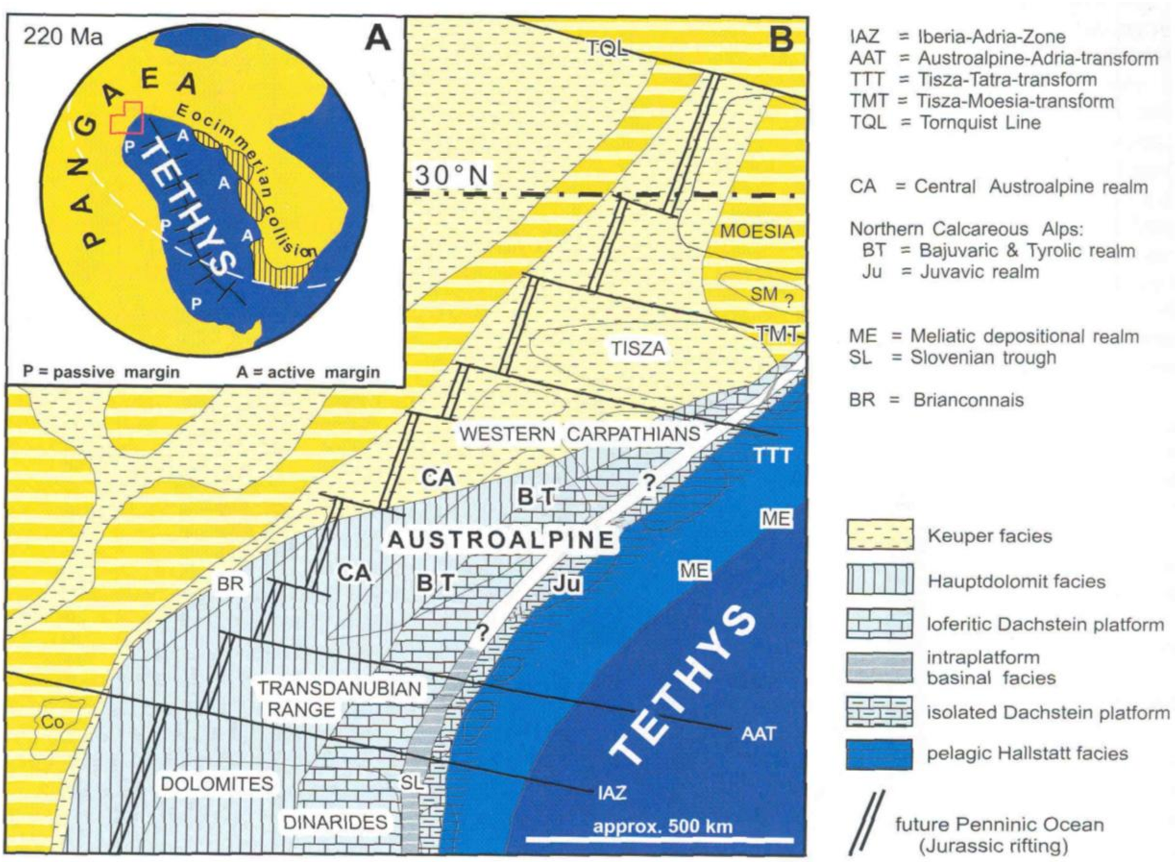

Fig. 2.8: Palaeogeography setting and facies distribution at the Alpine-Carpathian sector on the northwestern margin of the Tethys in Triassic times (Mandl, 2000).

Werfen Formation:

The Early Triassic (Scythian) was characterized by the widespread deposition of shallow shelf siliciclastics of the Werfen Formation, containing quartzites at the base, slates in the middle section and thin limestones in the uppermost part. The Werfen Quartzites consist of light green to white, well-bedded sediments with considerable thicknesses. The Werfen Shales appear as red, violet or green mica bearing shales and thin-bedded sandstones. At its upper boundary, the Werfen Limestone, with a poor fauna including Scythian ammonoids and conodonts, is about 30m thick and leads over to the carbonate dominated sedimentation of the Middle and Upper Triassic. For parts of the Dachstein Nappe, a thickness of 300m has been assumed (Mandl, 2000), but locally the Werfen Formation reaches thicknesses up to 500m (Tollmann, 1985).

Gutenstein Limestone/Dolomite:

The thin-bedded black to grey Gutenstein Limestones and Dolomites were deposited at the base of the Anisian. These bituminous and mainly micritic carbonates were sedimented in a shallow marine environment that was still anoxic. These carbonates achieve thicknesses of up to 240m. For the interesting area around Hallstatt about 200m are published (Mandl, 2000).

Steinalm Limestone/Dolomite:

During the Pelsonian (Middle Anisian), the Gutenstein-type sedimentation was replaced by the light grey, thick-bedded Steinalm Limestones and Dolomites. These algae-rich carbonates containing corals and crinoids were deposited in shallow marine environments. The Steinalm succession achieves thicknesses of about 100m in the Dachstein Nappe, whereas for the Hallstatt Nappe up to 250m have been recorded (Mandl, 2000).

Up to the lower Middle Triassic, sedimentation of the Dachstein Limestone Facies and Hallstatt Facies were comparable but with ongoing deepening of the Tethys, they began to differ (**see Fig. 2.9**). Pelsonian drowning and coeval block-faulting created a sea floor topography that was responsible for the subsequent differentiation into basinal areas of Hallstatt Facies and shallow carbonate platforms of the Dachstein Limestone Facies.

A further subdivision of the Hallstatt Facies into basinal areas (e.g. Reiflinger Basin) and intrabasinal ridges with reduced sedimentation has been presumed to have been caused by salt diapirism of the Permian evaporites (Mandl, 2000). Due to this differentiation the stratigraphy of the Dachstein and Hallstatt Nappes in the Middle and Upper Triassic times varies significantly and will be described separately:

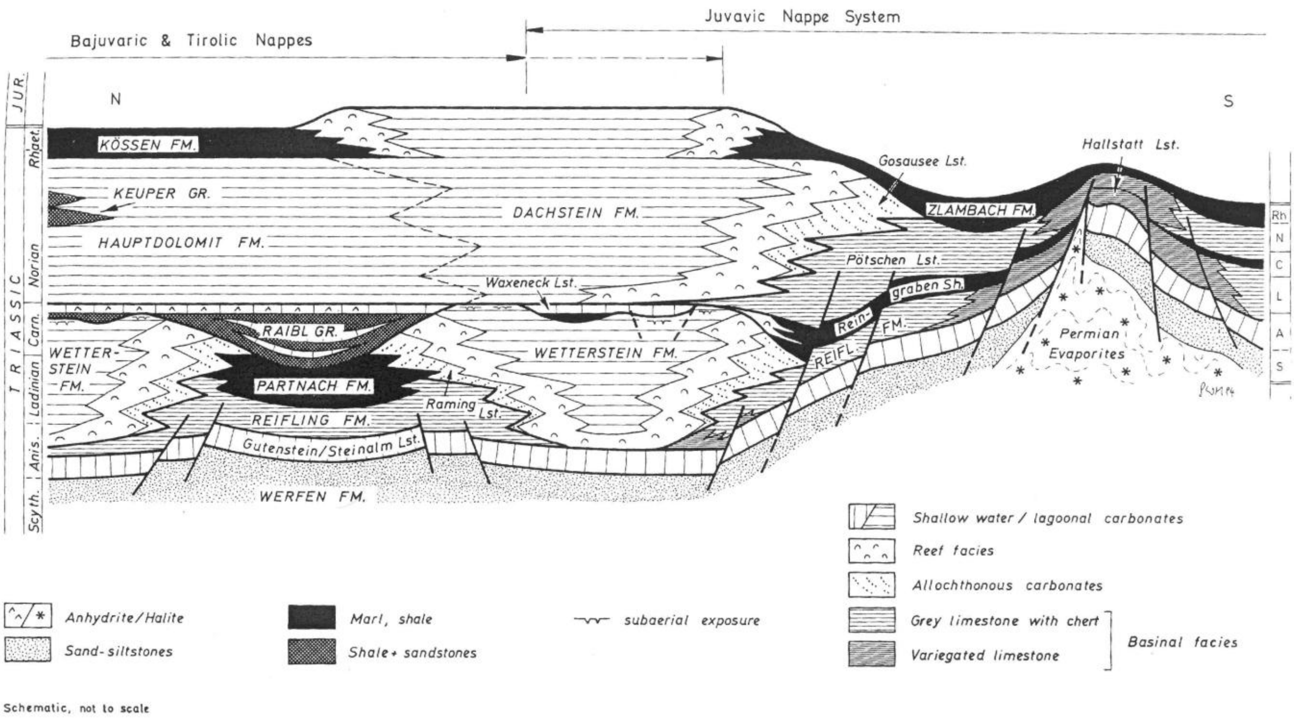

Fig. 2.9: Triassic stratigraphy in the central sector of the NCA, showing the differentiation into Dachstein Limestone Facies and Hallstatt Facies after Pelsonian drowning (Mandl, 2000).

Dachstein Nappe:

Due to the Pelsonian drowning the shallow marine conditions changed into pelagic conditions in the middle to late Anisian. Sedimentation of the pelagic carbonates like **Reifling Limestone** and **variegated Hallstatt Limestone** (see detailed description of these lithologies at **Hallstatt Nappe** within this chapter) prevailed until the Lower Carnian.

Wetterstein Limestone:

The sedimentation of the Wetterstein Limestone on the distal shallow marine shelf of the Thetys Ocean created the first major Triassic carbonate platform. In the Dachstein Nappe it achieves thicknesses of up to 800m. Propagation of the Wetterstein platform towards the basin during Ladinian up to the earliest Carnian is well preserved; only the initial stage of platform growth is not exposed (Mandl, 2000). Reef breccias, platform-derived bedded to massive allodapic limestones and distal carbonate turbidites are usual sedimentary features. Another typical attribute is the secondary dolomitisation that affected especially the lagoonal interior parts of the platform. Syn-depositional karst-structures within the platform reveal several regressions, as in the Middle Anisian when cavities were formed and vadose cements were deposited. The following carbonate deposition was interrupted by a second drainage during the Early Carnian. This Early Carnian sea level lowstand led to the exposure of the emerged platform and left an erosional surface on the top (Mandl, 2000).

Lunz-Raibl Group:

Due to the Carnian global sea level lowstand, the platforms emerged and the remaining basins received siliciclastic material from the European hinterland. Consequently the terrigenous Lunz-Raibl Group was deposited in large parts of the NCA. The Raibl Group is characterized by alternating sedimentation of black shales and carbonates. Intercalations of sandstones, especially in the third and uppermost shale horizon are typical. Locally sedimented evaporites indicate an increased salinity in the uppermost carbonate horizon. The shales and locally existing evaporites provided an ideal detachment horizon for the carbonates of the overlying Dachstein Formation **(see Fig. 2.2)**. As a result this formation with relatively low competence is tectonically detached and often missing or at least incomplete within the Juvavic Nappes of the central NCA (Piller et al., 2004). Thickness varies in a range from 10m up to a few hundred meters (Tollmann, 1985). In the Hallstatt Nappe this global sea level lowstand is represented by the terrigenous Rheingraben Shale.

Dachstein Formation:

In the Late Carnian, the sea level rose again, leading to the deposition of the second major carbonate platform. This Dachstein Limestone platform that continued until the Rhaetian reaches thicknesses of about 1200m, locally even up to 1500m. This huge sediment pile consists of two different depositional realms: a massive reefal limestone on the margin of the platform and bedded lagoonal limestones on the interior platform.

The unbedded, massive reef limestone is mainly composed of corals, hydrozoa and calcisponges (Faupl, 1997).

Periodic sea level changes caused a typical cyclic bedding of the lagoonal platform sediments, also called “Lofer-Facies”. These inter- to subtidal units build up three characteristic layers (A – C). The main sediment is a light-coloured subtidal limestone (layer C), usually at least 1m up to several metres thick. This layer is famous for large megalodonts, which have similarities to a cow`s track and therefore they are also known as “Kuhtritte” by the local people. Layer B that usually reaches maximum thicknesses of some decimetres consists of intertidal carbonates, mainly consisting of laminated limestones. The usually crinkled lamination represents filamentous algal mats. Layer A covers the weathered and solution-riddled surface of this limestone. This often reddish or greenish clayey limestones and are interpreted as former terrestrial soils. Due to its erosional origin Layer A is commonly not evolved as a continuous bed (Mandl 2000).

Zlambach Formation:

Increasing terrigenous input in the Rhaetian led to the sedimentation of the Zlambach marls. The Zlambach Formation consists of marls and limestones, which contain reworked corals with encrusting organisms. Towards the top of this lithology the carbonate content decreases and this regression terminated the Triassic carbonate platforms in the NCA (Tollmann, 1985).

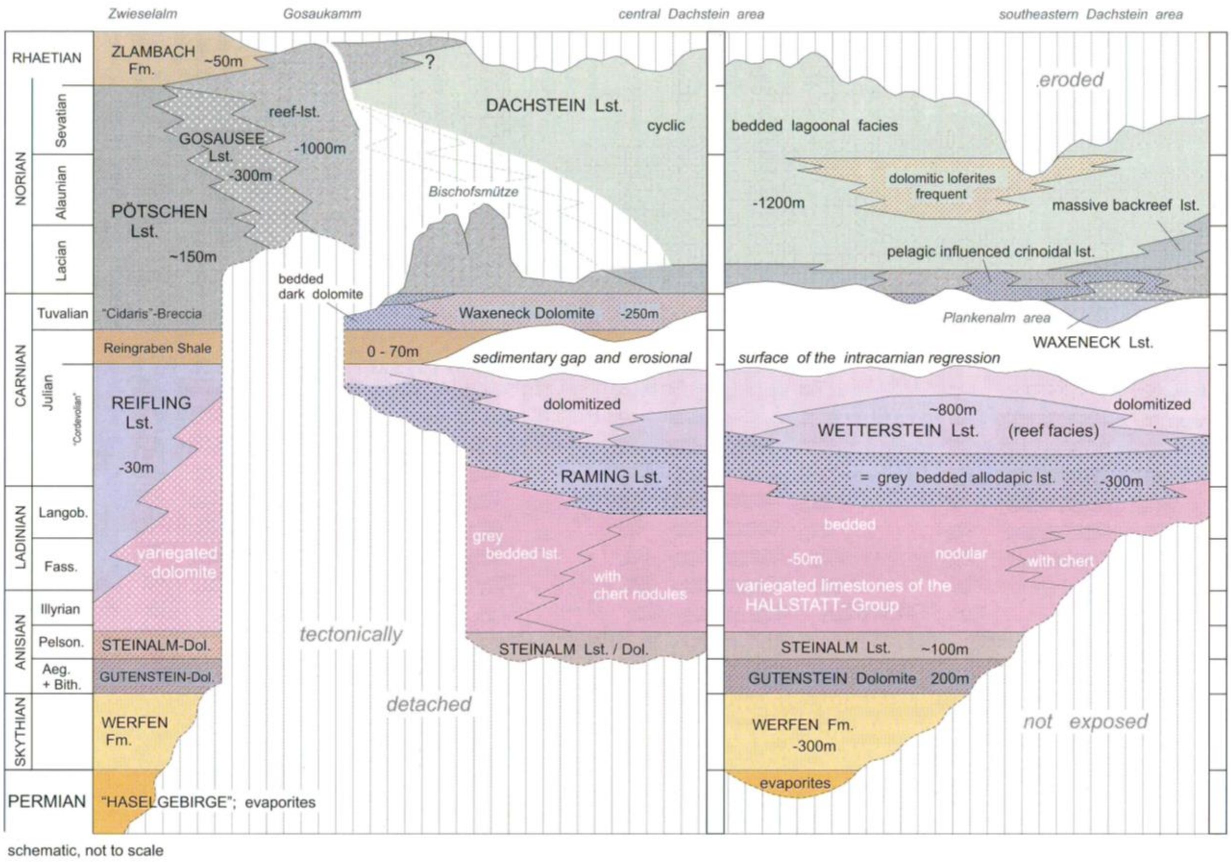

Fig. 2.10: Stratigraphy of the Triassic carbonate platforms within the Dachstein Nappe (Mandl, 2000).

Hallstatt Nappe:

The deep shelf environment, the Hallstatt Facies, was palaeogeographically situated south of the Dachstein Limestone Facies. The variegated limestones of Hallstatt, well known due to their richness in cephalopods, are developed in two different depositional realms: basinal areas and intrabasinal ridges with reduced sedimentation. Syndepositional block faulting and local uplift due to salt diapirism of the Permian evaporites are thought to be the reason for this differentiation (Mandl, 2000).

Reifling Formation:

The pelagic sedimentation of the Hallstatt Facies started with drowning of the Steinalm platform during the Pelsonian. The grey cherty Reifling Limestone represents the deep basin sedimentation, in contrast to red Hallstatt Limestones (e.g. Schreieralm Limestone) that cover shallow horst structures. Interlayers of marl and locally tuff are typical for the wavy bedded Reifling Limestones. For example a marl horizon of a few meters in thickness is frequent in the Late Anisian. The sedimentation of this lithology continues until the Ladinian to Lower Carnian (especially in the eastern NCA) but in the Hallstatt area the Anisian part dominates with thicknesses of up to 30m (Tollmann, 1985).

In general the deposition of grey cherty limestones, like the Reifling Limestone and the overlying Pötschen Limestone persists until the Norian.

Schreieralm Limestone:

Towards the ridges the grey cherty limestones change into well bedded red to violet micritic Schreieralm Limestones. As a consequence of the reduced sedimentation the existence of hardgrounds with ferromanganese crusts is typical. For the Schreieralm Limestone that was deposited from the Middle Anisian to the Early Ladinian thicknesses of maximum 10m to 15m are published (Tollmann, 1985). Deep cracks, filled up with red Schreieralm Limestone, indicate that the Hallstatt region was affected by brittle tectonics in the Late Anisian (Mandl, 2000).

Hallstatt Limestone:

The typically red Hallstatt Limestones represent a succession of several various lithologies, sedimented on the intrabasinal ridges. Deposition started in the Late Anisian and prevailed until the uppermost Norian. From the basin towards the (diapiric) ridges they change laterally either via variegated cherty limestones into bedded red limestones or via bedded grey limestones into light-coloured massive limestones (Mandl, 2000). During the Carnian Regression, carbonate production was interrupted by deposition of the Rheingraben Shale that split the Hallstatt Limestone in a lower and an upper succession. But the terrigenous sediments normally do not extend up to the top of diapiric high zones, so that the red bedded Hallstatt Limestones, which covered the tops of the narrow ridges, commonly were deposited undisturbed from the Anisian until the Norian (Mandl, 2000).

The red Hallstatt Limestones frequently show strong condensation and subsolution horizons with ferromanganese crusts. For example the thickness of the "upper red limestone" can be reduced from 25m to zero within a lateral distance of 200m (Krystyn, 1971). Most of classic ammonite sites of the Hallstatt Facies are located within the red limestone layers with reduced sedimentation.

Reingraben Formation:

The globally regression in the Middle Carnian led to the sedimentation of the clay rich Reingraben Shales. These bituminous shales are also known as "Halobien" shales and reach thicknesses of up to 5m in the Salzberg Facies (Mandl, 2000).

Zlambach Formation:

The Triassic carbonate succession was terminated by another major regression in the latest Norian and Rhaetian times. In this period Zlambach marls were deposited, as it was the case in the Dachstein Limestone Facies (**see chapter 2.2.2**, Dachstein Nappe).

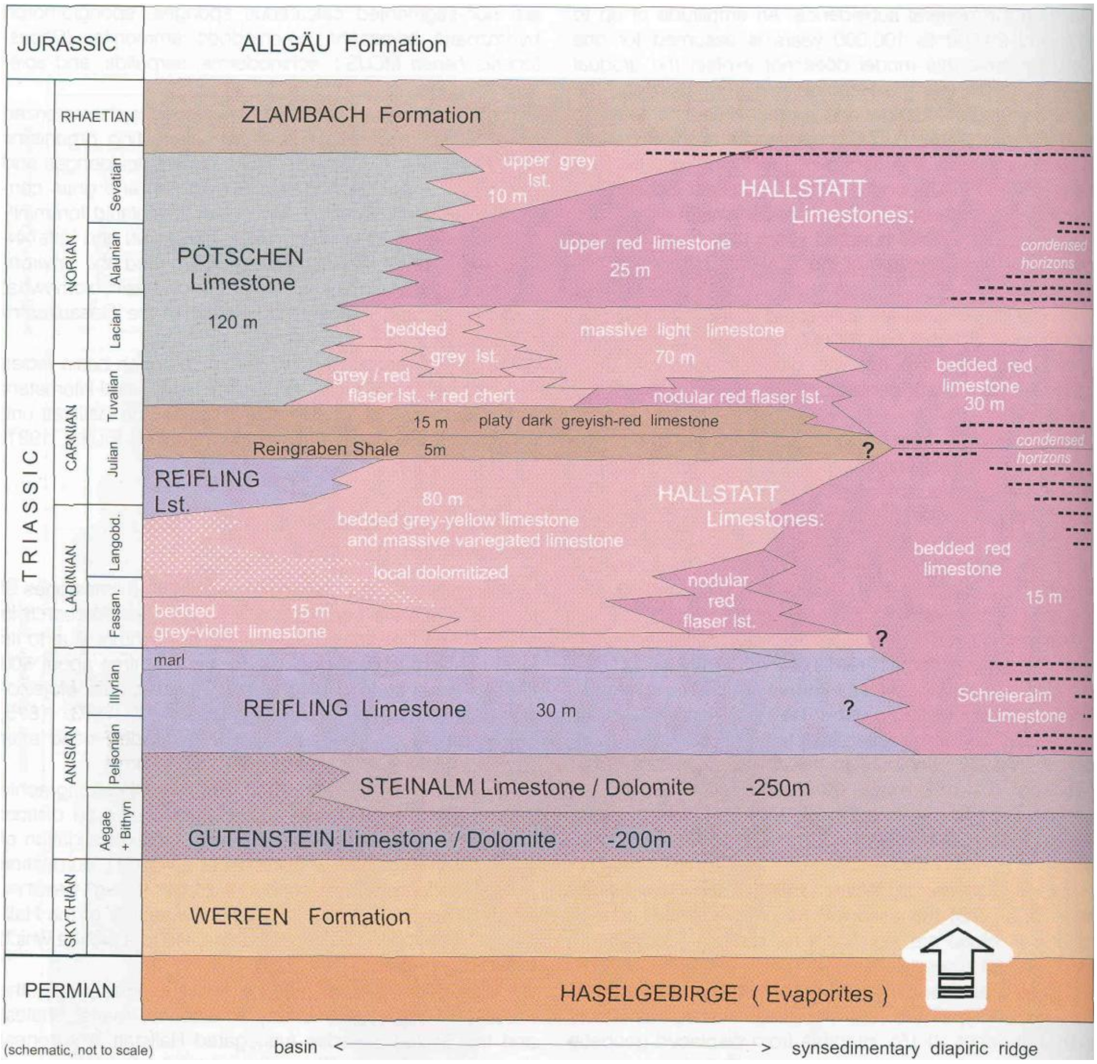

Fig. 2.11: Stratigraphy of the different Triassic sedimentation realms within the Hallstatt Nappe (Mandl, 2000).

2.3.3 Jurassic

At the beginning of the Jurassic the Austroalpine shelf, especially the southern NCA, within the realm of Juvavic Nappes, drowned completely. The basinal conditions prevailed until the Early Cretaceous with the exception of local shallow water carbonate platforms, like Plassen and Tressenstein Limestone. Both were deposited from the Late Jurassic to the Early Berriasian (lowest Cretaceous).

Drowning and synsedimentary faulting produced a complex seafloor topography with four main facies zones (Faupl, 1997):

- Cherty and limy-marly facies in the basins that reaches usually high thicknesses.
- Variegated nodular limestones are sedimented in a deep marine environment. Typical for these ammonoid bearing carbonates are very low sedimentation rates and consequently low thicknesses.
- Crinoidal and brachiopodal limestones deposited under shallower marine conditions, around the wave range.
- Development of reefs (restricted to the Malm).

Allgäu Formation:

The marls and cherts of the Allgäu Formation represent the basinal facies and were deposited in slumping basins of an anoxic environment. Due to the characteristic spotted appearance (owing to intense bioturbation), this lithology is also called "*Liasfleckenmergel*". The sedimentation started in the earliest Jurassic and persisted up to the Callovian (Upper Dogger). According to Faupl (1997) the chert content increases in the stratigraphic higher units. In the western NCA the Allgäu Formation can reach thicknesses of more than 1500m, in the central NCA thicknesses of up to several 100 metres are observed.

Adnet Limestone, Klaus Limestone, Agatha Limestone:

The Adnet Limestone was sedimented in a deep marine environment during the Lower Jurassic. It represents the facies of variegated ammonoid bearing limestones and achieves thicknesses of maximum several 10m. The Klaus Limestone was deposited above the Adnet Limestone in a similar milieu in Middle Jurassic times but obtains only some metres in thickness. Both, the Adnet Limestone and Klaus Limestone, comprise of red bioclastic wackestones, mainly consisting of nannoplankton. Their macrofauna contains abundant crinoids, brachiopods and ammonites (Böhm, 1992). Furthermore they both show low sedimentation rates that are documented by frequent ferromanganese crusts.

In the Malmian the red Agatha Limestone represents the deep marine ammonoidal limestone facies. It gains thicknesses of about 5m (Mandl, 2000).

Hirlatz Limestone:

The shallow marine facies with crinoidal and brachiopadal limestones is represented by the Hirlatz Limestone. It was deposited in the Liassic and is characterized by a thick-bedded to massive limestone of reddish or grey colour. Tollmann (1985) published a maximum thickness of roughly 100m.

Radiolarites, olistolithes and breccias (Grünanger Formation):

In Late Jurassic the seafloor deepened in whole NCA, especially in the Oxfordian the greatest water depth was reached. Radiolarite depositions in that period of time give evidence that even the calcite compensation depth was achieved. According to Tollmann (1985) and Mandl (2000) coevally breccias, olistolithes and large sliding blocks occurred as a consequence of Juvavic gravitational nappe movements during the initial stages of the Cimmerian Orogeny.

The Grünanger Formation represents a gravitational transported sediment in the Hallstatt area. This lithology consists of brecciated Dachstein Limestone with components that reach from several centimetres up to few metres in size. Usually the matrix of this breccia consists of red fine grained carbonatic material. As a consequence the Grünanger Breccia is often hardly distinguishable from original Dachstein Limestone that has undergone cataclastic deformation.

Large parts of the Hallstatt area are considered to be olistolithes, such as the northern slope of the Echerntal that may be constituted of a big sliding block of Dachstein Limestone (Mandl, 2000).

Plassen Limestone, Tressenstein Limestone:

The sedimentation of shallow marine reefs is represented by the Plassen and the Tressenstein Limestone. These locally developed shallow marine conditions are seen as a consequence of the Jurassic gravitational tectonics that formed a new seafloor topography. Especially above large Jurassic "sliding units" shallow water conditions led to the deposition of platform carbonates, whereas pelagic limestones filled the basins in between (Mandl, 2000).

The **Plassen Limestone** represents such a carbonate platform on an elevated zone. The typical white to light brown reef limestone can be distinguished into two different types (Tollmann, 1985):

- a thick bedded micritic type with poor fauna and
- a massive fossil rich sparitic type with onkoids and pseudooids, indicating more turbulent water in the external parts of the reef.

The type locality is situated at Mount Plassen on the northern border of the investigated area, where a respectable thickness of about 700m is published.

The **Tressenstein Limestone** a light brown, thick-bedded limestone was sedimented on the slopes of carbonate platforms. Consequently this lithology that bordered the open sea consists mainly of reef debris.

Oberalmer Limestone:

The Oberamler Limestone represents the pelagic sedimentation far from the reefs in the Upper Jurassic. This grey to light brown, well bedded micritic limestone is characterized by thin clay laminae on the bedding planes. Owing to the great water depth the fauna is dominated by aptychi but also some ammonites are found (Tollmann, 1985). The Oberalmer Limestone reaches a total thickness of about 800m.

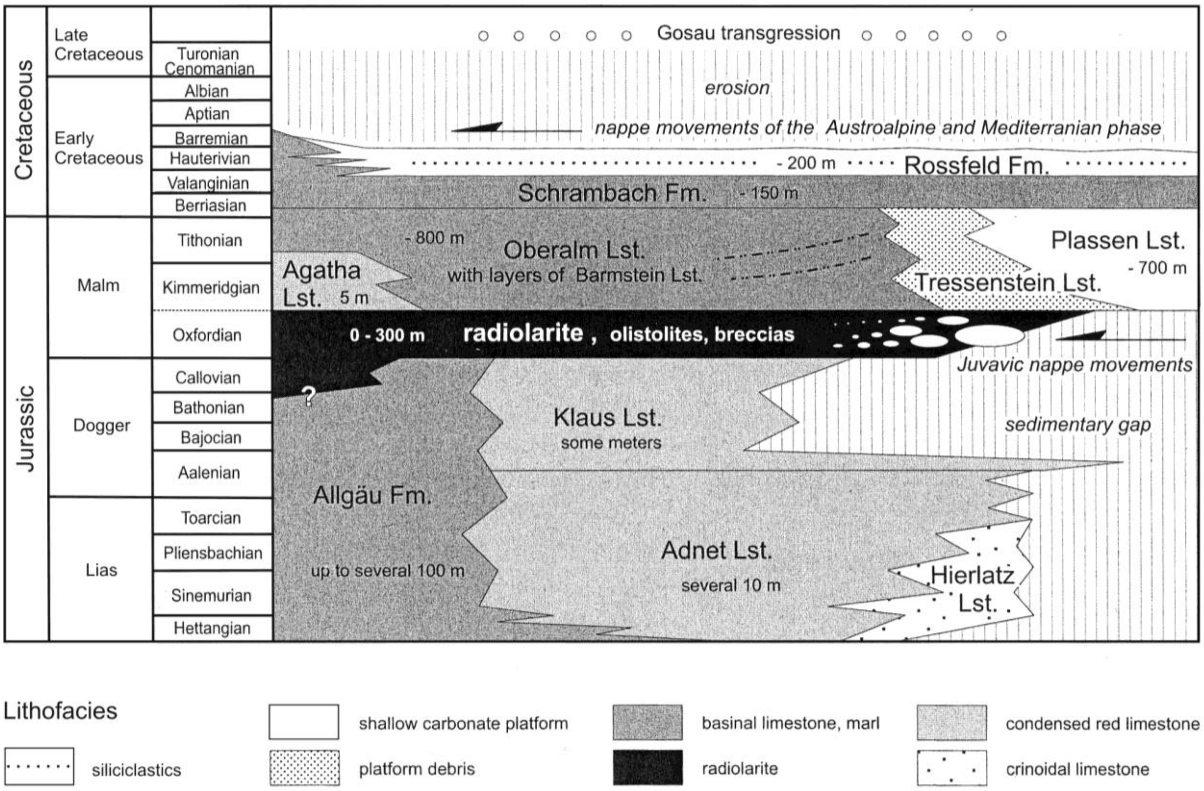

Fig. 2.12: Stratigraphy of Jurassic and Cretaceous within the central NCA (Mandl, 2000; modified after Böhm, 1992)

2.3.4 Cretaceous

As shown by microfossils, the facies of Late Jurassic carbonates persists up to the Early Cretaceous. Deepening and an increasing terrigenous input caused a gradual transition into the marly aptychus limestones of the Schrammbach Formation (Mandl, 2000).

Schrammbach Formation:

The grey well-bedded cherty limestones and marls of the Schrammbach Formation were sedimented in a pelagic environment and succeeded the Jurassic Oberalmer Limestone. The increasing content of marls towards the top, where even sandy intercalations occur, is characteristic for this lithology. Fossils like aptychi and ammonites indicate an Early Cretaceous age from Berriasian up to Barremian of the Schrammbach Formation that reaches a thickness of about 150m (Tollmann, 1985).

Rossfeld Formation:

Due to the beginning of the Eoalpine Orogeny in the Late Valangian (Early Cretaceous), deep water carbonates were ceased by the syntectonic clastic facies of the Rossfeld Formation (Faupl and Wagreich, 2000). Deposition began with grey marls, succeeded by turbiditic calcareous sandstones and coarse submarine breccias at the base of huge sliding masses. The progression of orogenic activity caused the beginning of nappe movement in the NCA accompanied by the migration of the sedimentation axis of the Rossfeld Formation from south towards the north, into structurally higher units (Mandl, 2000).

Gosau Group:

Due to the Eoalpine Orogeny, large areas of the NCA were uplifted and exposed to erosion. After a significant gap in the stratigraphy a following period of subsidence affected the NCA in Late Cretaceous times, which caused limno-fluviatil and marine sedimentation. The Gosau Group represents the sediments that cover the Austroalpine realm after the Middle Cretaceous orogenic peak. As a result of the abovementioned break of sedimentation and the Eoalpine nappe movement the base of the Gosau Group is marked by a major unconformity.

The Gosau sediments can be differentiated in a Lower Gosau Complex and an Upper Gosau Complex (Faupl et al., 1987):

The Lower Gosau Complex started during the Coniacian with basal alluvial conglomerates and coarse clastics of the **Kreuzgraben Formation**, which are exposed in an outcrop on the top of the Solinger Kogel within the investigated field area. The following fan-deltas represent a transitional facies to a shallow marine environment with marls, sandstones and lagoonal limestones (e.g. **Streiteck Formation**, **Hochmoos Formation**). In Early Santonian times the sedimentation of grey neritic marls (**Bibereck Formation**) indicate a peak of marine transgression within the Lower Gosau Complex.

The succession of the Upper Gosau Group starts in the Middle Campanian, after tectonic activities that changed the facies conditions and caused unconformities. The Upper Gosau Group is dominated by flysch sediments (“Flyschgosau”) that show turbiditic character (e.g. **Ressen Formation**). This upper complex is also characterized by a new spectrum of clastic material, which is dominated by metamorphic fragments. Deep marine fan sequences with red coloured marls and marly limestones (e.g. **Nierental Formation**) and a marl dominated slope facies (e.g. **Zwieselalm Formation**) can be distinguished.

3. Structural geology

3.1 Introduction

As mentioned in chapters 1 and 2 the main tectonic transport and the relation between the Dachstein and the Hallstatt Nappe, has been subject of vehement scientific discussions. As a consequence several questions in the Hallstatt area are not clearly answered until now. This diploma thesis addresses following topics:

- Direction of main shortening in the interesting area
- Possible valid structures in fold and thrust belts in respect to the geological environment
- Influence of the ductile evaporitic detachment (Haselgebirge) on the structural deformation style in the overlying brittle reacting carbonates
- The kind of contact between Hallstatt and Dachstein Nappe
- Limit the time of orogeny peak and consequently roughly determine the age of folding and thrusting
- Effect of the Alpine orogeny on the structure of the Haselgebirge – analyse the tectonically generated structures (**see chapter 4 and 5**)
- Deformation mechanisms that accommodated shortening (**see chapter 5**)

These topics have been tackled by following methods:

- Detailed structural investigations in the field
- Digitizing photographs to point out the structural geometries in the Echerntal
- Drawing a schematic profile through the Echernwand
- Microscopic analysis of several thin sections

One of the aims of this diploma thesis was to construct a balanced cross section but due to lacking of marker horizons and significantly changes in lithologies in the Echernwand this was not possible or at least it went beyond the scope of this diploma work.

Nevertheless balancing cross sections is a very important tool to relate the structures observed in the field to the different existing geological environments. Therefore a short compilation of balancing cross sections and the three main types of thrust geometries are given in this chapter.

3.2 Basics about cross section balancing

Due to cross-section balancing it became clear that only few different thrust geometries can evolve in fold and thrust belts and furthermore that those variable geometries depend on the geological environment (e.g. viscosity and thickness of detachment horizons and the overlying strata). Dahlstrom (1969) was among the first who claimed that just a limited suite of thrust geometries can be generated in a specific geological environment.

Generally available geological data from fieldwork or existing maps are insufficient to constrain the entire geometry of fold and thrust belts and to understand their structural complexity. On that account cross-section balancing was introduced by petroleum geologists in the 1960´s (e.g. Carey, 1962; Dahlstrom, 1969), in order to advance their interpretations and to test the validity of structural geometries. “Balanced geological cross-sections are an important aid to understanding thrust-belt structures and to estimating their hydrocarbon-bearing potential” (De Paor, 1988).

The technique is based on the concept that a balanced cross-section must not gain nor lose volume during the deformation process. Therefore the essential rule of the technique is that bed thickness and bed length throughout a section are consistent. Deformed-state cross-sections represent the geometry of structures as they appear in the field (after deformation). Restoration of deformed state cross-sections into their predeformational state is primarily reached by removing the displacement along the thrust faults and by straightening the fault related folds. Without creating overlaps or voids the faulted and folded beds should be reconstructed to their initial subhorizontal stratigraphic succession.

A deformed-state cross-section is called a **balanced cross-section**, if it is “admissible” and “viable” (Marshak and Woodward, 1988). **Admissible** means that the cross-section reflects the geometries observed on rock walls, mountainsides or road cuts in the field. In addition it depends on whether the geometries of these structures are likely to occur in the specific geological environment or not. **Viable** deformed state cross-sections can be restored to their original stratigraphic succession with constant volume (bed area) and without creating overlaps or voids (Marshak and Woodward, 1988). If thrust faults are not acceptable, for example if they cut down-section, they are called “out of sequence thrusts”.

Moreover viable cross-sections have to be constructed parallel to the direction of tectonic transport; otherwise material would be transported out of the section and the bed area can not stay constant. For example Marshak and Woodward (1988) point out that the section plane of a cross-section has to be within 5° of the thrust direction to enable a balanced result.

To gain plausible results the direction should always be:

- **parallel** to slip lineations on fault surfaces
- **perpendicular** to fold axes, the strike of bedding and the strike of thrust faults

For constructing an admissible and viable cross-section another fact about fold and thrust belts is crucial: The thrust faults do not develop at the same time! Analogue experiments (e.g. Huiqui et al., 1992) showed that usually the more internal faults are older than the faults generated towards the foreland. As a consequence structurally lower faults are younger than their overlying ones. The older faults can be folded and rotated into steeper position because of the movement of the basal younger faults. Such a sequence of faulting is called break-forward sequence or piggy-back sequence (because the older parts ride on the younger ones at the base; Marshak and Woodward, 1988). Due to the dominance of break-forward sequences, is has become a standard practice to restore fault displacements from the foreland towards the hinterland but sometimes break-back sequences in the contrary direction appear as well (Mc. Clay, 1992).

In order to describe the relative movement and shortening in fold and thrust belts and to define the area that is balanced, a reference frame is needed. Material that is included in the balancing procedure must not enter nor leave this reference frame, to satisfy the conservation of volume.

Two principal methods of cross-section balancing evolved:

- **Equal line length method**
- **Equal area method**

Equal-line-length method

This method requires that thickness and length of the involved beds are conserved during deformation. In order to conserve thickness and bed length, folds are only allowed to evolve by flexural slip and without penetrative strain, creating parallel fold geometries in competent layers. A cross-section is bed length balanced if all bed lengths and thrusts are constructed correctly, such that footwall and hanging wall cut-offs in the deformed section match up in the restored section (**see Fig. 3.1**).

As a result every ramp and every flat on the base of the hanging wall has its counterpart on top of the foot wall (e.g. Wilkerson and Dicken, 2001). This is a very useful finding because the shape of the base of the hanging wall – that can be recorded in the field – must have its counterpart along the top of the footwall – somewhere at depth. On the other hand if footwall geometries are measured in outcrops, their counterpart in the hanging wall can be constructed although these units have been eroded (Marshak and Woodward, 1988).

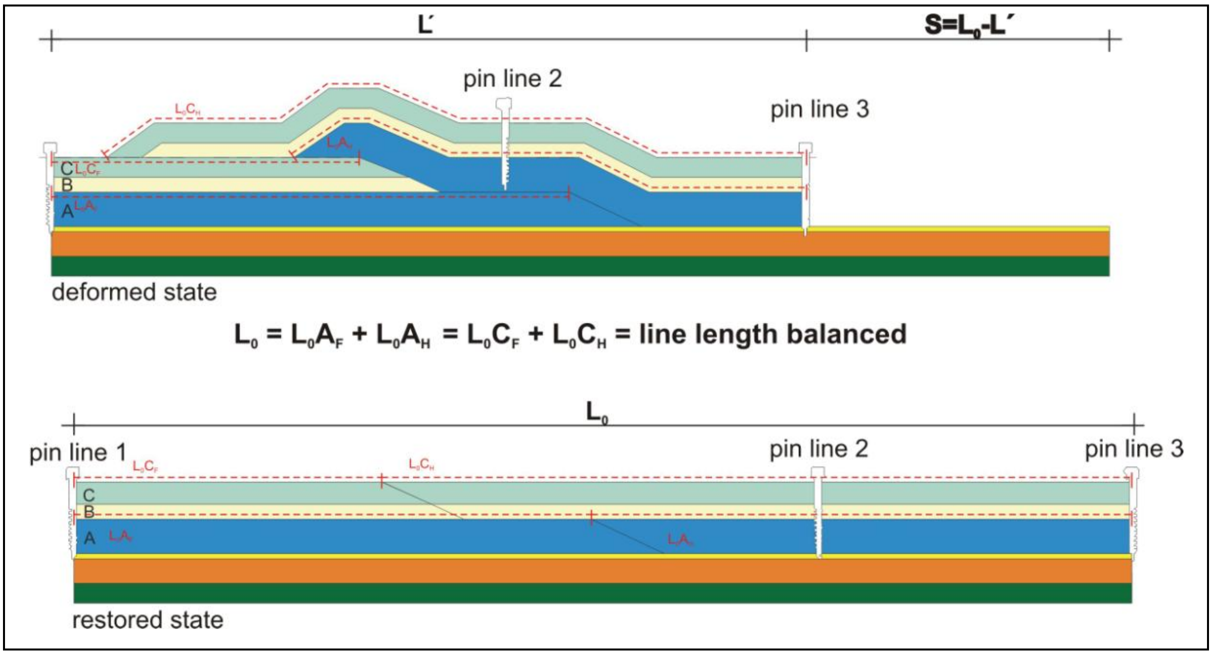

Fig. 3.1: Line-length balanced cross-section in a proper style (slightly modified after Grasemann et al., 2003). The stratigraphic beds of the deformed cross-section are exact as long as the beds of the restored section. Each flat and ramp in the hanging wall has its counterpart in the footwall.
The initial bed length (L_0) of the undeformed section has to equal the bed length in the deformed state cross-section. Furthermore the shortening (s) is defined by subtracting the length of the deformed section (L´) from its initial length (L_0).

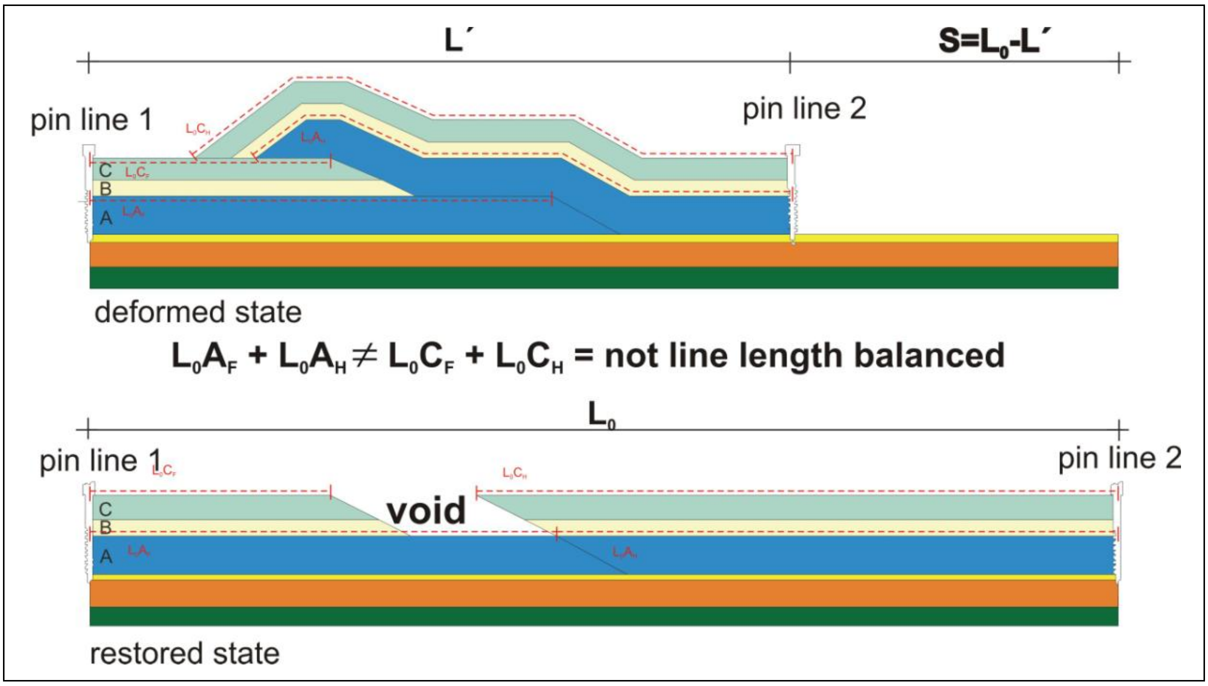

Fig. 3.2: Example of a cross-section that does not balance (slightly modified after Grasemann et al., 2003). In the deformed cross-section the flat in the footwall that was generated on top of horizon A has no counterpart in the hanging wall. Consequently a void in the restored state section developed between the foot wall and hanging wall elements of the beds B and C. Both beds are constructed to short in the hanging wall ($L_0C_F + L_0C_H. < L_0A_F + L_0A_H$). According to the above mentioned rules cross sections that do not balance will create voids or overlaps in the restored section if bed lengths are inconsistent.

Equal-area method

Mitra and Namson (1989) classified equal area balancing into two main categories, the **area restoration** and **excess area measurement**.

Cross sections that show significant thickness changes of beds have to be balanced by a**rea restoration.** Because area balancing alone does not always successfully constrain the exact shortening and thrust geometries Mitra and Namson (1989) suggest a combination of equal-area restoration and line-length restoration. That means a comparison of area balanced bed length with undeformed lengths of units that can be restored by the line-length method (e.g. key beds that have not undergone significant thickness changes). Since all units should provide the same undeformed length in the restored section the comparison will show if the equal-area section has been balanced accurately or not.

Mitra and Namson (1989) presented a method to determine the restored average bed length (l_a) by the relation of the area involved in deformation (A_x) and the original thickness of the unit (t) that can be verified in the undeformed foreland.

$$\mathbf{l_a} = \frac{\mathbf{A_x}}{\mathbf{t}}$$

The **excess area measurement** developed in order to determine the depth of the detachment or – if detachment depth is known – to calculate the regional shortening. “Excess area” means that area that has been deformed and uplifted higher than the regional elevation due to shortening. To refer to the constant volume model, this area has to be identical to the shortening area, which is determined by the depth to detachment and the amount of shortening **(see Fig. 3.3)**.

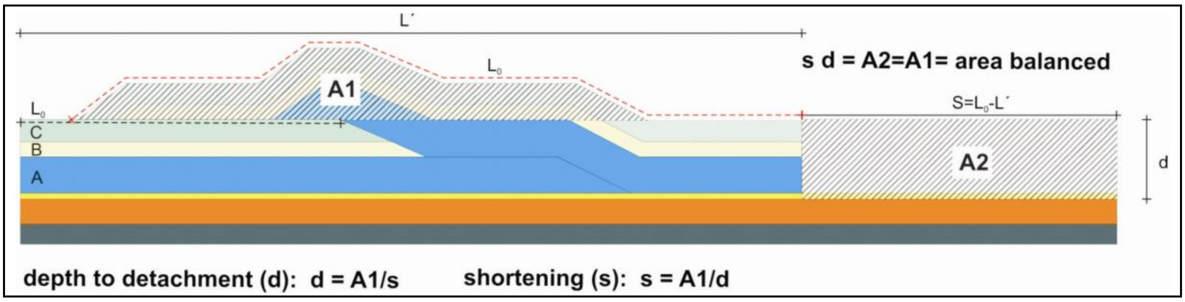

Fig.: 3.3: Area balanced cross-section (after Grasemann et al., 2003). The excess area (A1) above the regional elevation equals the area (A2) that was lost due to shortening. As a consequence the depth of the basal detachment can be determined if the excess area and the amount of shortening are known. Otherwise the shortening can be calculated if the excess area and the depth to the detachment (e.g. by drilling) are investigated.

3.3 Typical deformation structures in fold and thrust belts

In fold and thrust belts, folds are usually related to underlying thrusts (fault related folds). Due to seismic profiles all over the world in different fold and thrust belts that are influenced by thin skinned tectonics three main types of fold geometries established:

fault bend folds, **fault propagation folds** and **detachment folds**

3.3.1 Fault bend folds

This type of folds generates by movement of the hanging wall beds above a non planar fault. Fault bend folds, which often display more or less symmetric structures, show typical flat-ramp-flat geometries. Lower bedding parallel detachments step up into a higher detachment horizon in the direction of slip. Flats are those parts in the footwall or hanging wall that are parallel to the fault whereas ramps are parts of foot- or hanging wall that are cut through by the fault. Consequently beds of the footwall flat are parallel to the above lying fault, whereas beds of the footwall ramp and hanging wall ramp are lying discordant to the fault. In the hanging wall flat the sedimentary sequences appear parallel to the underlying fault. A stepwise development of a fault bend fold and the classification of the different parts (footwall and hanging wall ramps and flats) can be seen in **Fig 3.4**.

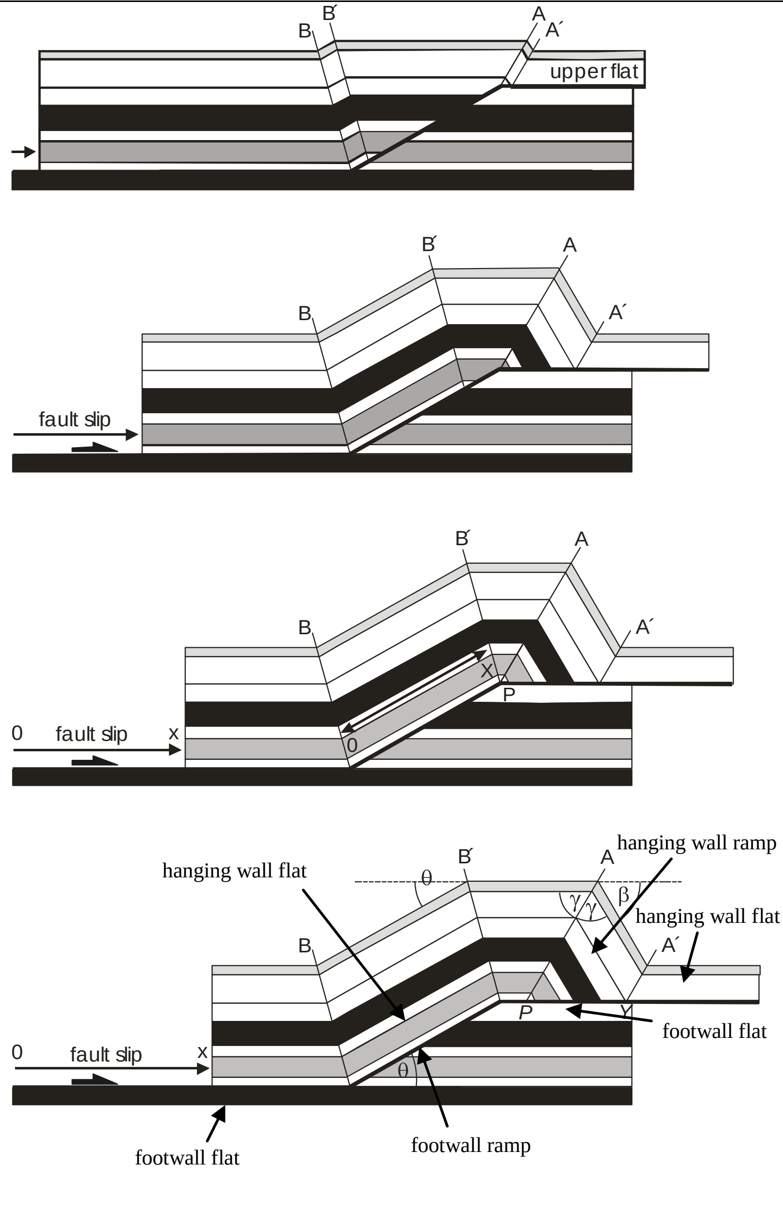

During the movement of the hanging wall over the ramp four axial planes are generated: A, A´, B and B´

As slip proceeds the beds migrate through the axial surfaces A and B that are fixed with respect to the footwall.

Axial surfaces A´ and B´ are fixed in the hanging wall and move with ongoing displacement along the thrust. B´ propagates exactly by the amount of displacement (0 → x) until the upper flat is reached.

Up to that moment axial surface A is fixed at the same inflexion point and the hanging wall beds migrate and rotate through it. During this bedding plane slip occurs and causes a steeper forelimb (hanging wall ramp) than the backlimb (hanging wall flat).

When B´ reaches the inflexion point to the upper flat it stops and gets fixed with respect to the footwall. But now A leaves its fixed position and moves along the upper flat with the hanging wall (Grasemann et al., 2003, after Suppe, 1983b)

Fig. 3.4: Stepwise development of a fault bend fold that reflects a simple step in detachment horizon (modified after Suppe, 1983b)

3.3.2 Fault propagation folds

Typical for this type of fault related folds is that during the development of the fold the underlying fault propagates into stratigraphic higher beds. Shortening in the beds lying stratigraphically above the fault tip (T) is admitted by pure folding. On the contrary beds lying stratigraphically below the fault tip accommodate shortening only by slip along the fault thrust. The displacement along this fault declines continuously to zero at the fault tip.

First a bedding parallel thrust cuts through the overlying units and forms a ramp. 4 axial surfaces evolve: **A, A´, B** and **B´.**

During expanding fault slip the beds are forced to migrate and rotate through A´ and B when they move from their horizontal position into the limbs of the growing fold (see red points 1 and 4).

A´ coincides through the whole deformation with the fault tip (T) and proceeds with it into higher stratigraphic units.

B terminates the backlimb and stays always fixed.

A and B´ coincide at the hinge of the fold, exactly at the same stratigraphic level as the fault tip is located. Together they migrate into higher units. While A stays in a fixed position in respect to the beds (see red point 3), the beds have to migrate through B´ during proceeding deformation (see red point 2) (Grasemann et al., 2003).

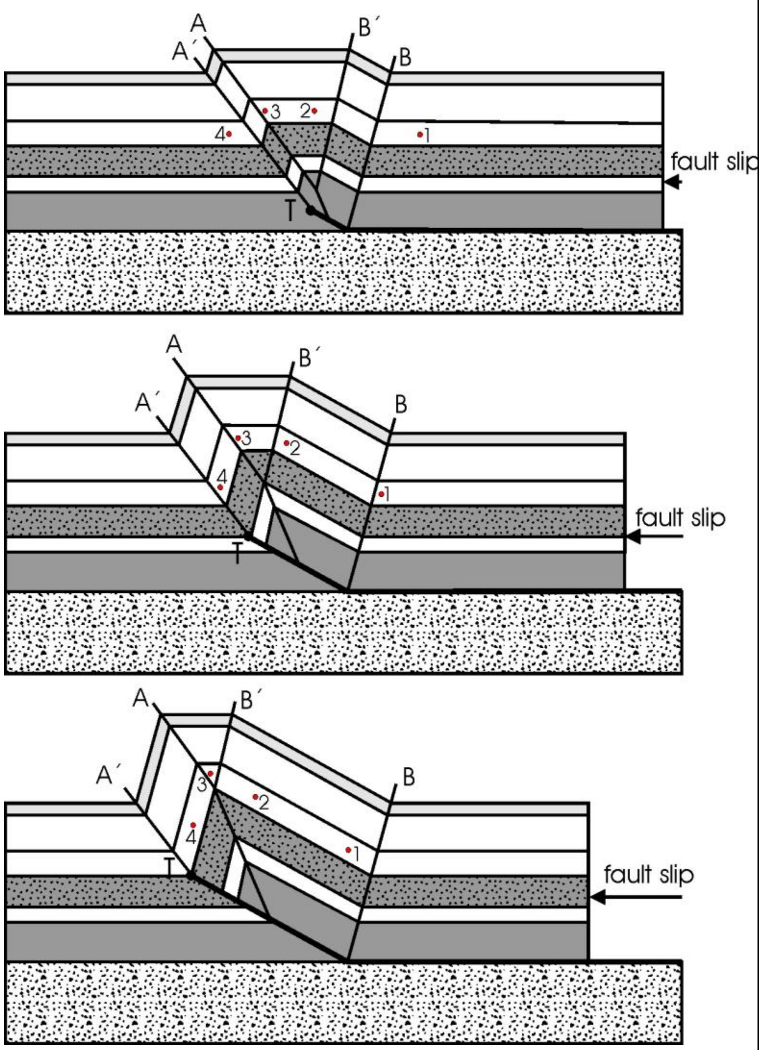

Fig.: 3.5: Stepwise development of a fault propagation fold (Grasemann et al., 2003, modified after Suppe, 1985)

3.3.3 Detachment folds

Detachment folds are fault related folds in relatively competent rock beds that accumulate incompetent rock units, usually consisting of evaporites or clay, in their core. In difference to simple “buckle folds” detachment folds are decoupled from the underlying and again more competent layers by a basal detachment.

Detachment folding occurs if shortening above a layer parallel blind thrust is accommodated by folding in the hanging wall (Jamison, 1987). Consequently the basal detachment does not cut upsection and neither in the hanging wall nor in the footwall cut offs are observed.

To constrain possible geometries and kinematic paths Homza and Wallace (1995) developed two geometric models of ideal detachment folds, one with fixed and the other with variable detachment depth. Detachment folds with constant depth of the detachment allow only few different geometric structures whereas the variable depth model shows a wide range of detachment fold geometries and kinematics (Poblet and Mc. Clay, 1996).

Moreover three different kinematic models for development of detachment folds involving a competent layer with constant bed length and thickness decoupled over a ductile unit are published by Poblet and Mc. Clay (1996). As shown in **Fig. 3.6** various different types of evolution of detachment folds are possible to gain the same final structure:

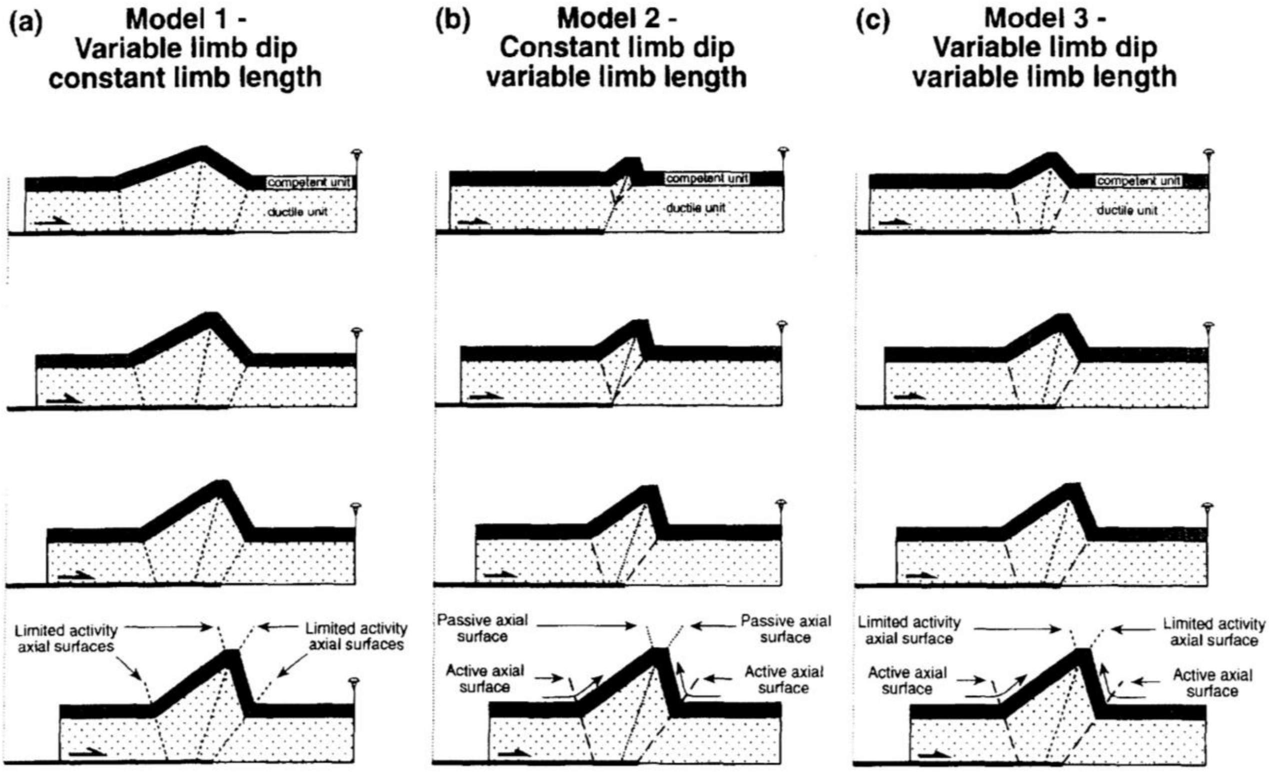

Fig. 3.6: Stepwise evolution of three different kinematic models for detachment folds where a homogeneous competent layer is detached over a ductile rock unit. Both the competent and the ductile units are area balanced in all models, but in the models 1 and 2 the ductile unit is only area balanced during shortening if a variable depth to detachment is assumed (Poblet and Mc. Clay 1996).

Model 1 (a) shows the development of the fold with fixed limb length but variable limb dip during shortening.

Model 2 (b) in contrary forms self similar folds with fixed limb dips and variable limb length during deformation

In Model 3 (c) variable limb dip and limb length are simulated.

Models one and two have the problem that the volume of incompetent material in the core of the fold can not increase linearly to the amount of shortening and consequently the depth to detachment has to change during deformation to enable these models. In model 3 variable limb dip and limb length enable an area balanced development of the detachment fold even if the depth to detachment stays constant (Homza and Wallace, 1995).

The constant depth to detachment model

The uplifted area in the core of a detachment fold with constant depth to detachment has to increase linearly to progressing shortening. Hence at least one fold limb must enlarge and hinge migration is forced in the competent layer. Due to the limited geometric structures of ideal detachment folds with constant depth to detachment both the depth to detachment and the amount of shortening can be determined by the observed geometry of the detachment fold.

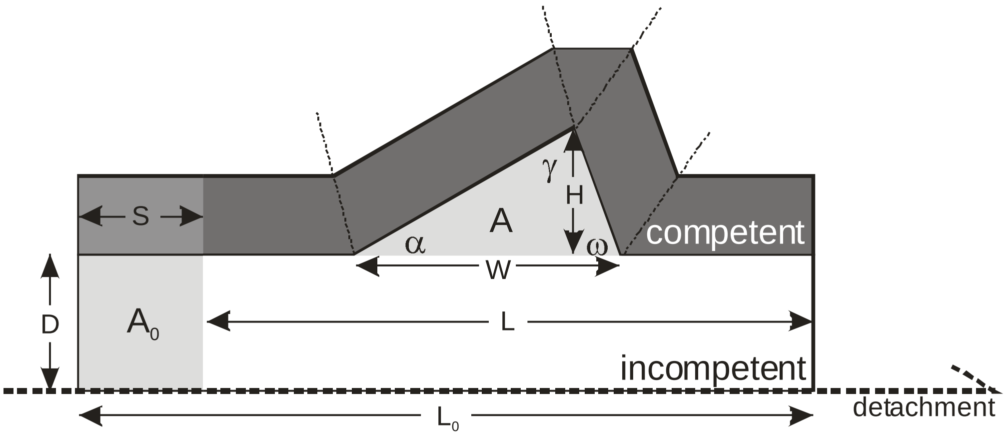

Fig.: 3.7: Schematic geometry of an ideal detachment fold with constant depth to detachment during deformation. Showing the main geometric relationships (Grasemann et al., 2003, modified after Homza and Wallace, 1995)

As seen in **Fig. 3.7** the shape of a detachment fault is determined by the triangle that defines the core with the incompetent material. For this triangle the essential geometric relationships are:

- W the base length of the fold
- H the height of the incorporated incompetent material
- α backlimb dip
- ω forelimb dip
- γ interlimb angle

The basic kinematical assumptions of detachment folds are that the competent units form parallel folds by flexural slip with a constant bed length during deformation and that the cross-sectional area is conserved during shortening. The incompetent unit in the core is forced to deform internally. Therefore an ideal detachment fold can be balanced by the following relationships:

competent layer: $S = L_0 - L$ = line balanced (see Fig. 3.7)

incompetent layer: $A_0 = SD = A = WH/2$ = area balanced (see Fig. 3.7)

These geometric relationships reference to the chevron fold type of detachment folds but can easily be upgraded for box fold structures with two hinges and a flat roof area in between (**see Fig. 3.8**).

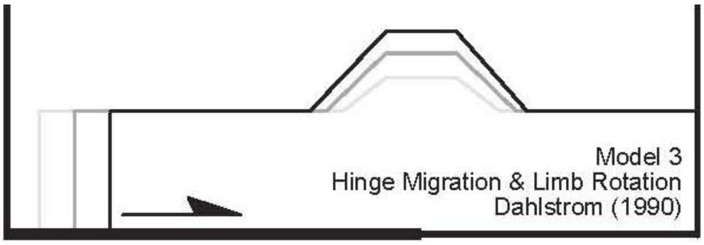

Fig. 3.8: Sample of a detachment fold with a flat roof area, developed with hinge migration and limb rotation (Wilkerson et al. 2004, after Dahlstrom 1990)

For the constant depth to detachment model following possibilities of kinematic evolution during ongoing shortening are given:

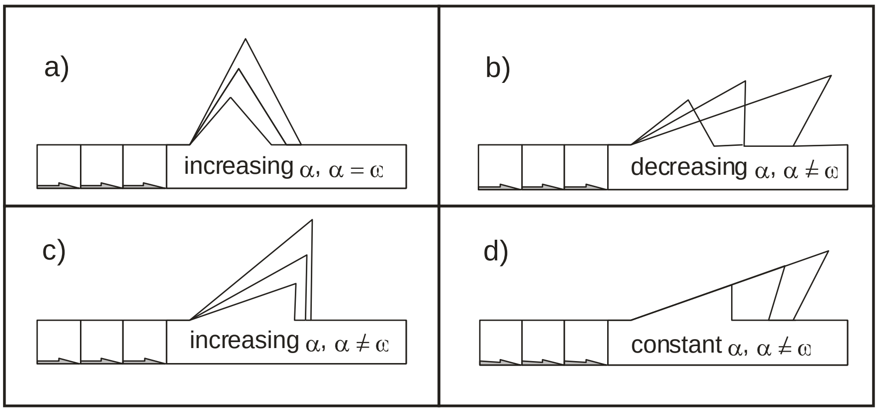

Fig. 3.9: Development of detachment folds with ongoing shortening (Grasemann et al., 2003, modified after Homza and Wallace 1995)

a) forelimb ω and backlimb α increase at same value – consequently a symmetrically fold arises

b) forelimb ω increases while backlimb α decreases

c) forelimb ω stays constant while backlimb α increases

d) forelimb ω increases and backlimb α stays constant

Variable detachment depth model

In this model the fold geometry defines the fold area but is independent from the detachment depth, therefore a wider range of structural geometries and kinematic deformation paths are possible. If the fold geometry is known either the original detachment depth or the final depth of detachment can be determined by the other (Homza and Wallace, 1995).

Two different cases of changing depth to detachment can occur:

1) final detachment depth is greater than original detachment depth
2) final detachment depth is lower than original detachment depth

If the final detachment depth is greater than the original one, the fold area (core of incompetent material) is smaller than the displaced area. In that case self similar folds with fixed limb dips and increasing limb length can evolve (**see Fig. 3.6**) Such layer parallel thickening beneath folds is well known from physical modeling of folds (e.g. Dixon and Tirrul, 1991) and from observations in natural detachment folds.

In the 2nd case vertical transport of material of the incompetent unit into the arising fold may cause thinning of the incompetent layer and generate a lower final depth to detachment than the original one. This phenomenon that enables “buckle folds” with constant limb length during proceeding deformation has also been recognized as well in physical models (e.g. Dixon and Tirrul, 1991) as in investigated natural folds.

To sum up detachment folds with a fixed depth to detachment exclude constant limb length model and self similar growth model with constant limb dip. Both require non-linear changes of the uplifted area and the shortening area. For these kinematic paths the variable depth to detachment model is needed. Although this model is more complex it might be a better approximation for natural detachment folds because variable detachment depth has been observed in natural detachment folds and furthermore fixed hinge growth of “buckle folds” is evidenced by natural observations and theoretical modelling (Homza and Wallace, 1995).

Moreover in literature various different models of geometric and kinematic evolution of detachment folds exist, e.g. thickening and thinning of the fore limb during shortening is simulated. Thinning of the fore limb leads to smaller inter limb angels (γ) and thickening to larger inter limb angels of detachment folds.

3.4 Structural geological data and interpretation

Detailed field analyses were done to gain knowledge about the kinematics and geometry of the Hallstatt Nappe and surrounding Dachstein Nappe in the particular area. The main focus of the structural field measurements was set on the northern slope of the Echerntal. The Echerntal is characterized by the steep, more than 1000m high rock face of the “Hirlatzwand” on the southern slope (for detailed information see Habermüller, 2005) and the about 300m high rock face of the “*Echernwand*” in the northern part. Therefore the field work concentrated mainly on the base of the Echernwand. Only in the western part of the Echernwand a small path, the so-called “*Gangsteig*”, leads through the rock face and facilitated structural measurements in higher units. More information about the geometry of the eastern upper part of the Echernwand was gained by digitizing photographs of the rock face. Significant outcrops are also located near the top of Hohe Sieg along an existing forest road.

To illustrate the fold and thrust geometries the main structures observed in the northern slope of the Echerntal were marked in photographs of the rock face and a schematic cross section has been drawn. Honouring the field measurements, it strikes ESE-WNW. As shown in **Fig. 3.10** the dip data at the base of the rock face in the eastern part of the Echernwand fluctuate, especially in areas with low dip angels. Therefore the measurements in the Gangsteig and the data from the outcrops near Hohe Sieg, which reflect the most significant structures in the investigated area, were used to constitute the direction of the main tectonic transport.

Furthermore to gain a 3 dimensional overview of the area a 3D model with GoCAD^{TM}, a geological object modeling software, was created. Therefore the interesting sector of the geological map of Austria 1: 50 000, Blatt 96, Bad Ischl (Schäffer, 1982) was draped over the digital elevation model (DEM) of the Echerntal and adjacent areas (**see Fig. 3.11**). This 3D-model helped to realize coherences between the relief and different lithologies more easily. Especially the kind of contact between the sediments of the Dachstein Nappe and the Hallstatt Nappe should be illustrated.

This 3D-model was also linked to the 3D-model of the Hallstatt saltmine, described in **chapter 4**, and facilitated to compare the subsurface geometry of the saltbody with the investigated surface structures.

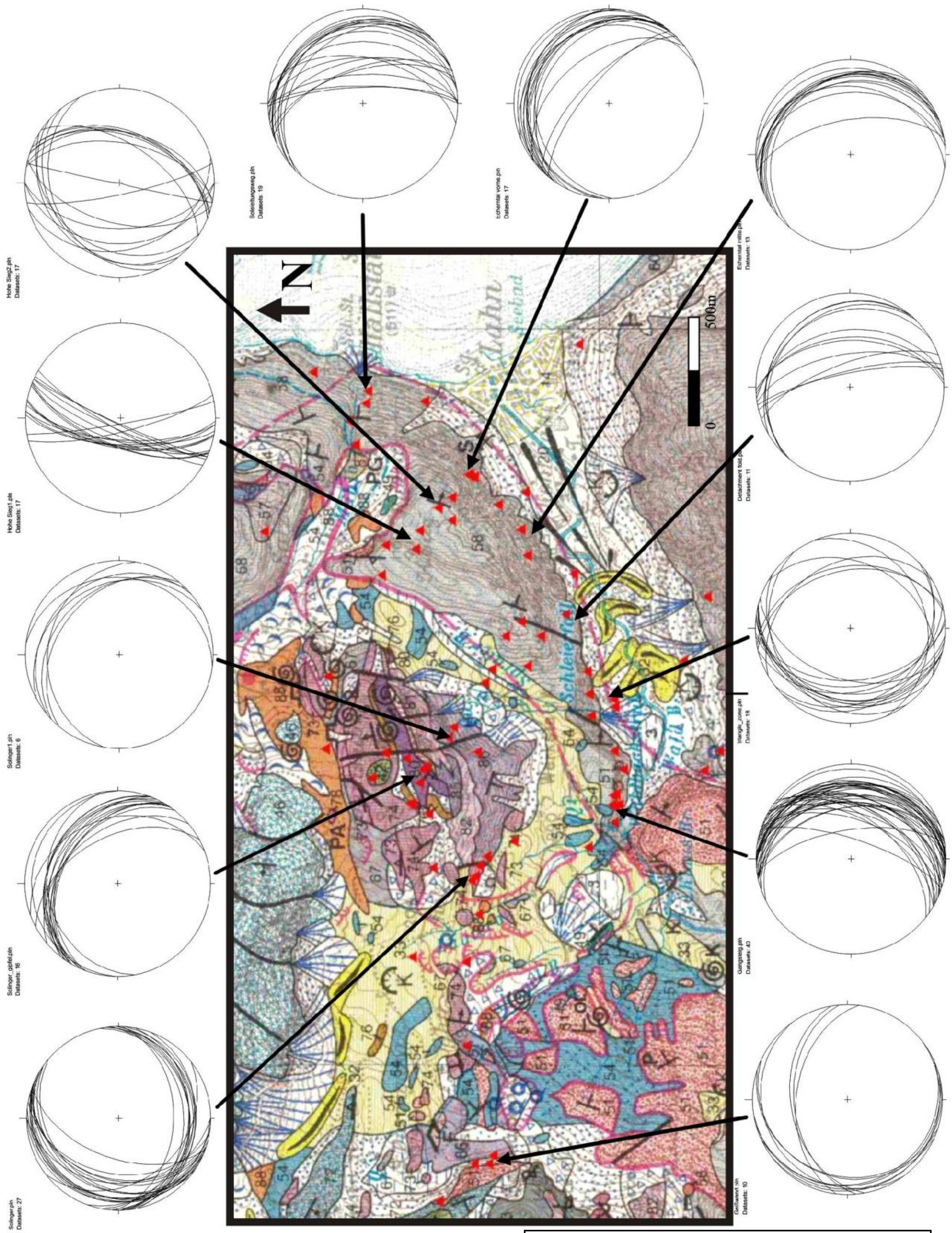

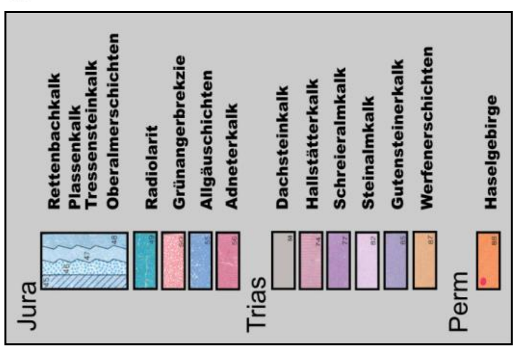

Fig.:3.10: Geological map of the Echerntal and adjacent areas (Schäffer, 1982). The relevant outcrops (red triangles) are marked. Bedding and thrustplanes are summarized in significant regions and shown in the surrounding plots. Yellow and white marked lithologies belong to Quaternary and recent times. The legend of the other relevant lithologies can be seen upwards.

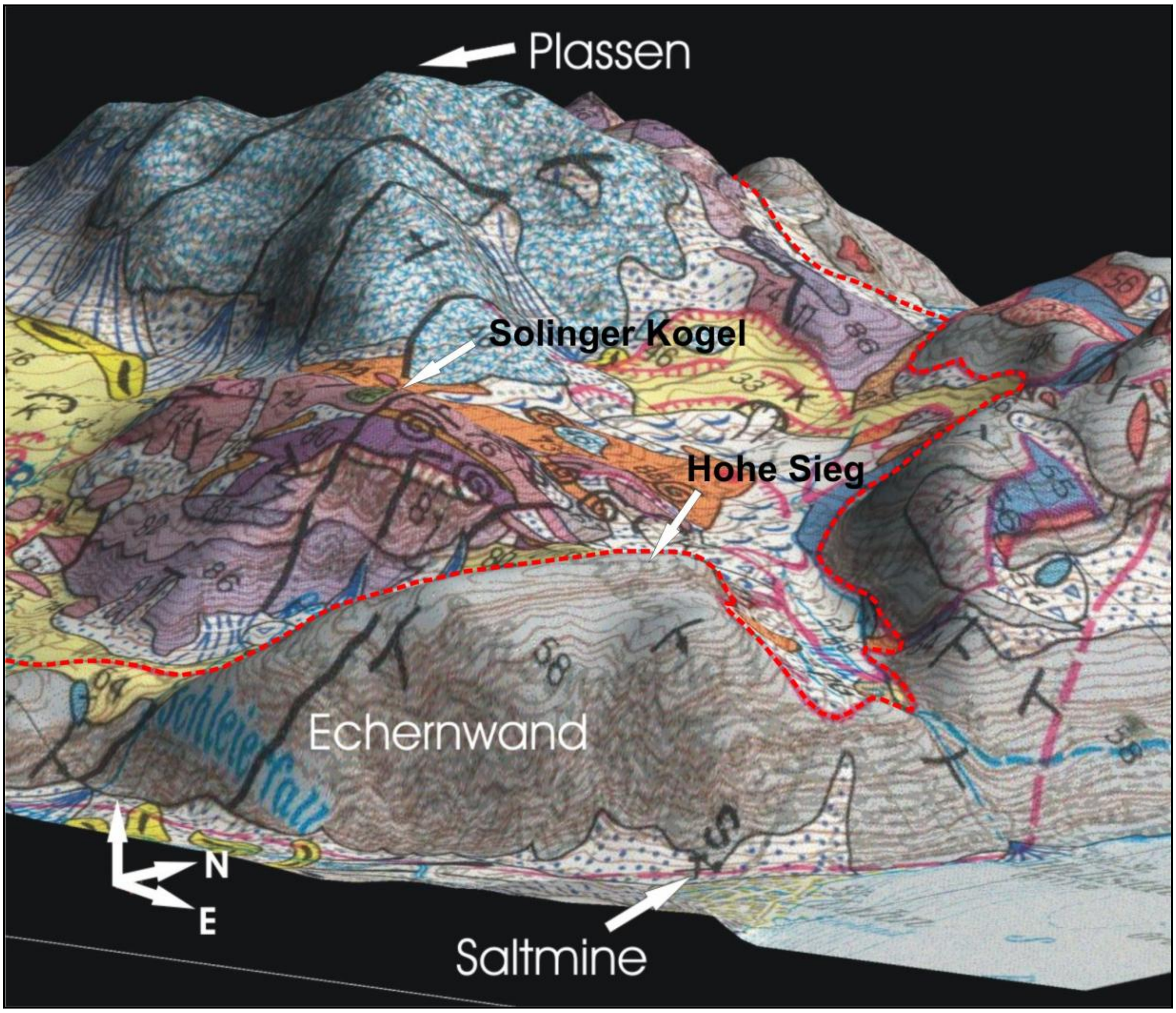

Fig. 3.11: 3D-model of the northern slope of the Echerntal. The geological map (Schäffer, 1982) was draped over the digital elevation model in GoCAD™. The red dotted line marks the border between the Hallstatt and Dachstein Nappes. The grey coloured lithology comprises of Dachstein Limestone and belongs to the Dachstein Nappe. For detailed legend of relevant lithologies see previous page.

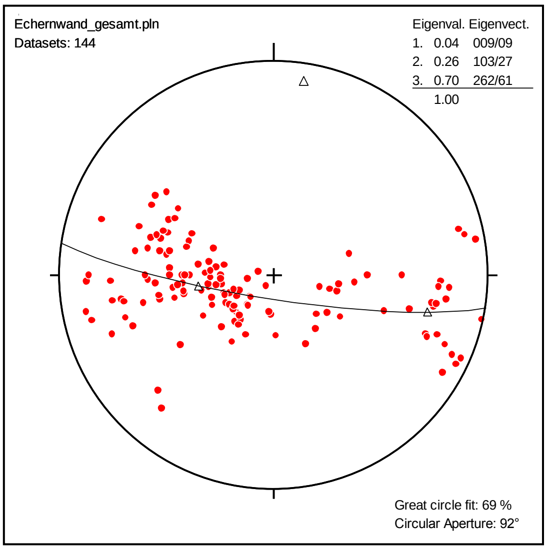

Fig. 3.12: Plot of all bedding planes (some of them with interbed slip) of the Echernwand and Hohe Sieg. The great circle in this plot (showing the average direction) indicates fold axes of the observed structures in this area that strike SSE – NNW. Consequently these fault related folds have to be generated in an ESE – WNW direction.

3.4.1 Observed deformation structures in the Echernwand

Moreover different thrust geometries could be observed in the field that are typical for thin skinned tectonics above more or less ductile detachment horizons. The Echernwand, wholly comprising of Dachstein Limestone, is divided into an eastern and a western part, due to a younger normal fault. Because of this normal fault trust geometries and structures of both parts can not be directly correlated. Both areas show the same direction of movement. In the eastern part the evaporitic detachment of the Haselgebirge is proved due to the investigations within the saltmine. An existing outcrop of Haselgebirge in the Erbstollen of the saltmine gives the evidence that the Haselgebirge is directly underlying the Dachstein Limestone in the frontal northern slope of the Echerntal. In the western part an evaporitic detachment horizon is possible too but is not verified until now.

Moreover in the whole Echernwand in addition to the basal detachment internal shortening structures (e.g. bedding parallel slip, thrust faults and duplexes) within the Dachstein Limestone are observed.

The most significant structures through the Echernwand beginning from the eastern frontal part proceeding to the west are listed on the following pages.

3.4.1.1 Eastern Part of the Echernwand

Detachment Fold

As already described Detachment folds require a ductile detachment that is able to migrate into the core of the fold during fold growth due to shortening. Because of that possibility detachment folds are known for their steep fore- and backlimbs. As shown in **Fig. 3.13** in the frontal northern slope of the Echerntal the bedding dips rise abruptly to very steep angles, indicating the structure of a detachment fold. Unfortunately not the whole geometry of the assumed detachment fold is preserved due to an out of sequence thrust that cuts the higher units of the structure downsection. Furthermore through the interlimb hinge area a younger fault cuts the bedding planes and so only the lower part of the backlimb of the fold can be observed on the rock wall.

But the location of dip steepening in the Dachstein Limestone correlates well with the position of the Haselgebirgs outcrop within the Erbstollen (**see Fig. 3.17**) and the structures observed at Hohe Sieg, which confirmed the thesis of a detachment fold.

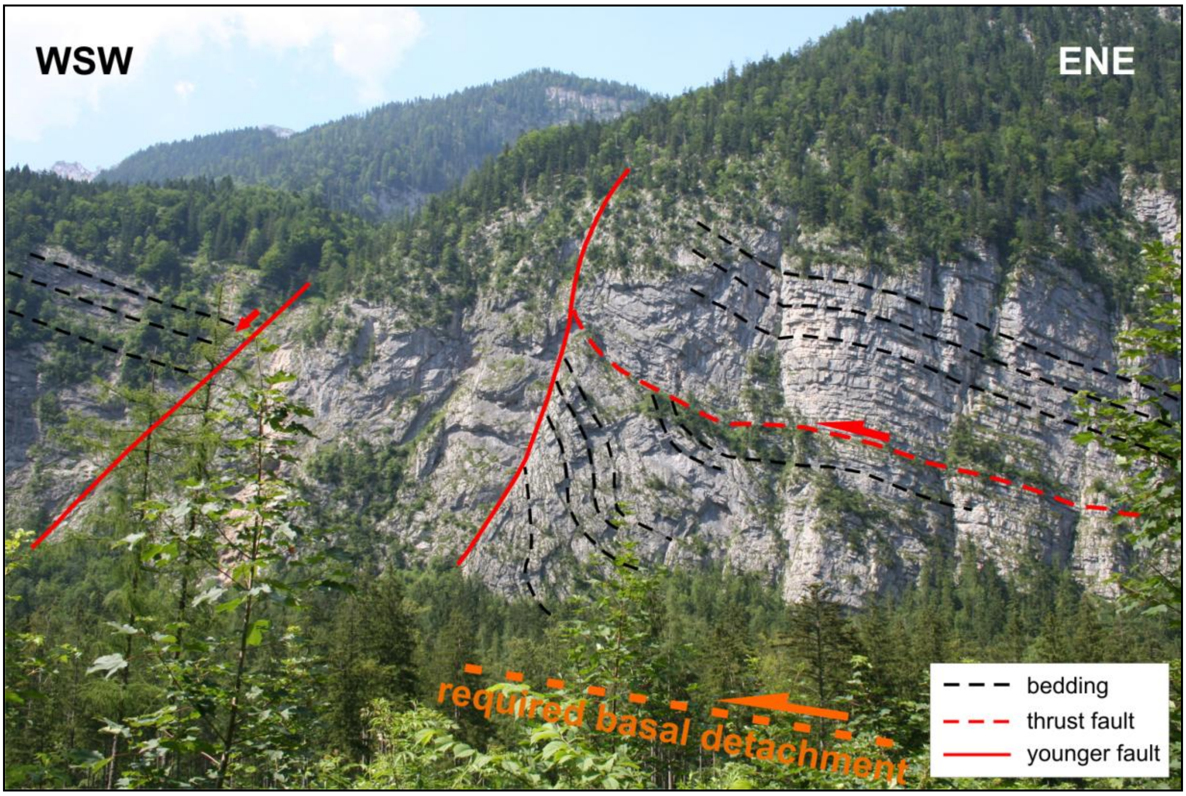

Fig. 3.13: Detachment fold. Immediately steeping of bedding planes requires a ductile basal detachment. Confirming the thesis of a detachment fold, the location of the structure correlates well with the outcrop of Haselgebirge within the Erbstollen. The structure is cut by an out of sequence thrust on the top (cuts bedding down section) and a younger fault limits the fold towards the west.
In the westernmost part of this picture a major younger normal fault takes place that separates the eastern and western part of the Echernwand.

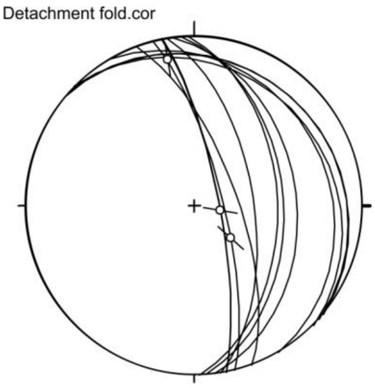

Fig. 3.14: Plot of bedding planes in the area of steepening dips. Some bedding planes show interbed slip but due to heavy weathering the direction of movement could not clearly be determined.

Hohe Sieg

A very distinctive outcrop is situated along a forest road near the top of the Hohe Sieg. The bedding planes are dipping steep towards the west. Therefore this part is seen as the steep dipping forward limb of the assumed detachment fold.

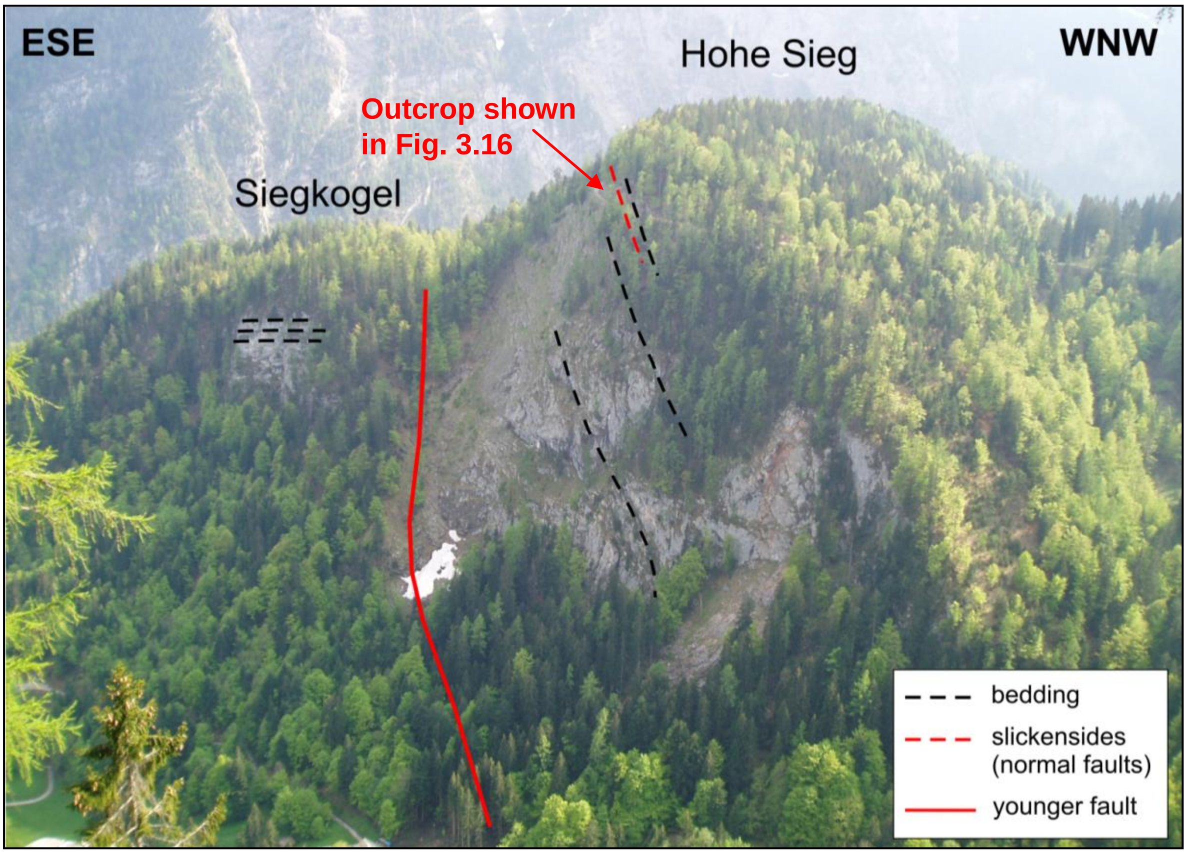

Fig 3.15: View from N to the backside of the Echernwand. The fault between Siegkogel and Hohe Sieg separates flat and steep lying areas of Dachstein Limestone. The steep towards WNW dipping bedding planes show interbed slip (see Fig 3.16) and are assumed to be the forelimb of the detachment fold observed in the Echerntal.

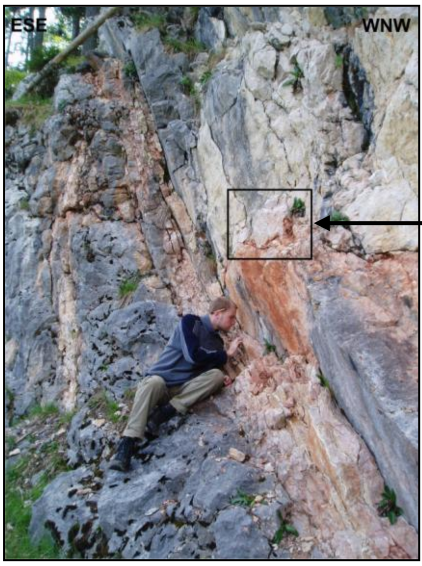

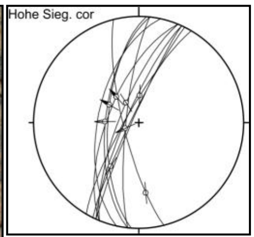

Fig. 3.16: Outcrop along a forest road near the top of Hohe Sieg. The extremely steep towards WNW dipping bedding planes show interbed slip evidenced by some calcite slickenfibres. As far as preserved these slickenfibres indicate normal faults.

This feature correlates well with the described backlimb structure in the Echernwand and the Haselgebirgs outcrop in the Erbstollen. A profile drawn by Schauberger and Medwenitsch (1951) demonstrates the relation of the steep dipping bedding planes of the Dachstein Limestone and the Haselgebirgs outcrop (**see Fig. 3.17**).

At the outcrops near the top of Hohe Sieg lineations on slickensides indicate movement mainly in ESE – WNW direction, but due to the weathering effect only few well preserved indicators for direction of movement, like slickenfibres of calcite are observed. Some of these slickenfibres indicate normal faults that suggest an interbed slip towards the WNW.

As seen in **Fig. 3.15** (also indicated in **Fig 3.17**) the fault between Siegkogel and Hohe Sieg separates clearly two different parts of the Dachstein Limestone. East of this fault strata is lying flat whereas west of the fault extremely steep bedding planes are observed. Interpreting this as the forelimb of a detachment fault the younger fault separating Siegkogel and Hohe Sieg may strike along the primarily hinge area of the fold. Hinge areas are often "weak spots" because the rigid limestones have to migrate through the fold hinges during growth of the fold. Consequently these areas are preferred zones for younger faults.

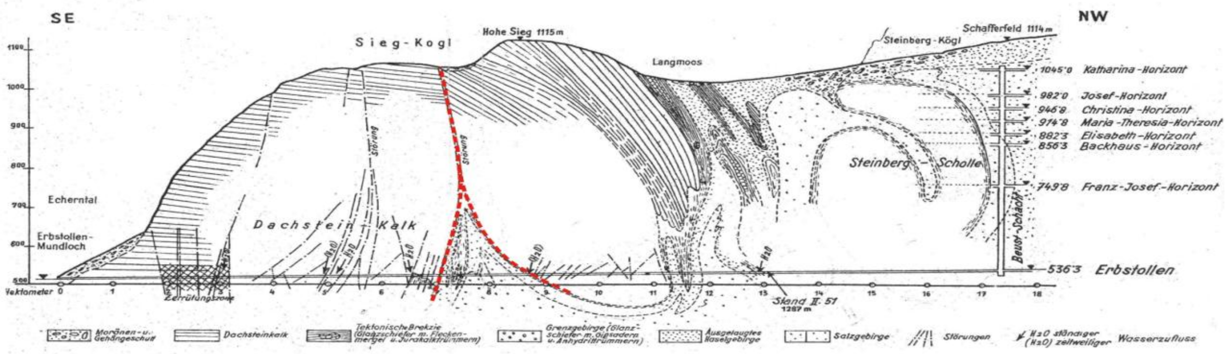

Fig. 3.17: Profile through the Echernwand along the Erbstollen (Schauberger and Medwenitsch, 1951). The fault separating Siegkogel and Hohe Sieg correlates with the Haselgebirgs outcrop in the Erbstollen.

3.4.1.2 Western part of the Echernwand

Triangle Zone

In the western part of the Echernwand a local backthrust was observed (**see Fig. 3.18**). Moreover this local backthrust that indicates top to east movement showed an unexpected feature when discovered at the first time. During investigating of the surrounding area it became soon clear that this is a local feature and that the general direction of main tectonic transport is top to WNW.

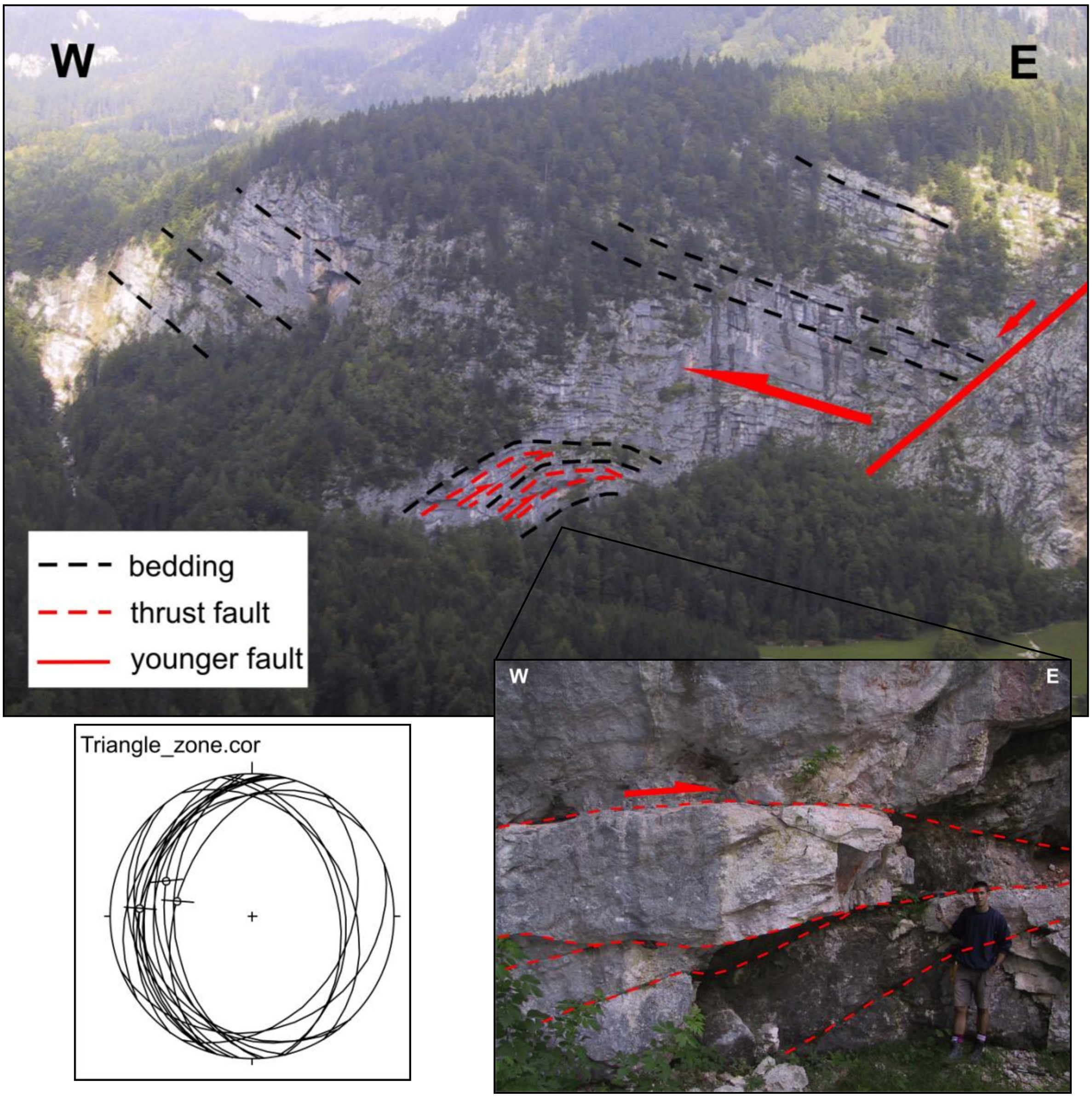

Fig. 3.18: Triangle zone or rather intercutaneous thrust wedge in the western part of the Echernwand. First indicating top to east movement but in relation to the other investigated structures it became clear that this is a local back thrust feature. As back thrust features are known for low-friction detachment horizons this structure indicates that the basal detachment of the western part of the Echernwand comprises of evaporitic Haselgebirge too.
The plot of this triangle zone area shows bedding planes dipping to East and West. Lineations were measured but due to heavy weathering no indication of shear sense was observed.

Backthrusts are typical structures that form above low-friction detachments that facilitate both foreland and hinterland vergent structures. This feature in the western part of the Echerntal led to the assumption that the evaporitic Haselgebirge makes up the basal detachment in this area too.

Because of the opposing bedding and thrust planes and the consequently generated triangular structures in the rock face backthrust structures are also known as “triangle zones” (**see Fig. 3.19**). A real “triangle zone” is a combination of two convergent thrusts with the same basal detachment that generate a triangular form between them (**see Fig. 3.19a**) (Mc. Clay, 1992). Moreover the term triangle zone is also used for zones of opposed thrust dips with different basal detachments, which more correctly should be described as intercutaneous wedges or passive roof duplexes (**see Fig. 3.19b and c**) (Mc Clay, 1992).

a) 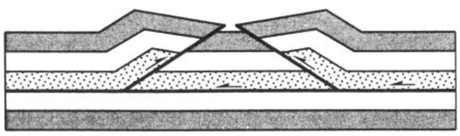	**Fig. 3.19a:** **Triangle zone: a combination of two opposing thrusts with the same basal detachment forms a triangle in between the thrust (Mc. Clay, 1992).**
b) 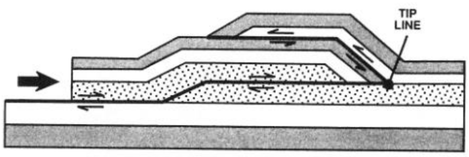	**Fig. 3.19b:** **Intercutaneous thrust wedge: A wegde bounded by a floor thrust at the base and a more or less passive roof thrust Mc. Clay, 1992).**
c) 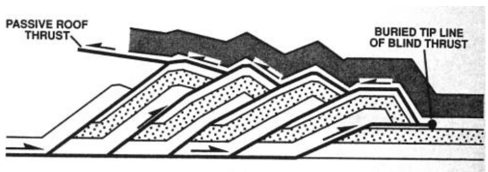	**Fig. 3.19c:** **Passive roof duplex: A duplex with a passive roof thrust that has been underthrusted by the duplex. Pssive roof thrust means that the sequences above have not been displaced in relation to the foreland (Mc. Clay, 1992)**

Fig. 3.19: Different backthrust geometries; backthrust features usually occur above low frictional detachment horizons (Mc Clay, 1992)

Fault bend fold and duplex structures at the Gangsteig

The westernmost part auf the Echernwand is characterized by a fault bend fold with ramps and flats and duplex structures. As described above it was possible to gain more detailed information in this part of the rock wall due to the Gangsteig, a small pass leading through the rock face. Fault bend fold and duplex structures clearly indicate top to WNW movement of the Dachstein Limestone. Fault gouge zones and slickensides can be observed along the thrusts that build up at least more than one flat – ramp – flat structure (**see Fig. 3.20**). As each flat and each ramp is forced to have its counterpart in the footwall (e.g. Wilkerson and Dicken, 2001), these structures have to exist in the footwall part too, which could not be investigated in the field.

Lineations observed on thrust and bedding planes show dominantly ESE-WNW direction of movement. Only few subsidiary lineations in N-S direction could be noticed. Calcite slickenfibres generated on thrust planes indicate top to WNW movement within interior shortening of Dachstein Limestone (**see Fig 3.21**).

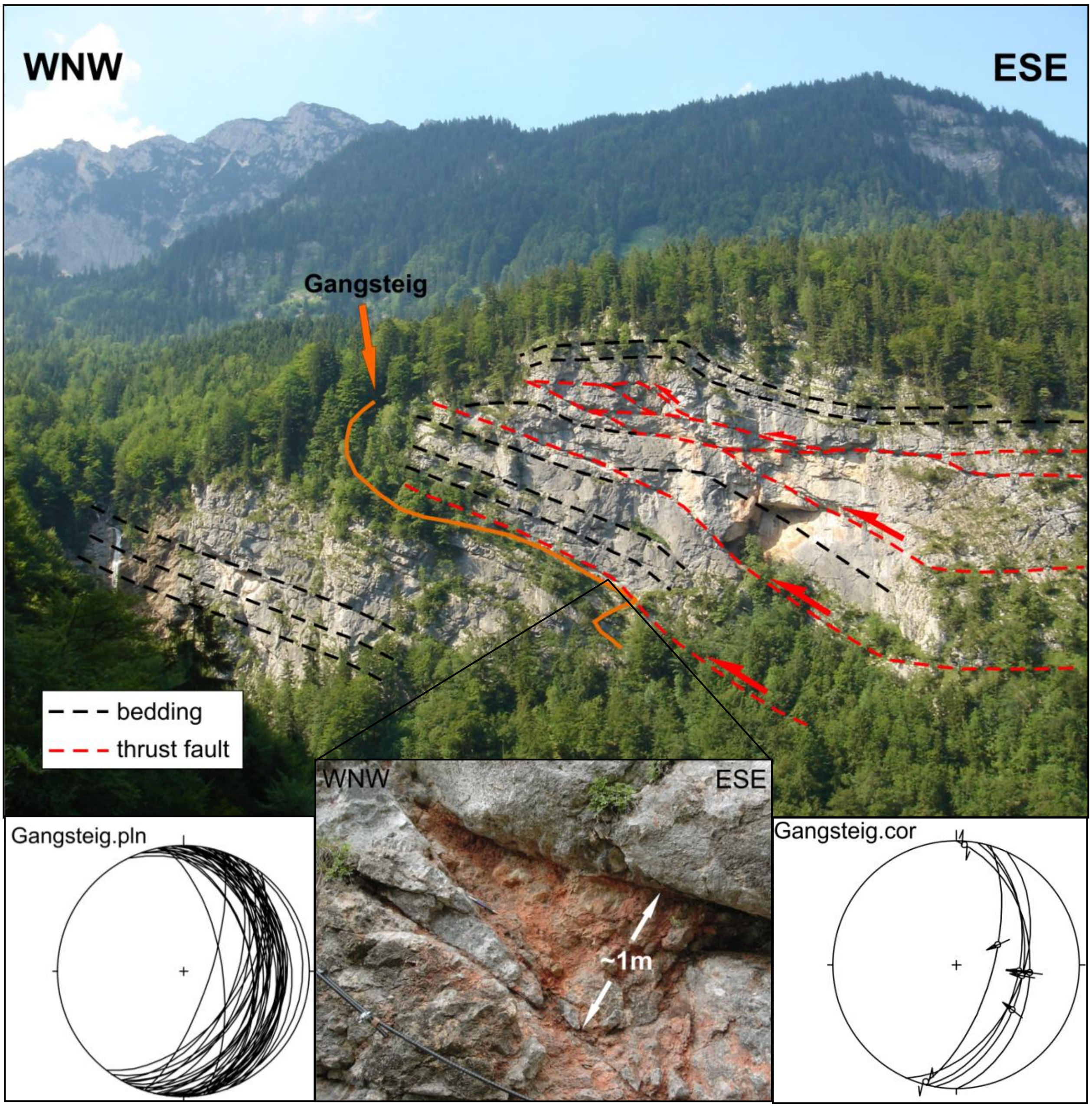

Fig. 3.20: Flat-ramp-flat geometries and duplex structures indicating top to WNW movement in the westernmost part of the Echernwand. Due to the Gangsteig direct inspections of the thrust faults, which generated up to 1m wide fault gouge zones, was possible. Slickensides observed as well in ramp areas as in flat parts show lineations that evidence the assumed direction of the main tectonic transport to WNW. On some slickensides a subsidiary lineation in approximately north-south direction was observed too (see plot at the right bottom).

Fig. 3.21: Slickensides with calcite slicken-fibres indicating top to WNW movement of the Dachstein Limestone.

In the upper part of **Fig. 3.20** some relatively small duplexes are generated during shortening. A duplex is an isolated part within the rock wall limited by thrusts at all sides. It is a common feature that duplex geometries occur at different scales. Multiple duplexes within one fault related structure are called second order duplexes (**see Fig 3.22**). Second order duplexes can generate in the ramp anticline of the footwall, the ramp anticline of the hanging wall and in the frontal zone of a ramp anticline.

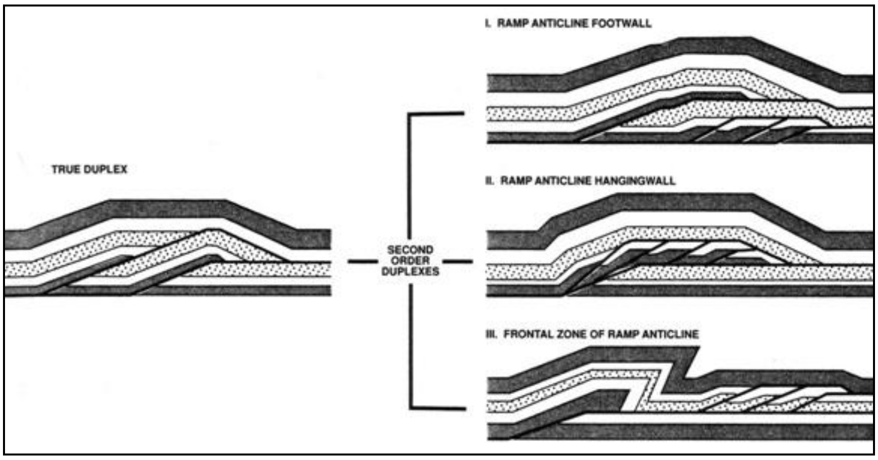

Fig 3.22: A true duplex on the left hand and different types of second order duplexes on the right hand. Small scaled second order duplexes were observed in the western part of the Echernwand (see Fig. 3.20). Usually duplex structures occur at various scales.

3.4.1.3 Panoramic view of the Echernwand and schematic profile

To receive an impression of the location of the different described structures within the Echernwand a photostitch of the northern slope of the Echerntal was generated. The most significant structures are marked in that picture. In the central part of this panoramic view a gap with no observed thrust geometries on the rock wall exists due to the younger faults that cut the structures laterally and due to the weathering effect enforced by the waterfall in this area (**see Fig. 3.23**).

As a consequence of the younger faults and the significant gap of geometrical structures, the schematic profile is split into an eastern and a western part. The eastern profile leads from the entrance of the saltmine WNW (roughly parallel to the Erbstollen) over the Hohe Sieg until the boundary between the Dachstein Nappe and the Hallstatt Nappe. This part is dominated by a detachment fold that requires a ductile material at the base. The Permian Haselgebirge constitutes that ductile basal detachment, evidenced by the Haselgebirgs outcrop in the Erbstollen. Thrusts cutting the underlying structures document that in addition to the detachment fold internal shortening of the Dachstein Limestone occurred.

The western profile starts at the distinctive younger fault west of the waterfall and leads through the westernmost part of the rockwall in WNW direction. As seen in **Fig. 3.24** this section is displaced to the south in respect to the Eastern part. The western part, where the basal detachment is not clearly determined, is characterized by the local backthrust forming a triangle structure and by ramp – flat – ramp geometries with second order duplexes in the westernmost area.

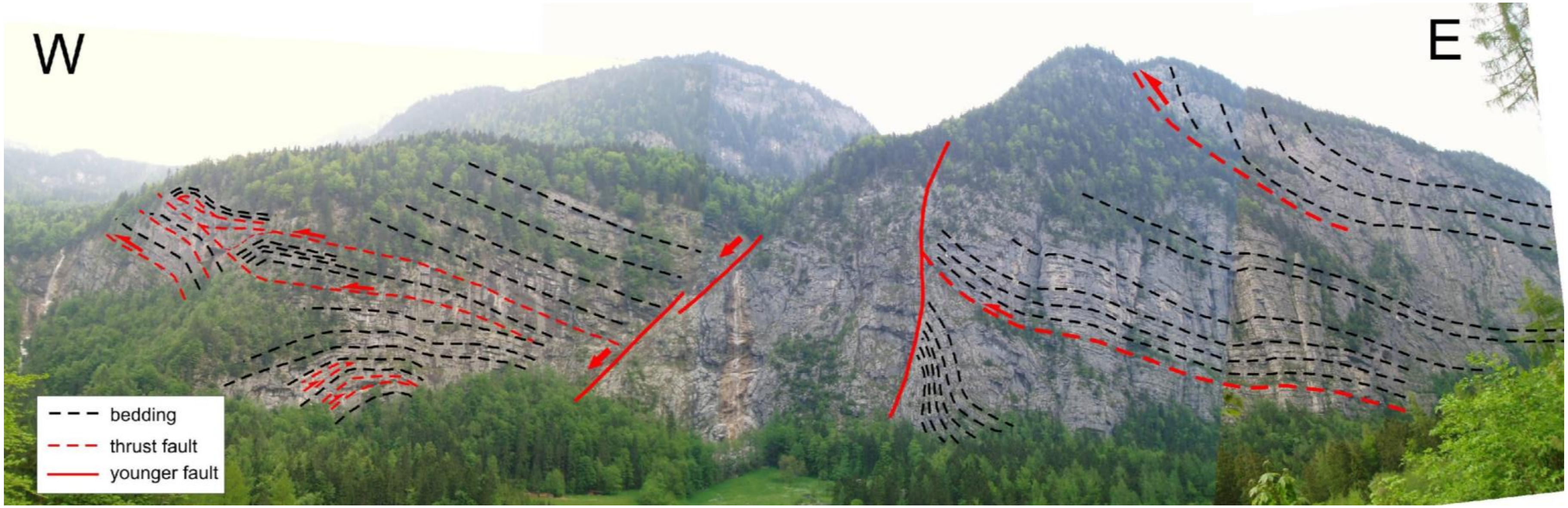

Fig. 3.23: Panoramic view of the Echernwand. Significant bedding planes, thrust faults and younger faults are marked in the picture. Due to the younger faults the structures cannot be correlated over the whole rock face. The tectonic structures clearly indicate that the Dachstein Limestone accommodate shortening with internal thrusts and folds in addition to the basal detachment.

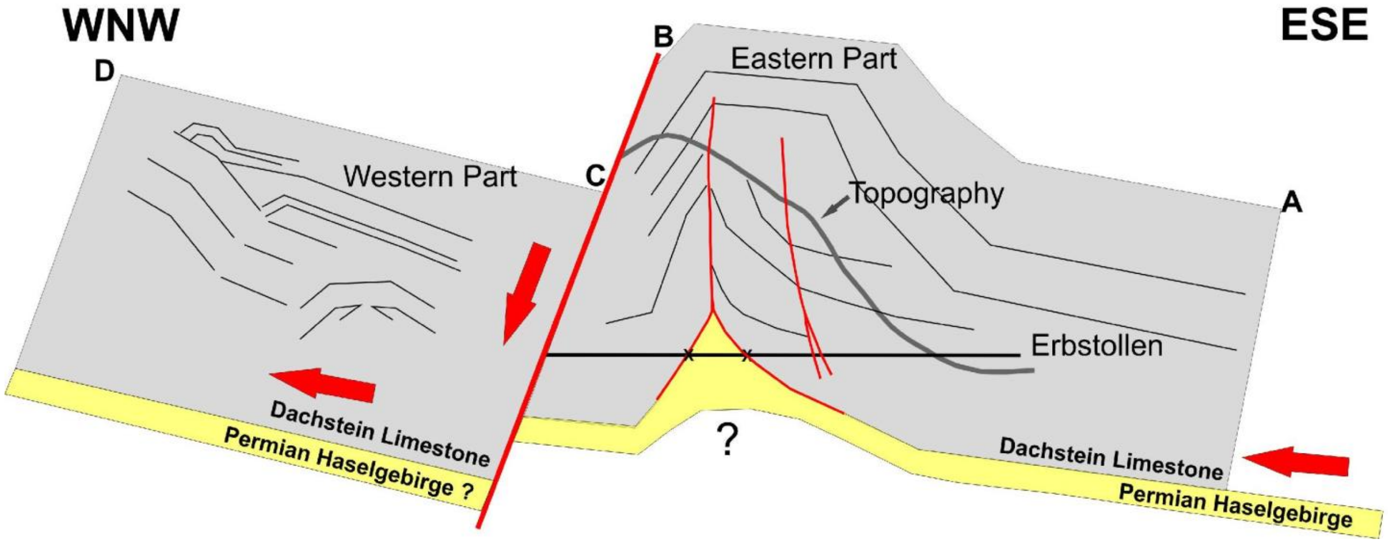

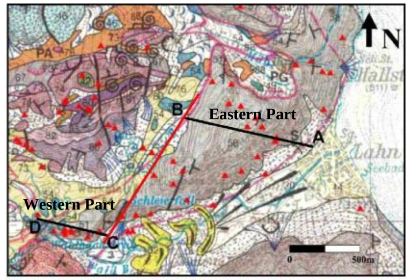

Fig. 3.24: Schematic profile through the Echernwand. Within the Erbstollen Dachstein Limestone directly overlies the Haselgebirge, indicating evaporites as basal detachment, whereas in the western section the basal detachment is undetermined. The small cutout of the Geological map shows the location of the eastern and western profile in top view.

3.5 Kind of contact between Hallstatt and Dachstein Nappe

As described in this chapter lot of spots indicate that the Dachstein Nappe overthrusted the Hallstatt Nappe at its southeastern boundary in a WNW-ward direction. The Haselgebirgs outcrop in the Erbstollen directly underlying the Dachstein Limestone and forming the core of a detachment fold and the thrust geometries that accommodate shortening within the Dachstein Limestone in the Echernwand are features that strongly confirm this thesis.

At the northern bound of the Hallstatt Nappe a major dextral strike slip fault as described by Arnberger, 2006, separates the sediments of the Dachstein and Hallstatt Nappes. This strike slip fault may be a result of significant changes of the basal detachment. Analogue modeling within a sandbox showed that the deformation front above a ductile detachment moves faster and farther forward than above higher frictional detachment horizons (Cotton and Koyi, 2000). As a consequence at the lateral boundary of different detachments a strike-slip “tear” fault generates. The ductile material within the core of thrust structures is able to migrate into that small pull-apart structure and accumulate in the tear fault zone (**see Fig. 3.25**, Cotton and Koyi, 2000)

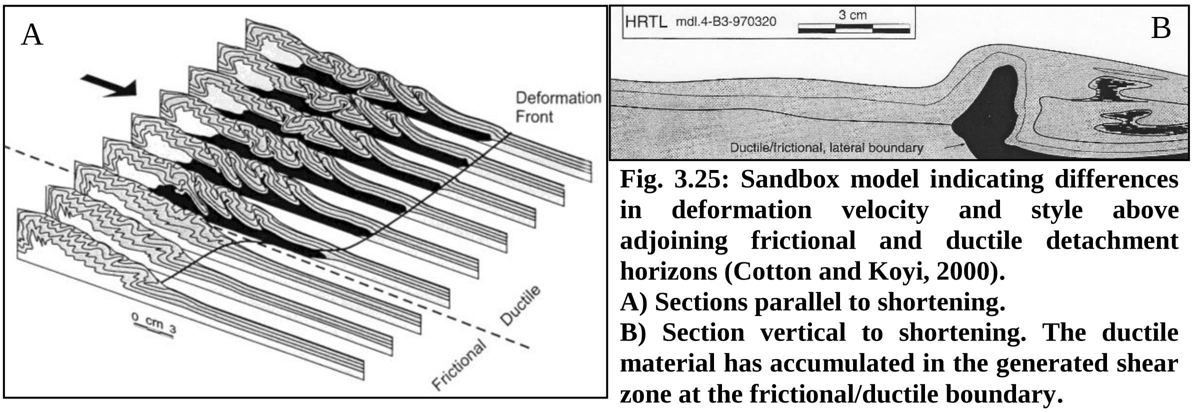

Fig. 3.25: Sandbox model indicating differences in deformation velocity and style above adjoining frictional and ductile detachment horizons (Cotton and Koyi, 2000).
A) Sections parallel to shortening.
B) Section vertical to shortening. The ductile material has accumulated in the generated shear zone at the frictional/ductile boundary.

These results of field analyses at the northern and southeastern boundary of the Hallstatt Nappe are in contradiction to the tectonic map of the Hallstatt area published by Mandl (2000) where the Hallstatt unit is drawn as a big gliding block lying above the Dachstein Nappe (**see Fig. 3.26**).

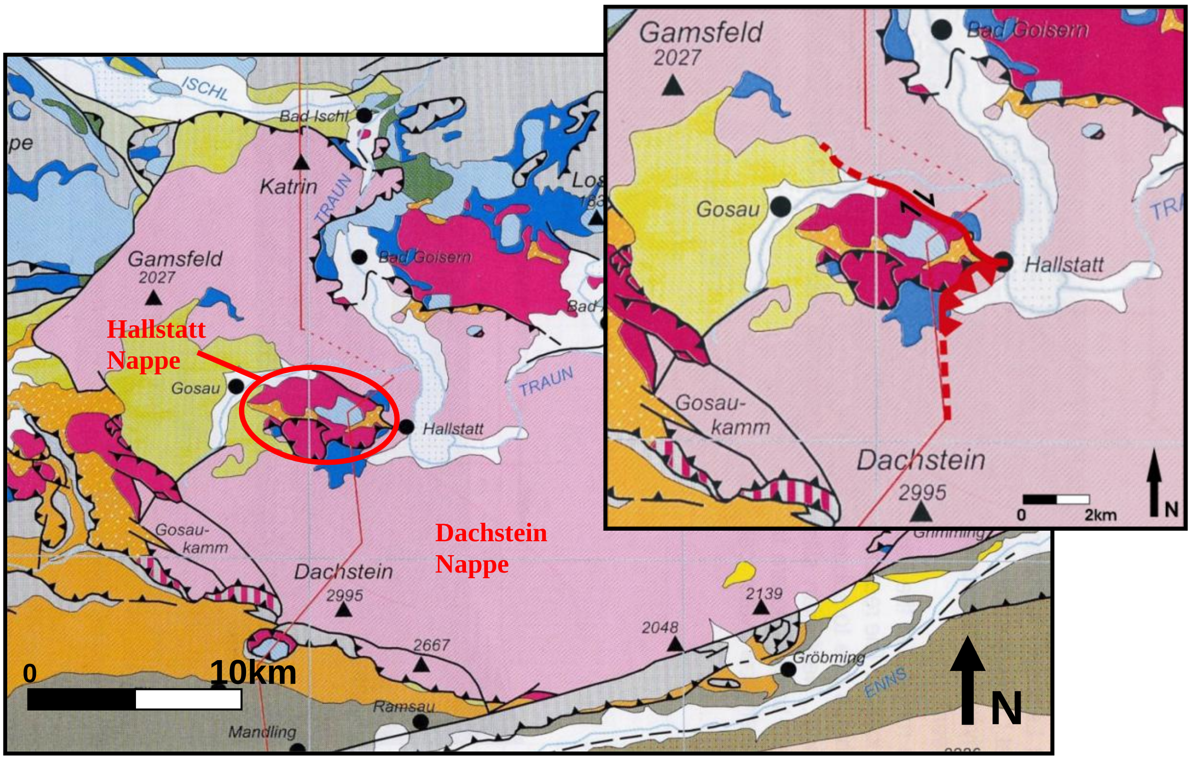

Fig.: 3.26: Tectonic map of the Hallstatt area (slightly modified after Mandl, 2000). As marked in the right map-section according to field observations the Dachstein Nappe overthrusts the Hallstatt Nappe at its southeastern boundary. The major strike slip fault at the northern boundary is suggested by Wagreich and Decker (2001) and confirmed by Arnberger (2006).

3.6 Time of thrusting

One of the aims of this diploma thesis was to limit the time of thrusting. The sedimentation of the limno-fluviatile to shallow marine Gosau Group marks a significant change of the tectonic setting within the interesting area and the whole NCA. These sediments overly the observed thrust structures discordant as well at Dachstein Nappe sediments as at Hallstatt Nappe beds. **Fig. 3.27** shows the bedding dips of Gosau outcrops in the surrounding area verifying their unconformities with the thrust tectonic affected rocks. As the deposition of the Gosau Group started in the Late Turonian the main tectonic thrusting in the interesting area must already have been terminated at that time.

As a consequence the thrusting is assumed to belong to the Early Cretaceous Eoalpine peak. For the tectonic setting of the Gosau Group sediments in the particular area (also the type-locality) a pull-apart basin is recommended by Wagreich and Decker (2001).

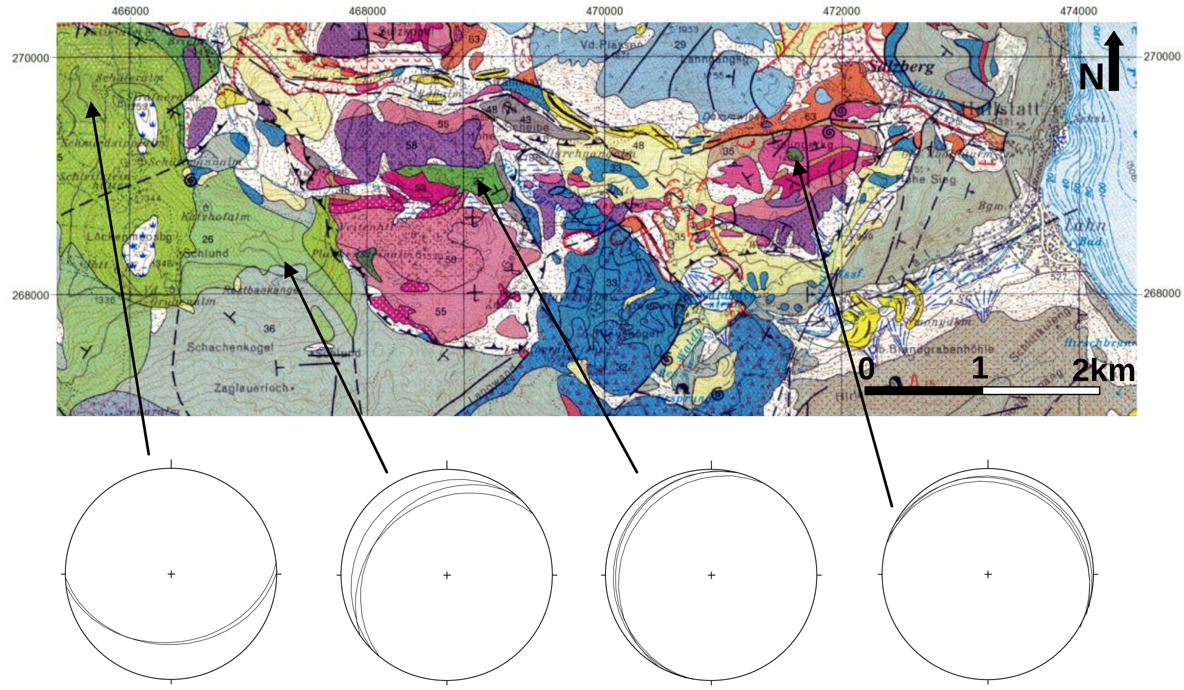

Fig. 3.27: Geological map of the Echerntal valley and surrounding area (Mandl, 1998). The bedding planes of Gosau outcrops show significant different dip directions than the underlying sediments affected by Eoalpine thrusting. The Gosau Group sediments are marked by the green colours.

4. Salt tectonics

4.1 Introduction

As mentioned in the chapters before a fold-and-thrust belt is usually located in the frontal region of a collisional range and characterized by tectonic shortening via growth of folds and thrusts above detachment horizons.

Due to the remarkable low shear strength of evaporitic units, the presence of the Permian Haselgebirgs Formation affects the mechanics and geometry of the studied fold-and-thrust belt significantly. Carter and Hansen (1983) mentioned that most rock types that are common in the upper 10km of the crust have similar frictional strength except shales and especially evaporites, which are much weaker. In particular halite can deform by viscous flow almost under surface conditions and at quite low differential stresses (**see Fig. 4.1**; Davis and Engelder, 1985).

Hence, evaporites are perfect detachment horizons, along which the overlying, brittle reacting sequences get decoupled. Due to their viscous deformation behaviour they can also facilitate folding by flowing into anticlines (**see chapter 3** Detachment folds) and are the preferred horizons for bedding parallel slip (Davis and Engelder, 1985).

Fig. 4.1: "Christmas tree" diagram showing the depth versus strength of various rock types. In comparison to the other rock types, halite reacts extremely weak and can deform by viscous flow under extremely low temperatures and shear stresses (Davis and Engelder, 1985).

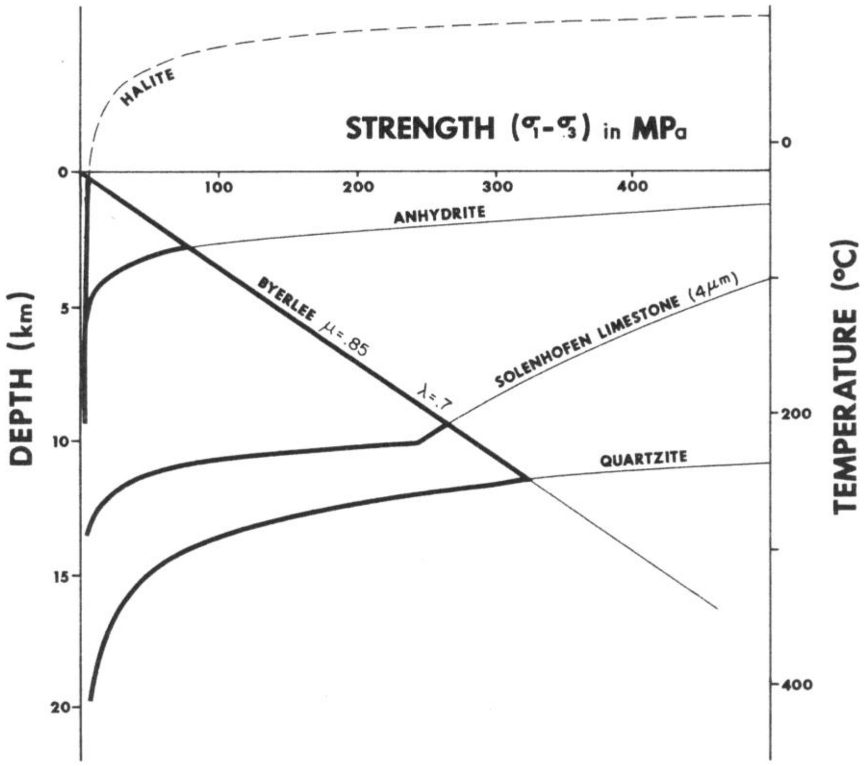

Moreover the low specific weight and viscosity of evaporites can cause diapiric upwelling, as long as there is no orogenic activity (Ramberg, 1981). While uprising and piercing the overlying sequences by an upward drag of the core of the diapir and downward drag of the circumfluent cover, it can produce a vast number of diapiric shapes (**Fig. 4.2**; Jackson and Talbot, 1989; Koyi, 1998).

Fig. 4.2: Different shapes of diapirs, controlled by viscosity contrast (m) of the surrounding material and the diaper itself. Another important aspect is the maturity of the diapir (Jackson and Talbot, 1989).

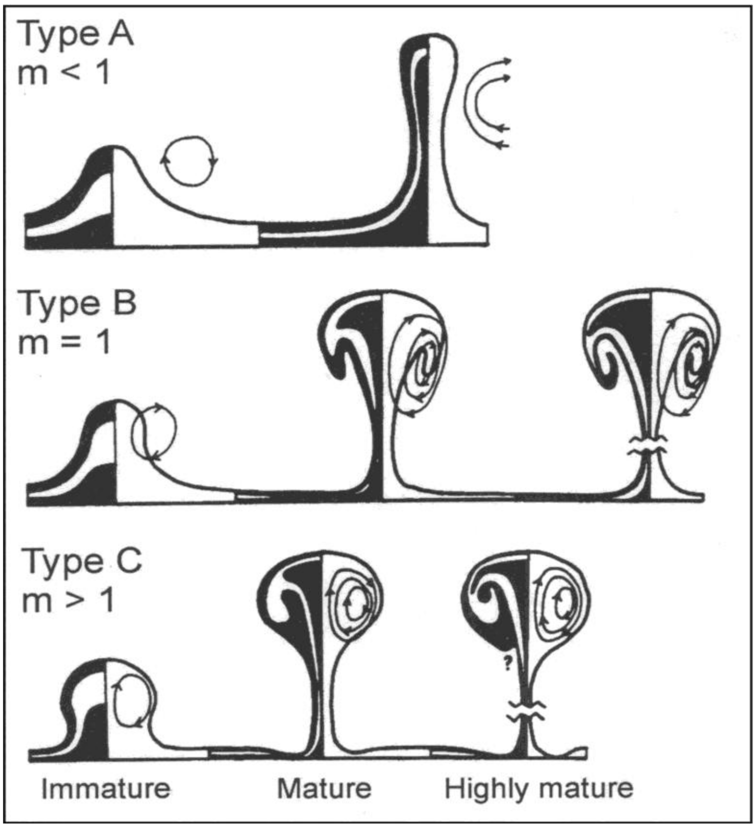

The Hallstatt salt deposit has undergone a polyphase development. At least the last stages of this salt body were totally controlled by the tectonically stressfield. As a consequence such diapiric shapes can not be observed in the Hallstatt saltmine.

At the structurally base of large parts of the NCA nappes evaporites of the Haselgebirge are present and constitute the major detachments for alpine thrusting (Tollmann, 1985). The development of the current composition of the Haselgebirge, a polymict breccia, has been debated for a long time and was interpreted quite variously. Within the clayey-salty matrix especially the halite rich sections of the Haselgebirge display obvious foliations. Whereas Schauberger (1955) suggested a complete sedimentary origin of these planar features, Medwenitsch (1949) was among the first who interpreted them as mylonitic structures. Today it is commonly accepted that due to penetrative Alpine deformation no primary depositional sequences can be preserved in the Haselgebirgs Melange. Especially the analysis of strain textures in evaporites verified the tectonic development of the Haselgebirge (Spötl, 1988 and Spötl and Hasenhüttl, 1998).

As a result of its high mobility, the Haselgebirge provides a complex tectonic history. The post depositional evolution, after sedimentation in a continental rift-setting, started with diapiric upwelling of the evaporites, which was recorded in the overlying Late Anisian carbonates (Mandl, 1984a). As described in chapter 2, the arising diapiric ridges were responsible for a facies distribution during the Middle and Late Triassic, as they created submarine highs in between the deep marine basins (Mandl, 1984a; Lein, 1987). Tollmann (1981) claimed that in the late Jurassic and Early Cretaceous times these evaporites acted as detachment horizon for gravitationally induced glide tectonics. Owing to Alpine thrust and nappe tectonics, the strongest deformation of the Haselgebirge happened from Middle Cretaceous to Late Eocene. During that period the Jurassic diapirs were probably displaced and intensely tectonized. Huge components of shales, marls and Mesozoic carbonates got incorporated into the visco-plastic reacting Haselgebirge. The original sedimentary bedding in the evaporitic units was completely destroyed (Spötl, 1989).

In the investigated area around Hallstatt, the Haselgebirge is more or less restricted to the Hallstatt Nappe. Analogue modelling by Davis and Engelder (1985) demonstrates that the presence of salt facilitates different deformation styles, what can also be observed in the field as described in chapter 3. For the purpose of correlating salt related surface structures with their underlying Haselgebirgs-detachment, a 3D-model of the salt body, based on subsurface maps of the saltmine of Hallstatt (courtesy of Salinen Austria AG) was created in GoCAD™. This 3D-model is related to the DEM (Digital Elevation Model) of the study area.

4.2 Subsurface structural data and interpretation

Field analysis in the mylonitic Haselgebirge focused on determination of the internal structure in relation to observed deformational geometries in the overlying strata. To get more information about the internal structure cleavages, fold axes and fold axial planes were measured and the shear sense was determined by examination of porphyroclasts. Due to the low viscosity of halite, especially the portions of Haselgebirge that contain high concentration of halite (i.e. "*Kernsalz*") validate the mylonitic character of the Haselgebirge, as isoclinal folds and porphyroclasts dominate in these areas. Furthermore thin-sections of anhydrite and "*Glanzschiefer*" samples (**see chapter 5**) were created and investigated. Structures in the thin-sections evidence the mylonitic character as well. Mylonite is a strictly structural term that refers only to the fabric of the rock and does not give any information on the mineral composition. "A Mylonite is a foliated and usually lineated rock that shows evidence for strong ductile deformation and normally contains fabric elements with monoclinic shape symmetry." (Passchier and Trouw, 1996). As a result, evaporites can be seen as an analogue material that develops characteristic structures of crystal plastic deformation nearly at surface temperatures, which are usually observed in quartz-feldspar rocks, deformed under greenschist facies conditions (350-500°C, 0,2-1GPa).

4.2.1 3D-Model of the salt deposit in Hallstatt

For the purpose of better understanding of the structural relation between the Haselgebirge and its overlying strata and of course to localize the saltbody itself, a 3D-model of the saltmine of Hallstatt was generated. For the localization of outcrop points, measurements and the relationship between structural elements inside the saltmine the 3D-model was very helpful too. It is based on the maps of the different horizons of the saltmine (courtesy of Salinen Austria AG) that were digitized and georeferenced.

As far as encountered by the saltmine up to now, the Haselgebirge forms an elongated body, almost 3km long and about 500m wide, that strikes NW – SE. The main access at the basal level (Erbstollen) is situated at the frontal northern slope of the Echerntal at an altitude of 514m above sea level – about 6m above the level of Lake Hallstatt (508m). From their up to 1219m altitude, the saltmine consists of 14 horizons and several shafts. The most important levels between Erbstollen and Kaiser Josef Hz. (970m) were used for 3D modeling (**see Fig. 4.3 and 4.4**).

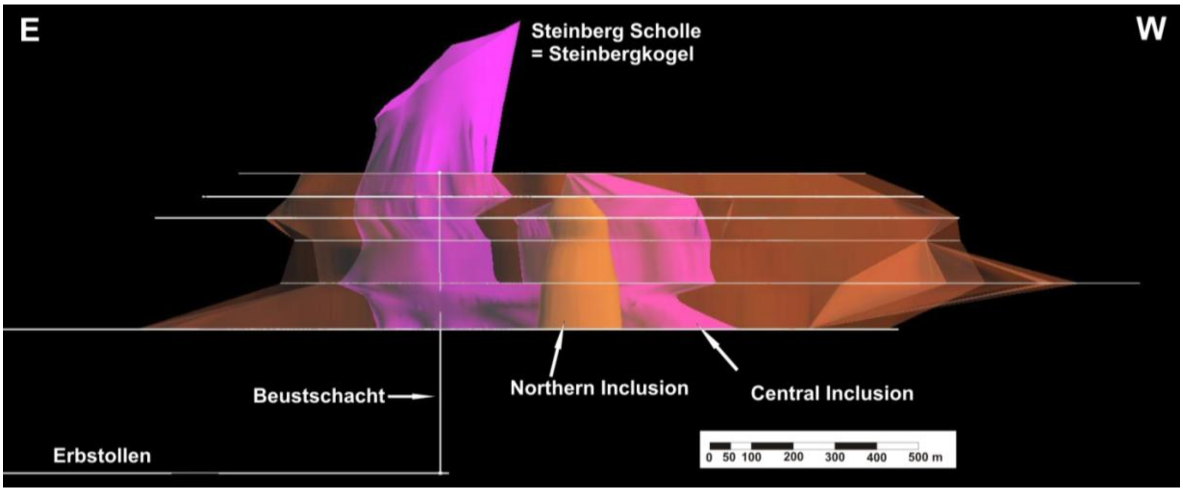

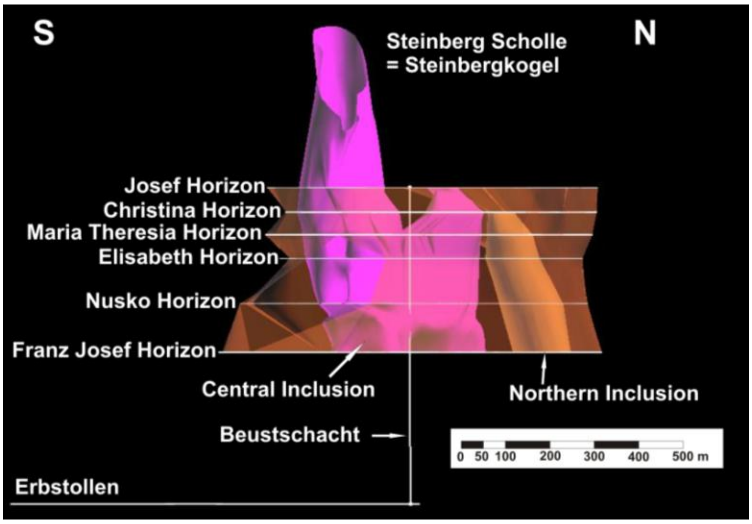

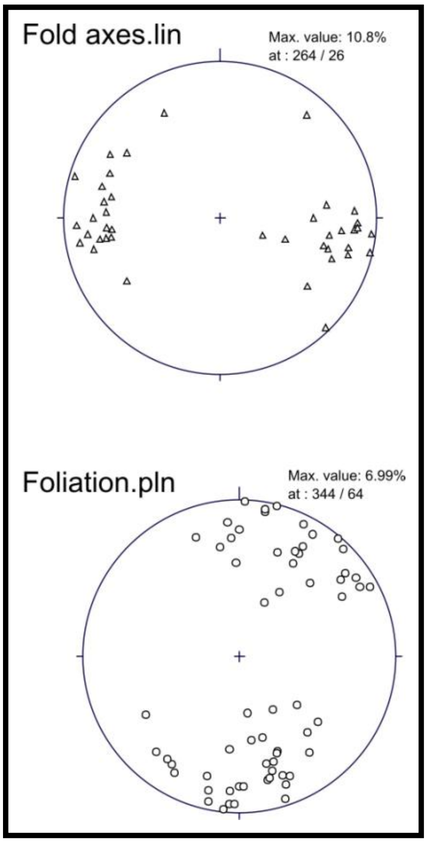

Fig. 4.3: Cross sections through the generated 3D-model of the Hallstatt salt deposit in horizontal view; 2 times exaggerated. The Horizons that were used to construct this model are named in the S – N section. The Steinberg Scholle within the saltmine crops out to the surface at Steinbergkogel. Steinbergscholle and Central Inclusion comprise of Hallstatt Limestone whereas the Northern Inclusion consists of an Upper Permian red bed sequence (Spötl, 1987). On the right hand plots of the measured fold axes and foliations within the Hallstatt Saltmine are shown. For detailed plots and their position in respect to the saltbody see next page Fig. 4.4.

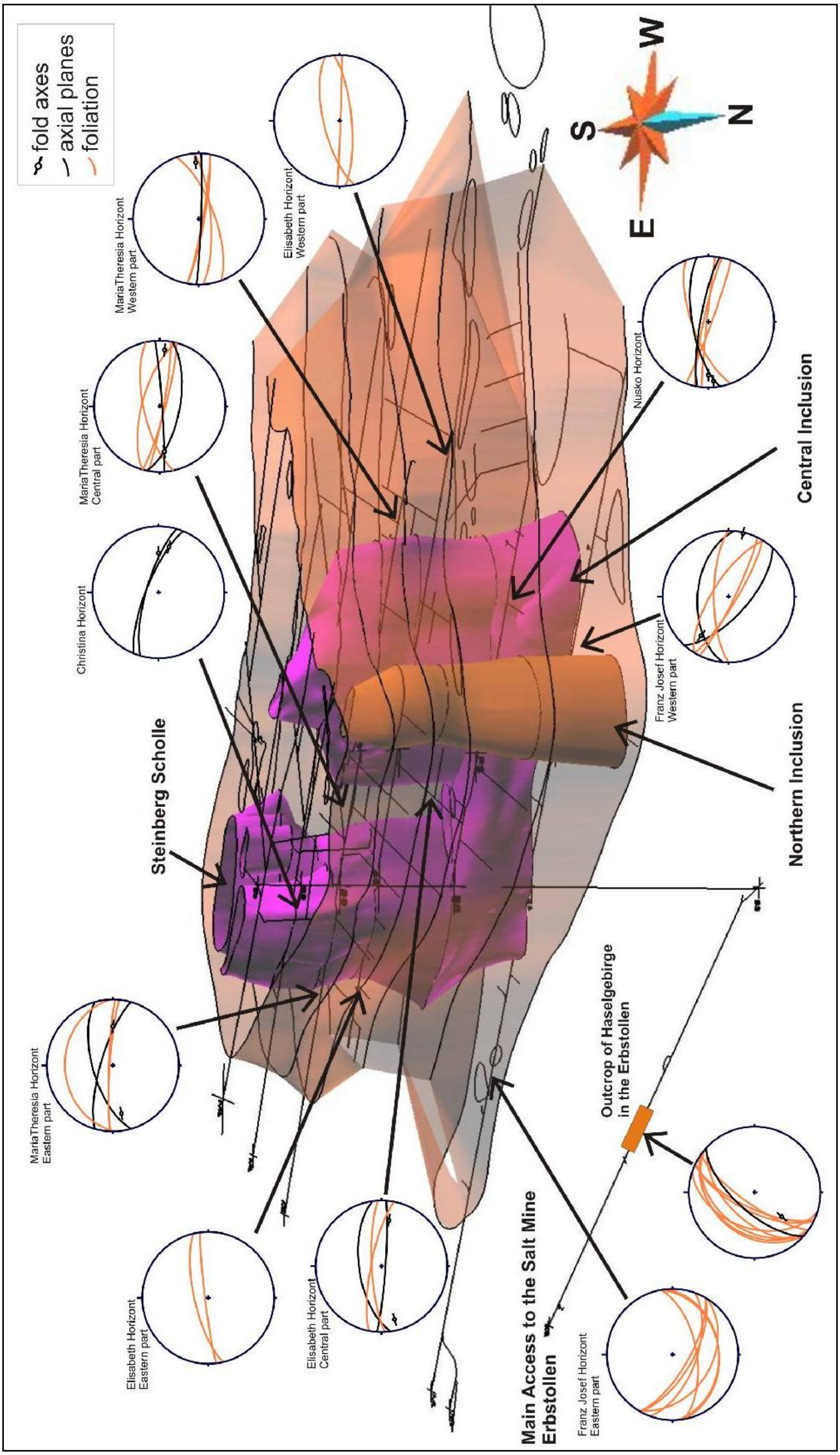

Fig. 4.4: Oblique view towards S of the 3D-model of the Hallstatt Saltmine; 3 times exaggerated. Structural data of the Haselgebirge (fold axes, axial planes and foliation) mainly strike E – W related to a big strike slip shear zone. Only the Haselgebirge encountered in the Erbstollen shows different measurements indicating that this outcrop is related to WNW directed thrusting (see Fig. 4.5)

As shown in **Fig. 4.3 and 4.4** within the saltbody several bigger lenses of different materials are incorporated, mainly elongated parallel to the general strike of the salt deposit. The biggest of these lenses is the “Central Inclusion”, an up to 1000m long and nearly 200m broad lens of Hallstatt Limestone. This limestone lens makes up the core of the saltbody. The “Northern Inclusion” consists of an Upper Permian red sequence with silty-clayey rocks and intercalated sandstones (Spötl, 1987). This tectonically isolated lens probably presents the facies between the salt pan and the alluvial fan (**see Fig 2.6**). Anhydrite clasts within the stratigraphy higher parts of the Northern Inclusion confirm evaporitic sedimentation environment (Spötl, 1987). Another significant inclusion comprising mainly of Hallstatt Limestone in the eastern part of the salt body is the “Steinberg Scholle” that crops out to the surface at “Steinbergkogel”. The Steinbergkogel correlates well with the sediments observed at the “Solinger Kogel” but it is separated by an E – W trending fault from the supposed mother rock.

The whole structure is influenced by those large rigid inclusions and also a relation between the position of salt- or clay-rich areas with respect to the inclusions is obvious. Halite rich zones in favour take place along the border of the saltbody and around the large rigid inclusions. On the other hand in some relatively high pressure zones, e.g. at unconformities along the elongated inclusions, clay rich zones developed due to pressure solution. These portions consist only of the non dissolvable rocks and because of the intense deformation several small polished slickensides are established and give these rocks a “shiny” appearance. Therefore clay rich border rocks are called “*Glanzschiefer*”.

In general the elongated form of the saltbody together with the steep dipping E – W striking axial planes with the more or less horizontally lying fold axes and the dextral sense of shear (proved by rotated porphyroclasts, **see chapter 4.2.2**) indicate that Hallstatt salt deposit is related to a major dextral strike slip fault. This is in good accordance to the investigated deformational structures at the surface (Arnberger, 2006).

As mentioned already in chapter 3 the Haselgebirge outcrop in the Erbstollen within the Dachstein Limestone shows contrary features than the described saltbody. Foliation and axial plane strike ENE – WSW and suggest that the evaporites in this outcrop were related to WNW directed thrusting. It indicates that the Permian Haselgebirge in the Hallstatt area originally made up the basal detachment horizon for thrusting towards WNW but probably in a later stage the evaporitic sediments migrated into the strike slip fault and generated the Hallstatt salt deposit as it appears today.

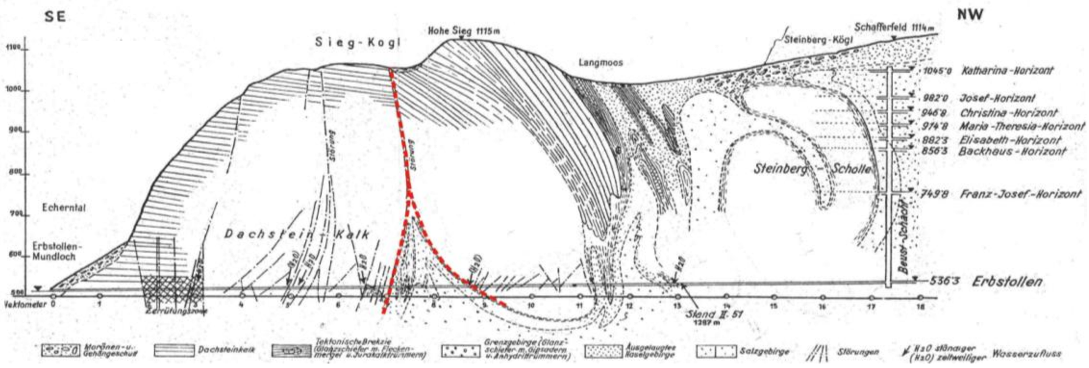

Fig. 4.5: Profile along the Erbstollen (Schauberger and Medwenitsch, 1951). The outcrop of Haselgebirge in the Erbstollen within the red marked faults indicates that the evaporites primarily were related to WNW-directed thrusting.

4.2.2 Mantled porphyroclasts

Porphyroclasts are components of resistant materials that keep a larger size than grains in the matrix. Those clasts can be seen as remnants that resist the deformation due to the rheological contrast between the relatively hard minerals of the porphyroclast and the more viscous matrix. Consequently the matrix is wrapped around the rigid clasts and typical fabric elements of mylonites are generated that provide essential shear sense indicators. Porphyroclasts are commonly flanked by tapering grain aggregates and form a structural unit with them. If those aggregates consist of the same material as the porphyroclast itself, they are called mantels. If they have a different composition they are named strain shadows. Due to the flow in the matrix, mantled porphyroclasts usually form wings that extend on both sides of the clast, parallel to the foliation in the mylonite (Passchier and Simpson, 1986).

Passchier and Trouw (1996) classified five types of mantled porphyroclasts:

Θ-type porphyroclasts lack wings completely

Φ-type clasts have a mantle with orthorhombic symmetry

σ-type clasts have a monoclinic shape symmetry that is defined by a wide mantle with two planar and two curved faces near the porphyroclast. The difference in elevation of the wings on both sides forms a stair-stepping geometry.

δ-type clasts have narrow wings with characteristic bends flanking close to the porphyroclast. δ-clasts do not necessarily show stair-stepping, but the embayment of matrix near the core yields a reliable shear sense indicator

Complex mantled porphyroclasts have more than one set of wings.

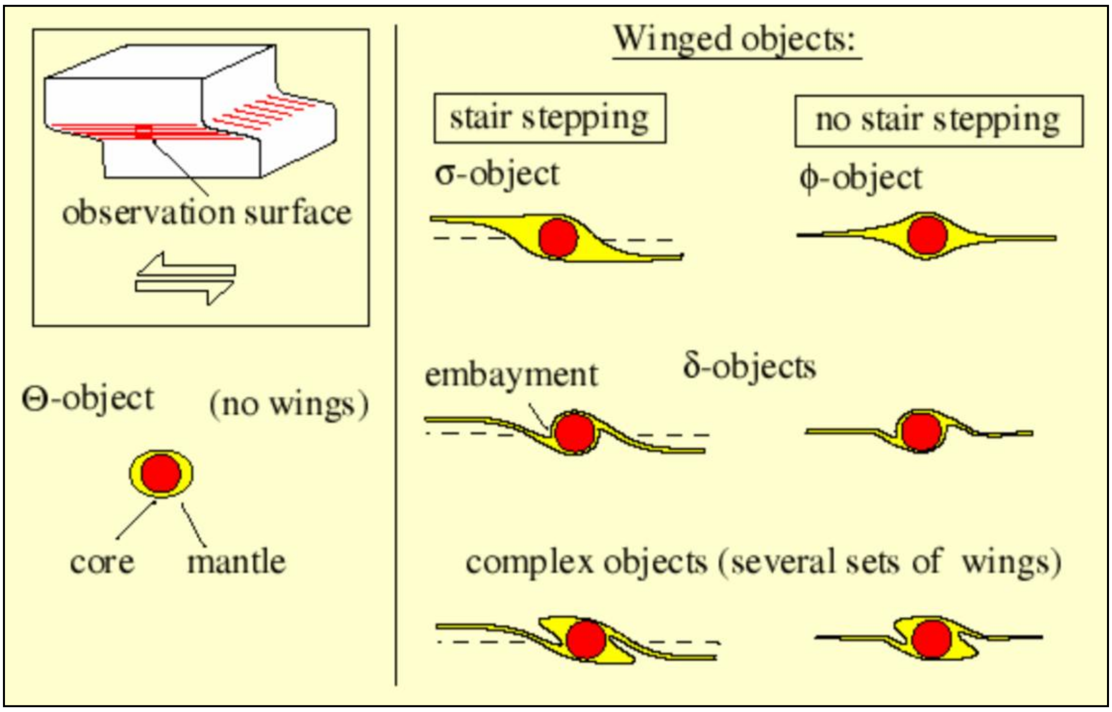

Fig. 4.6: Classification of mantled porphyroclasts at sinistral sense of shear after Passchier and Trouw (2005)

The internal asymmetry of σ-, δ- and complex clast types can be used as shear sense indicators. Stair-stepping of the wings shows a step up in the direction of movement of the upper block. δ- and complex porphyroclast types only appear in large strain mylonites, while σ-clasts are found at small strain as well.

In the Haselgebirge clay, anhydrite, polyhalite and sometimes sandstone form rigid inclusions within the ductile halite matrix and are deformed to σ- and δ- clasts, consistently showing a dextral shear sense. That means for the local situation that the northern block (in respect to the southern block) moves towards the E.

Due to the position of the observed clasts, most of them are situated on the tunnel`s roof, the first impression of sinistral sense of shear has to be flipped into dextral shear sense in top view (see Fig.4.7; Fig 4.8).

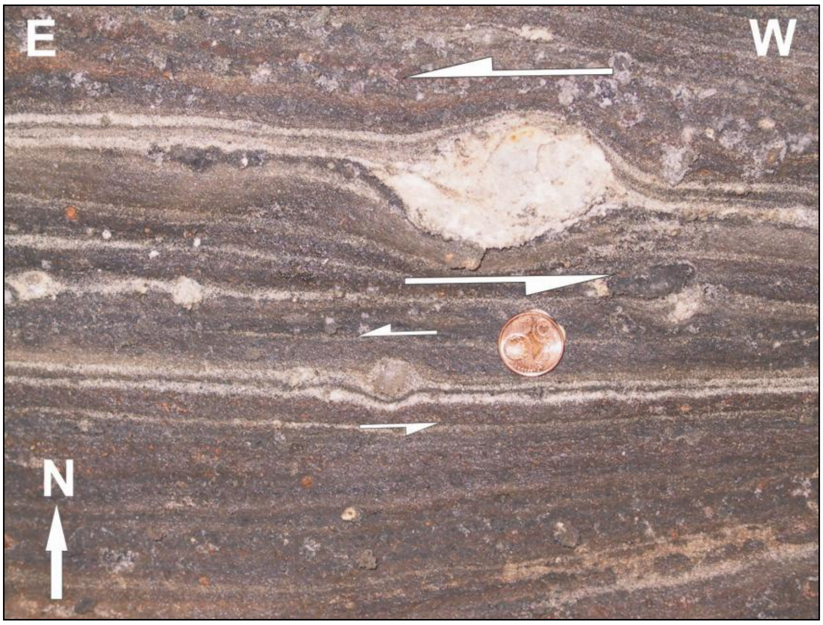

Fig. 4.7: σ-clasts on the tunnel`s roof at Maria Theresia Horizon (near Beustschacht), showing dextral shear sense (view upwards!). As described in the text the indicated sinistral shear sense has to be flipped to gain the correct sense in map view. The clasts in this picture consist of pure halite ("*Salzaugen*"), which is more competent than the salty-clayey matrix.

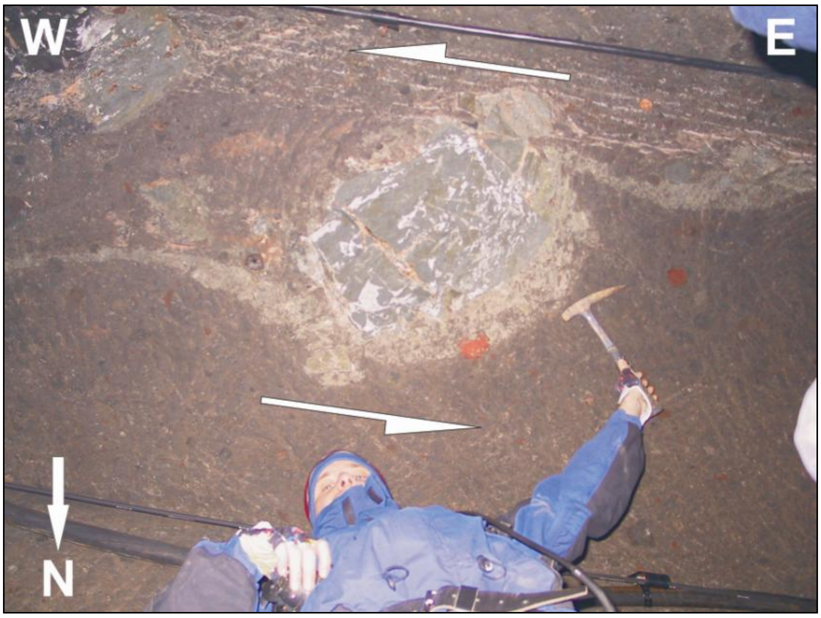

Fig. 4.8: δ-clast on the tunnel`s roof at Franz-Josef Horizon (800m west of the tunnels entrance). The clast, comprising of black shale, shows dextral shear sense (view upwards!).

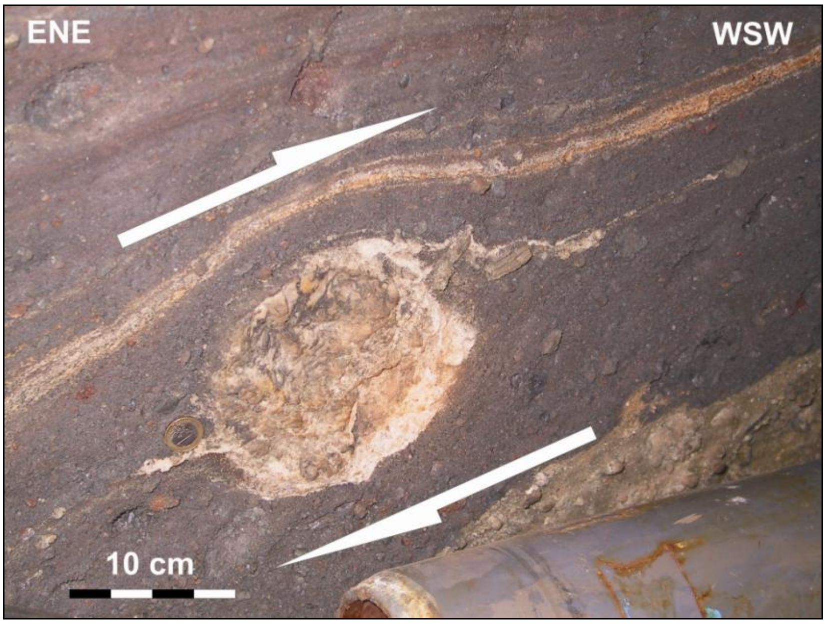

Fig. 4.9 δ-clast in Grausalz at the Franz-Joseph Horizon (580m west of the tunnel`s entrance). In contrast to the other shown clasts, this one is not situated on the roof and therefore the indicated dextral shear sense is the correct one! The dextral shear sense of this clast is determined by stairstepping of the wings. This clast shows stairstepping although it is almost parallel to the Foliation – perhaps a local stressfield with a different direction of extension is developed.

4.2.3 Isoclinal folds and cleavage

Stretching lineation that points out the direction of movement is not developed within the Haselgebirge of Hallstatt since halite is able to recrystallize very easily, overprinting primary existing lineation. However, in the most cases the axial planar foliation of tight or isoclinal folds in a high-strain mylonite cannot be distinguished from the main foliation (**see Fig. 4.10**; Passchier and Trouw, 1996). Such folds are known as oblique folds and commonly decrease in amplitude and fade out laterally. This indicates that the fold axis is parallel to the lineation and hence fold axes can be used to determine the direction of tectonic transport. Several authors (e.g. Jordan, 1994) used fold axes of isoclinal folds as kinematic indicators in evaporites.

An important fact is that there are obvious differences in the geometry of structures between sections cut normal and parallel to the stretching lineation. Sections normal to the lineation of a mylonite show relatively little deformation or orthorhombic structures, whereas in sections parallel to the lineation, the deformation fabric is much stronger and structures with monoclinic symmetry, which can be used as shear sense indicators, are common (**Fig. 4.10**; Passchier and Trouw 1996).

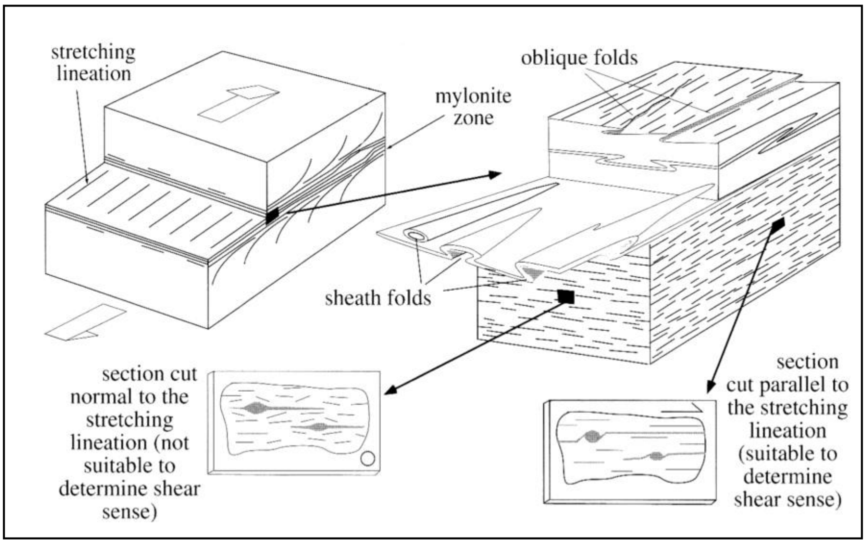

Fig. 4.10: Schematic diagram showing the geometry of a mylonite zone and the nomenclature used. Only sections that cut perpendicular to the foliation and parallel to the stretching lineation are suitable to determine the shear sense! (Passchier and Trouw, 1996)

In the Hallstatt salt mine the fold axes usually strike more or less horizontally in E - W direction, whereas the axial planes and axial plane cleavage are dipping steeply towards north and south (**see Fig. 4.3 and 4.4**).

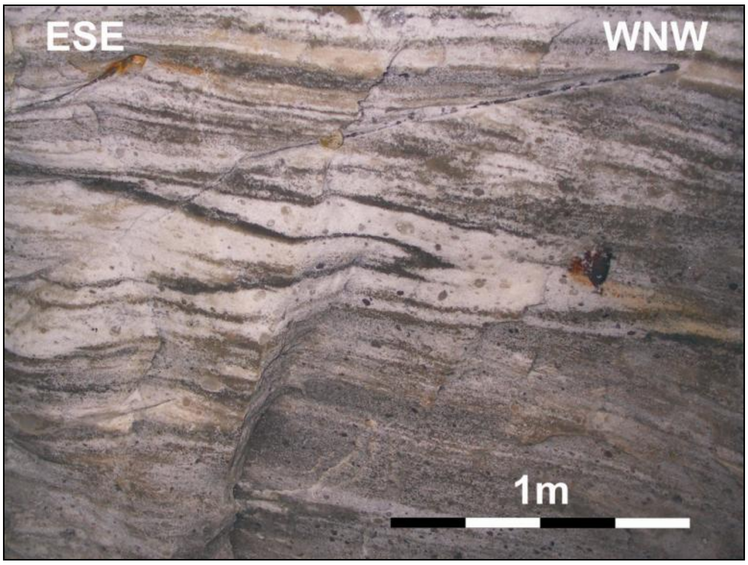

Fig. 4.11: Isoclinal folds in the mylonitic "*Liniensalz*" of the Haselgebirge, on the tunnel`s roof of Maria-Theresia Horizon (near Paussaner Ablass.). The subhorizontal fold axes (262/20) are used to determine the direction of shear.

Fig. 4.12: Isoclinal folds in "*Grausalz*" on the tunnel`s roof of the Christina Horizon (near Tuschwerk).
The fold axis is (128/30) indicates the direction of the shear.

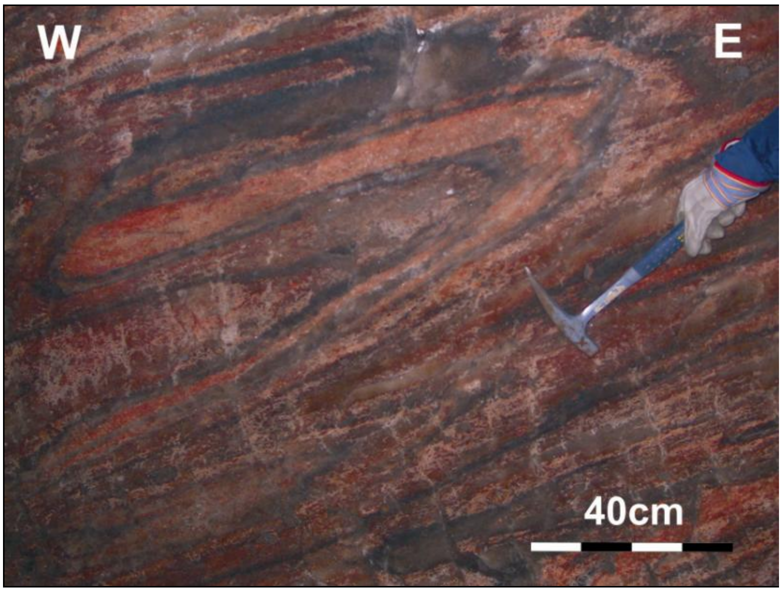

Fig. 4.13: Isoclinal fold in red Kernsalz at Elisabeth Horizon (near Beustschacht). The fold axis is (256/18) displays the direction of the shear.

Fig. 4.14: Isoclinal folds at Maria Theresia Hz. (Vernier Kehr). This mylonitic fold, developed in Kernsalz, shows second order S-shaped folds on the upper limb.

As mentioned already these E – W striking axial planes with subhorizontally fold axes and the dextral shear sense, proved from the mantled porphyroclasts suggest that the Haselgebirge structure of the Hallstatt salt mine is related to a major dextral strike-slip fault, which is in good accordance to the observed structures in the surrounding rocks and the shape of the 3D-model.

4.2.4 Fibrous veins, strain shadows and recent stress field

More deformation structures of the Haselgebirgs Melange are isolated and elongated fibrous veins and strain shadows. Many deformed rocks contain “dilatation sites”, as veins and strain shadows, which are interpreted as an effect of rearrangement of material by local dilatation and precipitation. The development of fibrous veins and strain shadows is associated with the circulation of fluids in the host rock. If the fluid pressure exceeds the smallest principal stress σ_3, dilatant conditions are achieved and voids can open and get immediately filled by fluids at any depth. The presence of tension gashes, veins that lie at a high angel to the extension direction, also implies that the differential stress in the rock was relatively small. Veins, including a small angel to the extension direction, are known as slickenfibres (e.g. along bedding planes in the case of flexural slip) (Passchier and Trouw, 1996).

Often void opening and filling is a continuously process during a deformation phase. In such cases, the evolving fibres of these veins and strain shadows can record information on the deformation path.

Four types of fibre growth in veins are common in nature. Divided by their geometric relation to the wall rock these are (Passchier and Trouw, 1996):

1. Syntaxial growth: The fibres are in continuity with the wall rock crystals and hence the oldest part of the fibres lies along the edge of the vein. A median line marks the final position of the growth surface.
2. Antitaxial growth: The fibres grow from the centre outwards. Consequently the oldest part of the vein is along the median line. Two growth surfaces develop, along the contact with the wall rock. Such veins usually consist of other material than the wall rock.
3. Composite growth: Composite vein types show both a syntaxial and an antitaxial component. At the contact between the different vein segments, where the youngest parts of the vein are situated, two growth surfaces are present.
4. Ataxial growth: The fibres are in continuity of the wall rock but lack a localized growth surface. Young and old parts of the fibres, which grow by repetitive fracturing at different sites, can be mixed throughout the vein. No median line is developed.

In many veins, fibres are supposed to be displacement controlled, that means that they usually grow in the opening direction of the vein and as a result the fibres record relative changes in movement direction of the wall rock and may form a curvature that can be used for kinematic analysis. Important is that syntaxial and antitaxial veins show mirror symmetry deflections due to their opposed growth directions. Composite veins prove both senses (**see Fig. 4.15**).

In the Haselgebirge of the Hallstatt salt mine the fibrous vein fillings are mainly comprised of halite and rarely of gypsum. Anhydrite, claystone or shales usually make up the wall rock. A lot of tension gashes were observed in the "*Blättersalzgebirge"* and the "*Tontrümmergebirge"*. The fibres of halite, both in veins and in strain shadows indicate the youngest deformation events and the recent stress field, as halite fibres tend to recrystallize very quickly. Some halite vein fillings of different growth show both fibrous and recrystallized parts even if it seemed not to be much difference in their age (**see Fig. 4.16**)

Fig. 4.15: Development of the four types of veins with displacement controlled fibres described above. A change in the relative orientation of the extensional ISA can cause curvature of the growing fibres which can be used for kinematic analysis. The sense of the curvature of the veins depends on the type of the vein (Passchier and Trouw, 1996).

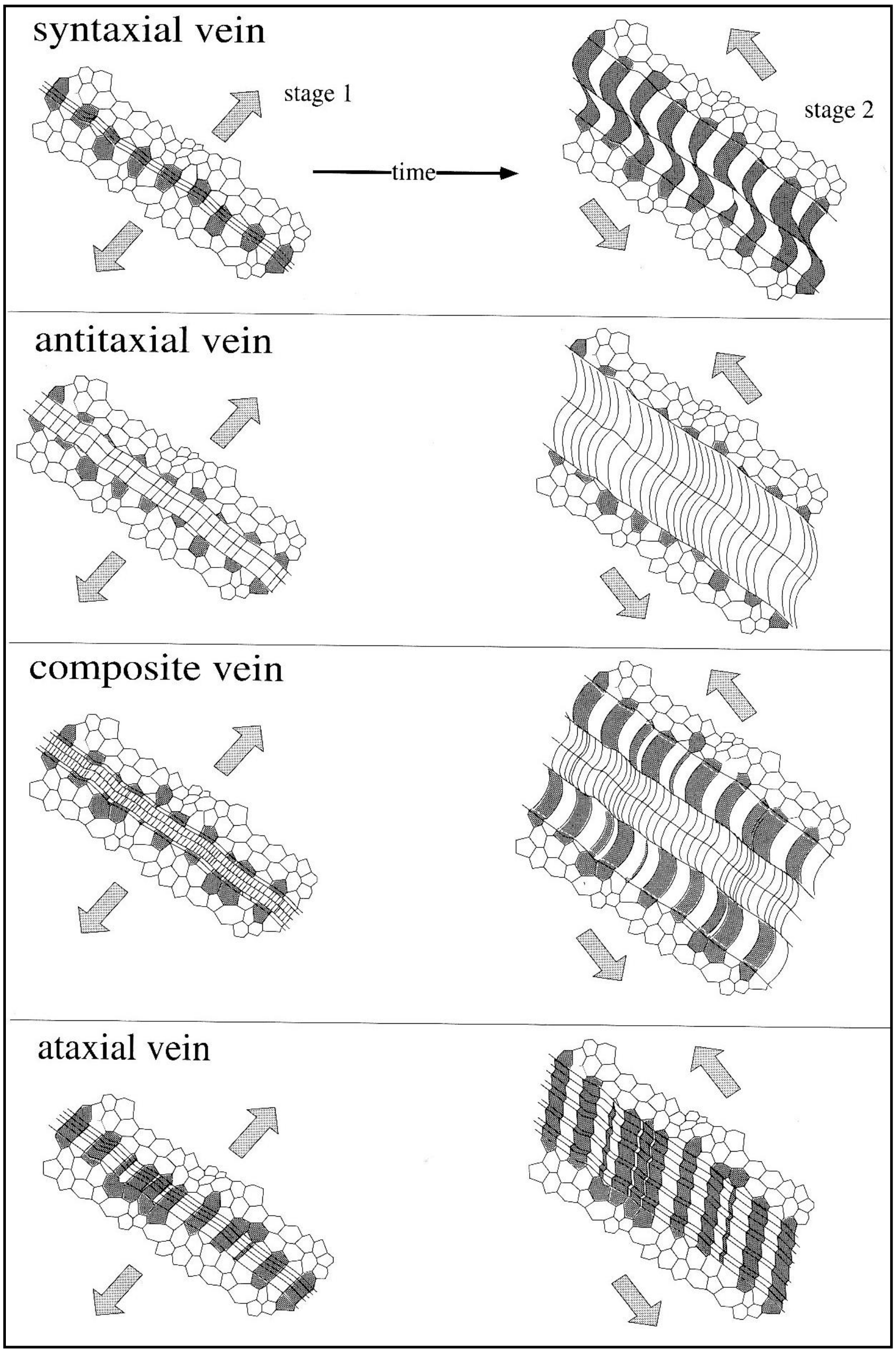

In contrast to the E – W trending mylonitic strike-slip structures, proved by the mantled porphyroclasts and the isoclinal folds, these youngest structural elements in the Hallstatt salt mine are created by extension in E – W and shortening in N – S direction. As a result the veins predominantly opened in E – W direction and if fibres are preserved they are elongated in the same direction. The veins commonly are only slightly rotated and feature no or slight curved geometry, hence a more or less coaxial deformation during their opening is assumed.

Fig. 4.16: Composite type vein at Elisabeth Horizon. The vein filling consists of halite, which is recrystallized in the older parts (inner red part; orange part on the left edge), whereas the fibrous fabric in the younger parts is well preserved.
The fibres (285/14) show the opening direction of the vein. Due to their light curved geometry a minor rotation of the stretching ISA during void opening is evidenced.

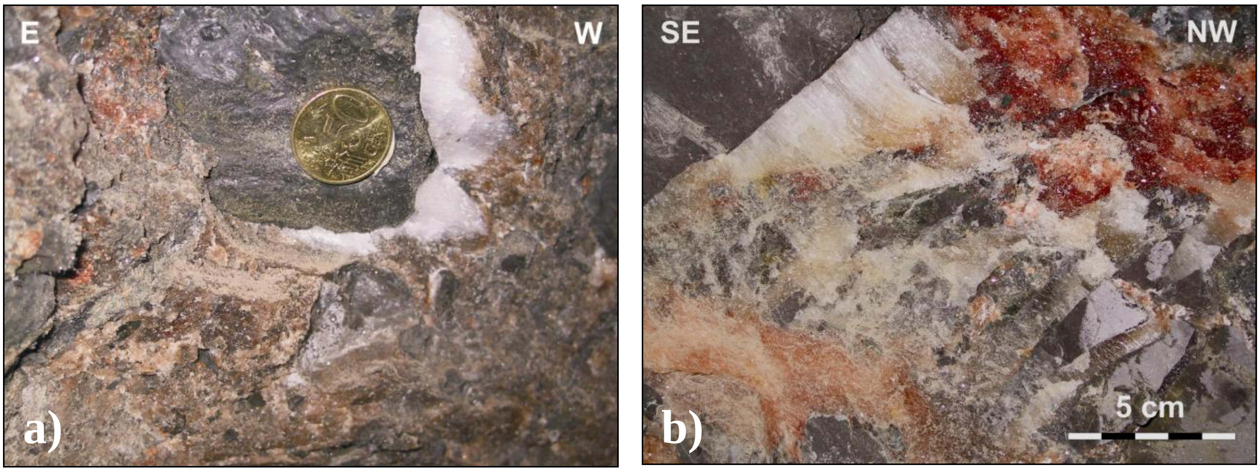

Fig. 4.17: Fibres of white halite in the strain shadows of clasts. a) A clast of black shale in "*Grausalz*" at Elisabeth Horizon (crossing of Kleinkehr and Schrammelkehr) showing fibres (234/20) of white halite in its strain shadow. b) Shows slightly curved fibres at the edge of an inclusion of black shale in "*Blättersalz*" at Elisabeth Horizon (Fleissnerkehr). The curved geometry of the fibres indicate a rotation of the stretching ISA during their genesis in the strain shadow of this inclusion but influenced by the clast (e.g. rotation of the clast) this has to be seen as very local phenomenon.

More evidences for the recent stress field in the Haselgebirge Melange, that show the same direction of shortening, are deformations of the equipment and the tunnels in the modern salt mine. For example rigid markers like rail tracks (on the tunnels bottom) do not show intense damages in E – W directed tunnels, whereas in N – S directed tunnels severe bending can be observed.

5. Microstructures

5.1 Introduction

In addition to the observations in the field, as well in the saltmine as in the covering carbonates several samples were taken and thin-sections were generated to gain detailed information about the microstructures. Especially the mechanics of deformation of the mainly brittle reacting carbonates and the more ductile reacting evaporites were investigated. Therefore samples were collected mainly in areas that record large displacement of the rocks, for example along major thrust faults in the Echerntal. Thin-sections of the Haselgebirge were only made from anhydrite- and clay-rich portions of the saltbody due the dissolvable character of halite (**see chapter 5.3**). To gain kinematically meaningful results the samples were taken orientated and thin-sections were cut parallel to main tectonic transport direction, indicated by the lineation. If a thin-section is cut parallel to the transport direction recognized in the field, shear sense observed in the field can be directly related to shear sense indicated by microstructures (Passchier and Trouw, 2005).

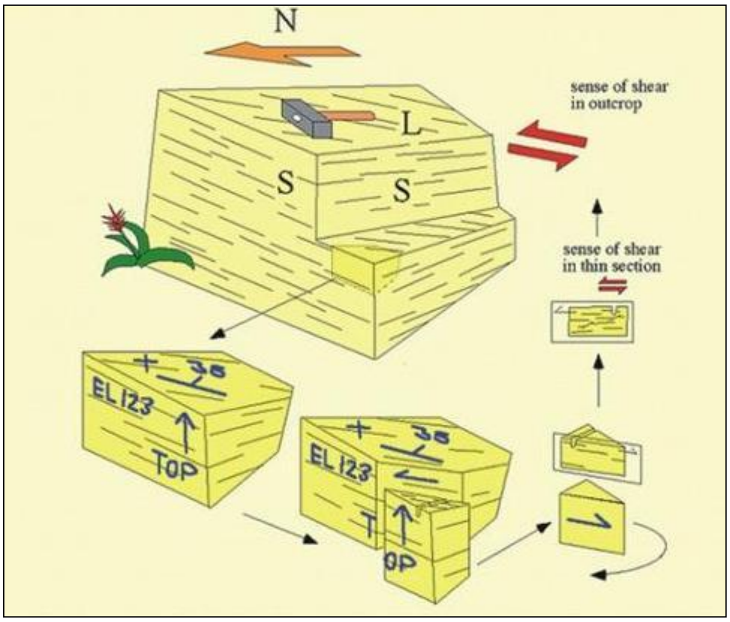

Fig. 5.1: This figure shows the correct method to take an orientated sample in the field and to produce an orientated thin-section from that sample (Passchier and Trouw, 2005).

- **The top of the sample and the direction of dip have to be marked.**
- **The chip cut out of the sample with a diamond saw has to be parallel to the lineation.**
- **An arrow indicating the top surface and the orientation is marked on both the chip and the sample**
- **This arrow has to be correctly reproduced on the thin-section**

Moreover some samples from the Haselgebirge that showed scratched and polished surfaces on clayey clasts were taken and examined under the scanning electron microscope (SEM) (**see chapter 5.5**).

5.2 Different deformation processes

Rocks can deform by various different deformation mechanisms. Which deformation process or which combination of processes occurs, depends mainly on chemical parameters (mineralogy of rocks and composition of intergranular fluids), physical parameters (temperature and pressure) and the strain rate (Grasemann and Fusseis, 2000). In this chapter a short compilation of the dominant rock deformation mechanics observed in the generated thin-sections is given. Starting from low temperature or high strain rates, like cataclasis or pressure solution, continuously leading to high temperature or respectively low strain rates, like mylonitic structures, twinning or dynamic recrystallisation.

The observed microstructures can be used to determine deformation conditions and mechanics. Different temperature and pressure conditions, sense of displacement and deformation history are reflected by typical fabrics and mineral aggregates. An important fact that must not be neglected is that due to the typical “weak” deformation behaviour of evaporites and shales, ductile mylonitic deformation mechanics happen at already relatively low temperatures in these rocks, as mentioned in **chapter 4.**

Generally the deformation in rocks is not spread homogeneously. A frequent type of heterogeneous deformation is a shear zone, which constitutes a planar high strain zone that accommodates the displacement of relatively rigid wall-rock blocks (Passchier and Trouw, 1996). Shear zones are classified into brittle shear zones (faults) and ductile shear zones. As seen in **Fig. 5.2**, ductile shear zones appear at higher metamorphic conditions than brittle ones do.

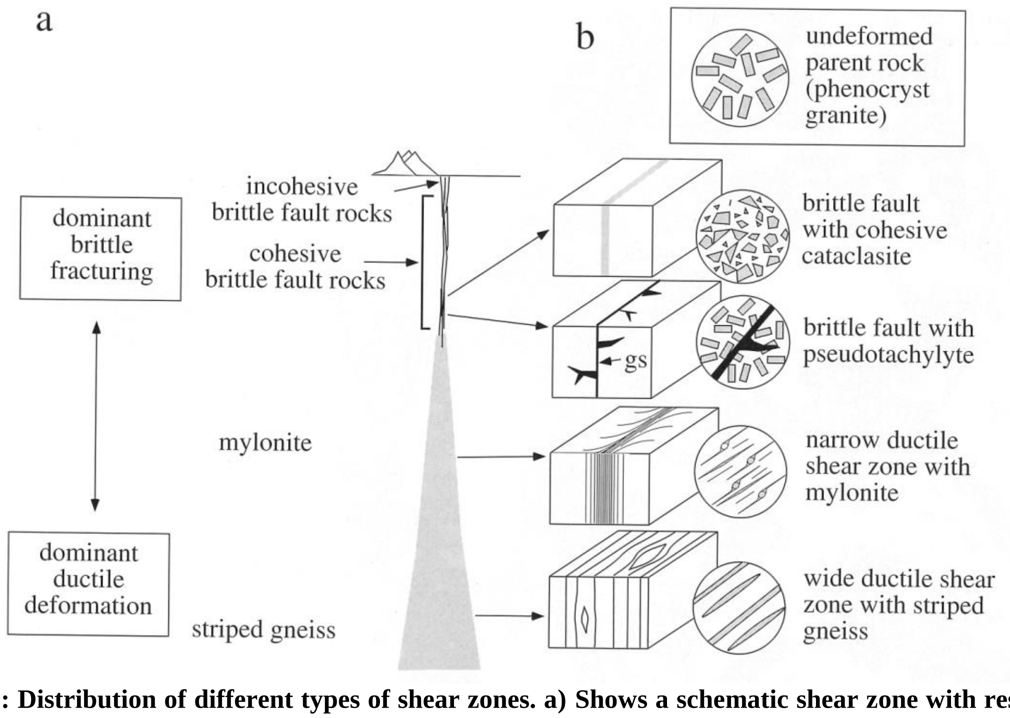

Fig. 5.2: Distribution of different types of shear zones. a) Shows a schematic shear zone with respect to the depth. b) Shows the different rock types that are generated in the shear zone with increasing depth and metamorphic grade based on a phenocryst granite as parent rock. The abbreviation “gs” means generation surface (Passchier and Trouw, 1996).

5.2.1 Cataclasis

Cataclastic flow happens under brittle conditions at low temperature and high strain rates. This process causes mechanical fragmentation of rocks and subsequent sliding and rotation of the generated components. Cataclastic flow is preferred under high fluid pressure conditions that are responsible for typical veins in cataclasites. Breccias, cataclasites and fault gouges, with different relations between fragments and fine grained matrix, are typical rock types that are dominantly generated by cataclastic flow. Breccias comprise more then 30% fragments within fine grained matrix, cataclasites less than 30% and fault gouges are indicated by only few large fragments isolated in the matrix. They take place along brittle fault zones that often show sharp borders to the undeformed host rocks (shear zones), whereas gradual decrease of the brittle deformation within the host rock is observed rarely (Passchier and Trouw, 1996).

In thin-sections cataclasites can be differentiated from ductile deformed rocks by:

- the large range of existing grain size
- fragments that show straight sharp boundaries and usually contain angular outlines
- the frequent occurrence of polycrystalline rock fragments

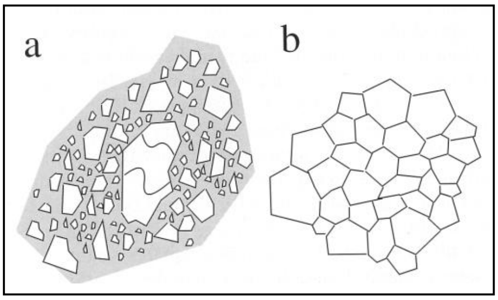

Fig.: 5.3:
a) Cataclastic fabric with components of all sizes, embedded in a fine grained matrix. Some fragments showing angular grain boundaries.
b) Shows a recrystallized fabric with little diversity of grain size in contrast (Passchier and Trouw, 1996).

5.2.2 Pressure solution

During the process of pressure solution components get dissolved at their grain boundaries at relatively high differential stresses. This happens at grain contacts that show a high angle to the instantaneous shortening axes (ISA). As the solubility of grains or minerals is higher under high stress material gets dissolved at grain contacts and redeposited at localities with relatively low differential stress. That may happen at adjacent pore spaces (as shown in **Fig. 5.4)** or otherwise after a solution transfer over a larger distance in sites like veins or strain shadows. Pressure solution occurs at diagenetic to low metamorphic conditions.

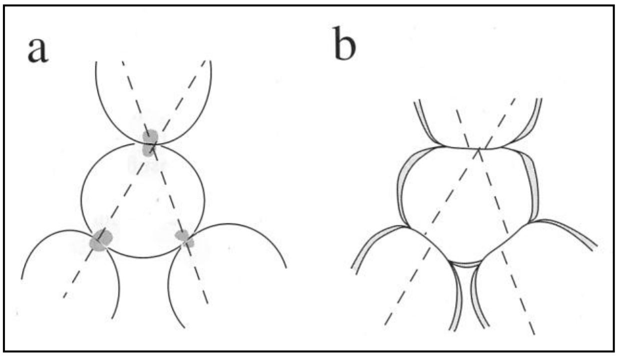

Fig.: 5.4:
a) At grain contacts the differential stresses are relatively high (indicated by the grey dots)
b) Pressure solution occurs at that points and affects the shape of the components. Dissolved material is redeposited in adjacent pore spaces (indicated by grey boundaries).
The marker lines crossing at the contacts of grains in a) seems to be displaced in b) due to the dissolved material (Passchier and Trouw, 1996).

In thin-sections pressure solution is indicated by truncated components, by surfaces rich in opaque and clayey minerals and by new grown minerals in strain shadows. The displacement along pressure solution layers is in most cases only an apparent offset due to dissolution of rock material (**see Fig.: 5.4**). An impressive example of pressure solution layers are stylolites that are very common in carbonates.

Stylolites form perpendicular to the maximum compressive stress, as pressure solution is facilitated under high stress. Compressive stress may be caused by overlying sediments, generating bedding parallel stylolites or by tectonic compression, inducing more horizontal transverse stylolites (Andrews and Railsback, 1997).

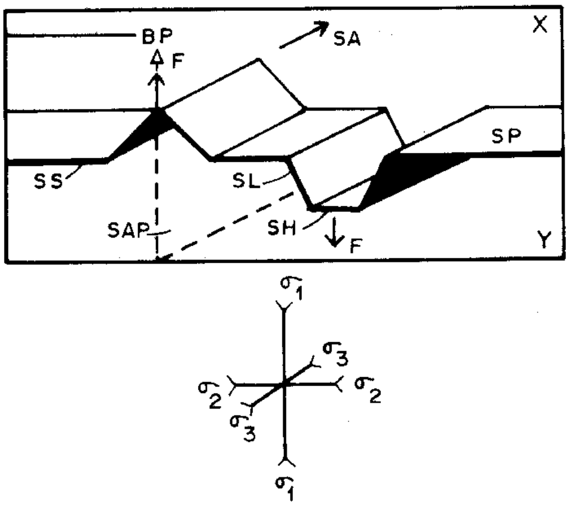

Fig 5.5: Profile of schematic stylolite showing the different parts of the stylolite in respect to the stress field (Sinha-Roy, 2002). The graphic below the schematic stylolite shows its stress system ($\sigma_1 > \sigma_2 > \sigma_3$). The other parameters used in this figure are:

BP	**bedding plane**
F	**stylolite facing**
SA	**stylolite axis**
SAP	**stylolite axial plane**
SH	**stylolite head**
SL	**stylolite limb**
SP	**stylolite plane**
SS	**stylolite seam**

As seen in the **Fig. 5.5** the stylolite faces in the main stress direction so the peaks of the stylolite can also be used as shear sense indicator, if they are generated in an oblique direction to the stylolite plane.

5.2.3 Intracystalline deformation

Commonly crystals show anomalies in their lattice. Such lattice defects can be subdivided in point defects and line defects. Point defects show vacancies or interstitials with missing or added lattice points. Line defects are additional half lattice planes that cause an edge dislocation at their end. During intracrystalline deformation dislocations within the crystal lattice migrate through the crystal. If the dislocation migrates along a plane through the crystal it is called dislocation glide. Dislocations are described by the Burgers vector that determines the direction and minimal amount of displacement.

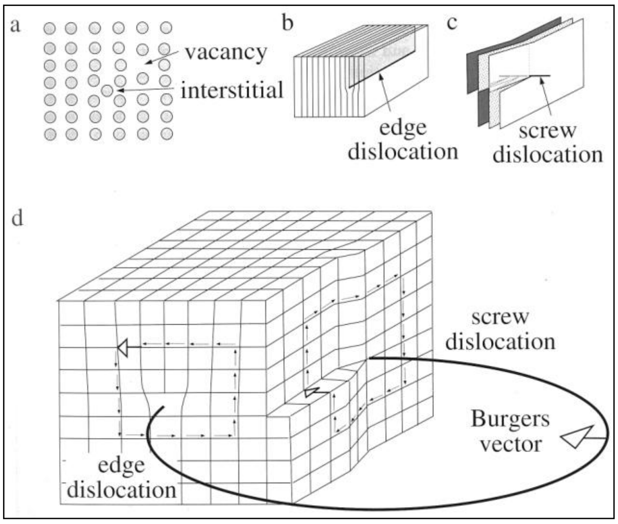

Fig. 5.6: Chrystal lattice defects (Passchier and Trouw, 1996)

a) Shows the two different possibilities of point defects

b) Shows an edge dislocation caused by a distorted half lattice plane.

c) Shows a screw dislocation that is defined by a twisted lattice.

d) Shows screw and edge dislocation areas in a crystal. A marker grid (small black arrows) is used to determine the Burgers Vector marked by the open arrows.

An important effect of intracrystalline deformation is the development of a lattice preferred orientation (LPO), which is the result of preferred migration directions of dislocations through the crystal. Due to that the crystallographic orientation of rock building minerals develops in a preferred orientation too.

In thin sections crystals are observed that show undulose extinction, which means they do not extinguish homogeneously in the microscope with crossed polars. LPO indicates dislocation creep.

5.2.4 Deformation or mechanical twinning

Some minerals create deformation twinnings in addition to dislocation features. Twinning can only happen in specific crystallographic orientations and furthermore only a relatively small amount of strain can be accommodated. Therefore twinning usually occurs in addition with other mechanisms like pressure solution, dislocation creep or recrystallisation. Twinning is a process that happens at low temperature most likely in plagioclase or calcite minerals.

In contrary to growth twinnings, mechanical twinnings, which are originated if stress rises above a critical value, mainly are tapering at the end. The twin boundary act as a mirror plane and separates the undeformed (untwinned) part from the twinned the area.

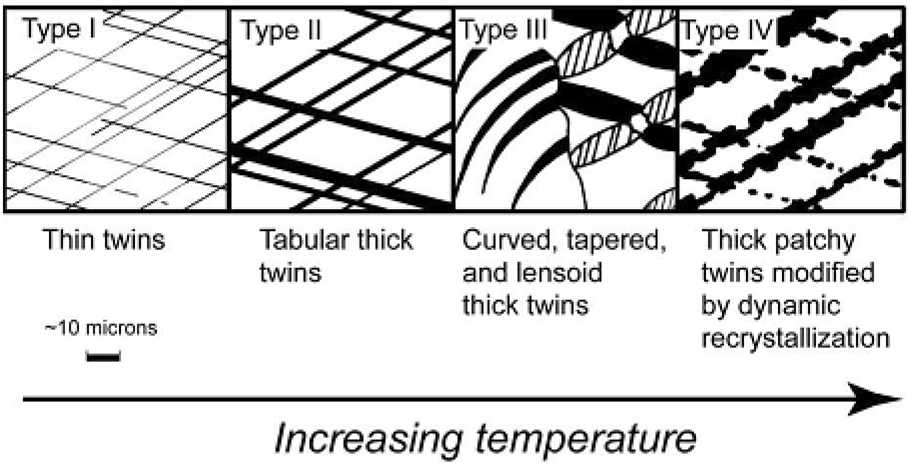

Fig. 5.7: Schematic deformation twinnings of calcite in respect to increasing temperature (Ferrill et al., 2004; after Burkhard, 1993).

5.2.5 Dynamic recrystallisation

If two chemical identic crystals with different dislocation density are neighbours, the atoms of the more deformed crystal (high dislocation density) are displaced slightly to fit to the lattice aggregate of the crystal with low dislocation density. As a consequence the grain boundary is moved and the less deformed crystal grows at the cost of the more deformed one. This process is called grain boundary migration – recrystallisation (GBM). Due to the migration the grain boundary may bulge into the adjacent crystal and form new small crystals. Rarely small isolated nucleates grow within a strongly deformed crystal, decreasing the dislocation of the aggregate. These processes that lead to a reorganization of the deformed material are called bulging and are shown in **Fig. 5.8**. If crystals are nearly completely substituted by their neighbour so-called "left-over" grains may remain. Their identical lattice orientation indicates the existence of a primarily larger grain (Jessell, 1986)

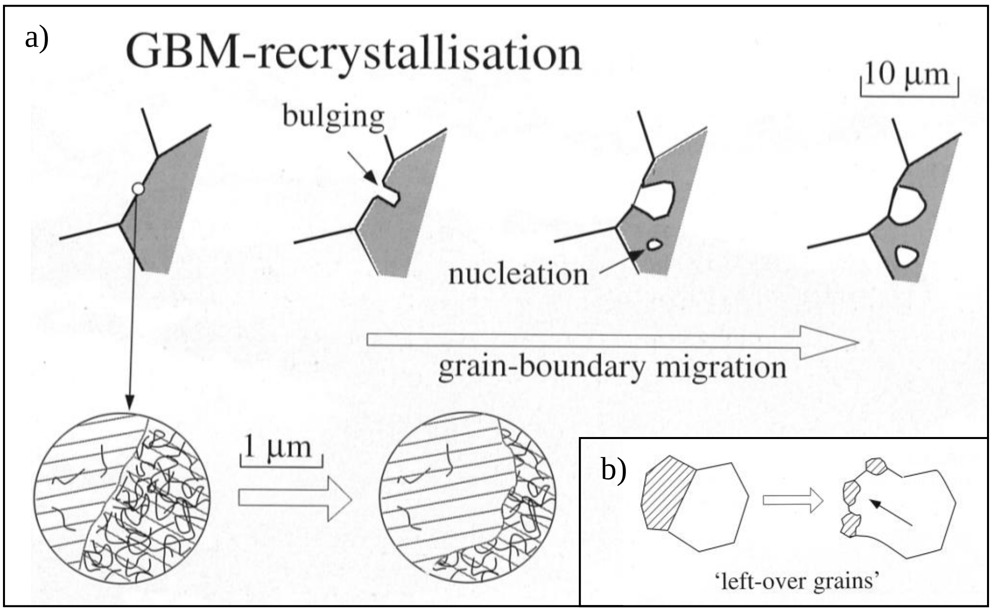

Fig.5.8: a) Grain Boundary Migration (GBM): Different dislocation density of neighbouring crystals leads to bulging into the grain with the higher dislocation density. Even the nucleation of a new isolated crystal within a strong deformed crystal (high dislocation density) is possible. (Passchier and Trouw, 1996)
b) After proceeding GBM only little fragments of the primarily crystal are left-over, showing the same lattice orientation on (Passchier and Trouw, 1996, after Jessel, 1987)

The 2nd type of dynamic recrystallisation is subgrain rotation recrystallisation (SR) where a subgrain rotates due to migration of dislocations into the subgrain wall. Due to this rotation an angle between the lattice orientation on both sides of the subgrain develops and with progressing deformation a new crystal is evolved.

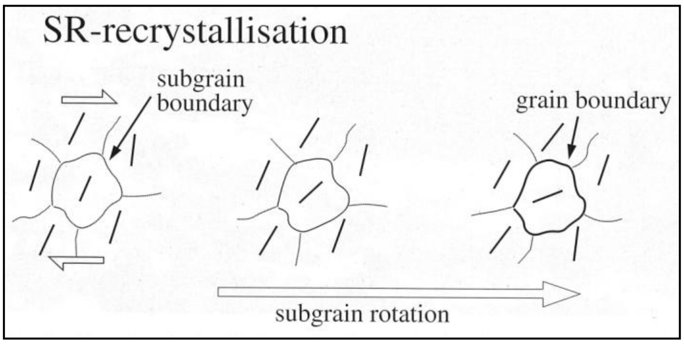

Fig.5.9: Subgrain rotation due to progressing migration of dislocations leads to the development of a new crystal. The black bars show the lattice orientation of the subgrains.

In thin-sections typical microstructures that evidence dynamic recrystallisation are aggregates of larger grains with undulose extinction that show subgrains and smaller crystals of roughly same grain size (similar to the size of subgrains). Due to the uniforlm size of the new grains after recrystallisation, a completely recrystallised fabric sometimes is hardly to distinguish from an equi-granular fabric that has not been recrystallised (Passchier and Trouw, 1996). Nevertheless dynamic recrystallised rocks usually show in addition to quite consistence grain size, evidence of internal deformation and lattice preferred orientation.

5.2.6 Static recrystallisation

Grain boundaries are, similar to lattice defects, areas of internal free energy in crystals. Decreasing the total surface of grain boundaries leads to reduction of the free energy. For this purpose straight grain boundaries and large grains are best fitting fabrics. Grain boundary area reduction often happens post deformative and especially in mono-mineralic rocks or rock fragments it will lead to the development of triple junctions with interfacial angles of about 120°. This process that minimizes the free energy of the system is called **static recrystallisation** or **annealing**.

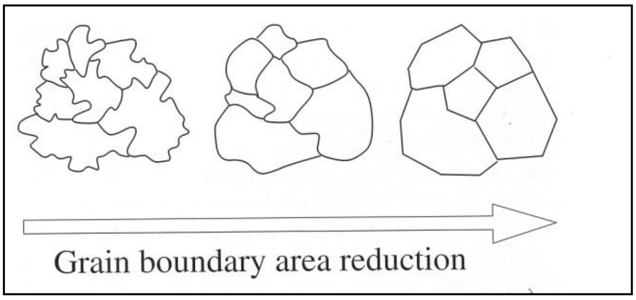

Fig. 5.10: Process of grain boundary area reduction, tackled by straightening grain boundaries and growth of the grains. Irregular grain boundaries established during deformation and dynamic recrystallisation (Passchier and Trouw, 1996)

5.3 Thin-sections of Dachstein Limestone in the Echerntal

The most instructive samples from the Dachstein Limestone at the northern slope of the Echerntal are shown and described in this chapter. The typical deformation features within the carbonates are cataclasis, pressure solution and partly deformation twinning. The samples in the field were mainly taken along main thrust faults were deformation appears stronger due to the movement along these faults. **Fig. 5.11** shows the location of the thin-sections in the field area (northern slope of the Echerntal).

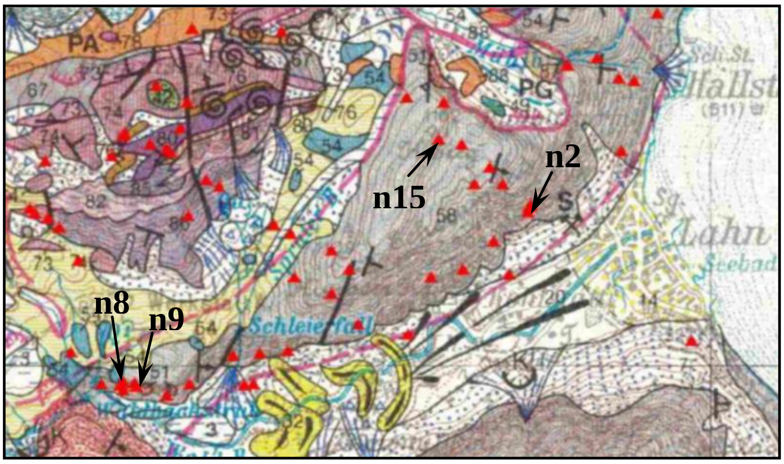

Fig. 5.11: Detail of geological map (Schäffer, 1982). The black arrows mark the outcrop points of the described thin-sections within the Dachstein Limestone.

5.3.1 Thin-section n2

Thin-section **n2** that originates from a sample of Dachstein Limestone taken in the frontal part of the Echerntal shows an ultra cataclastic fabric. The progressive evolution of cataclastic flow led to an ultra cataclasite fabric by grain size reduction and fluid processes. Already cataclastic deformed and partly cemented material broke up again into smaller grains to accommodate the displacement. The brownish coloured areas show the interaction between cataclastic deformation and fluid processes, facilitated by pressure solution. The fluids within the limestone cemented the components after cataclasis. Otherwise calcite veins of crystallised fluids got broken up again by the ongoing cataclastic flow.

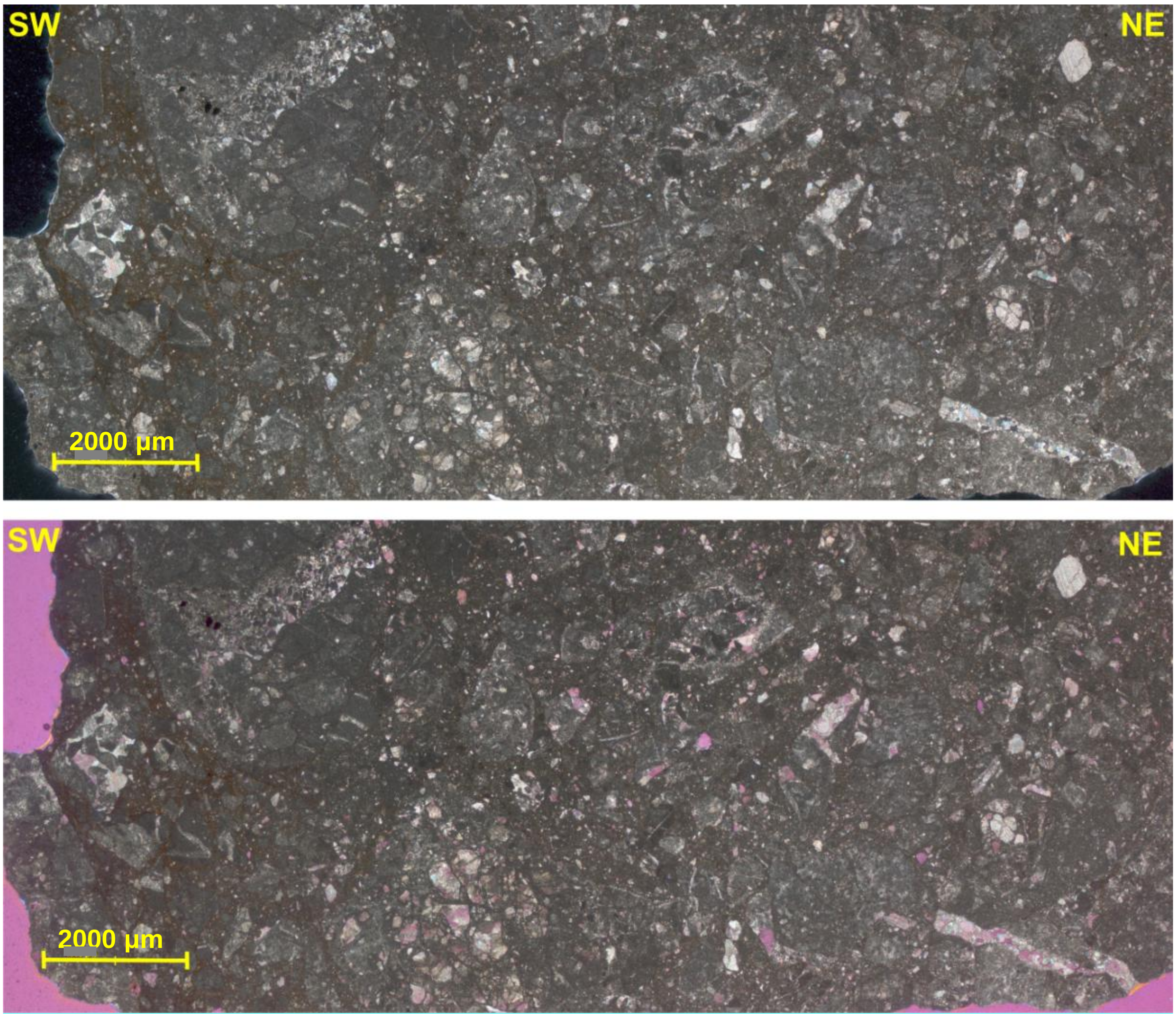

Fig 5.12: n2: Overview of an ultra cataclastic fabric within the thin-section n2 of Dachstein Limestone in the frontal Echerntal. Angular fragments of different grain sizes exist. Already cemented areas of the cataclasite broke up again and also older veins, filled with calcite, are fractured by ongoing cataclastic flow (see at right bottom). The upper picture is photographed under crossed polarised light (CPL), the lower one with inserted gypsum plate.

5.3.2 Thin-section n8

The thin-section n8 originates from the westernmost part of the Echernwand. The sample was taken nearby an obvious thrust plane. The fossil bearing Dachstein Limestone shows partially cataclastic flow and distinctive pressure solution that also makes up a sc-fabric (s: shear band; c: cleavage) indicating dextral shear sense with top to west movement (**see Fig. 5.15**). Within this carbonate different generations of veins are observed and the calcite vein-fillings show deformational twinning. The older generation of veins shows recrystallised small and slightly contaminated grains, whereas the younger ones are characterized by larger blocky grains. Syntaxial vein growth is observed as in the outer parts of expanded veins the calcite crystals are recrystallised and the inner parts show the younger generation with larger grain sizes and relatively fresh deformational twinnings.

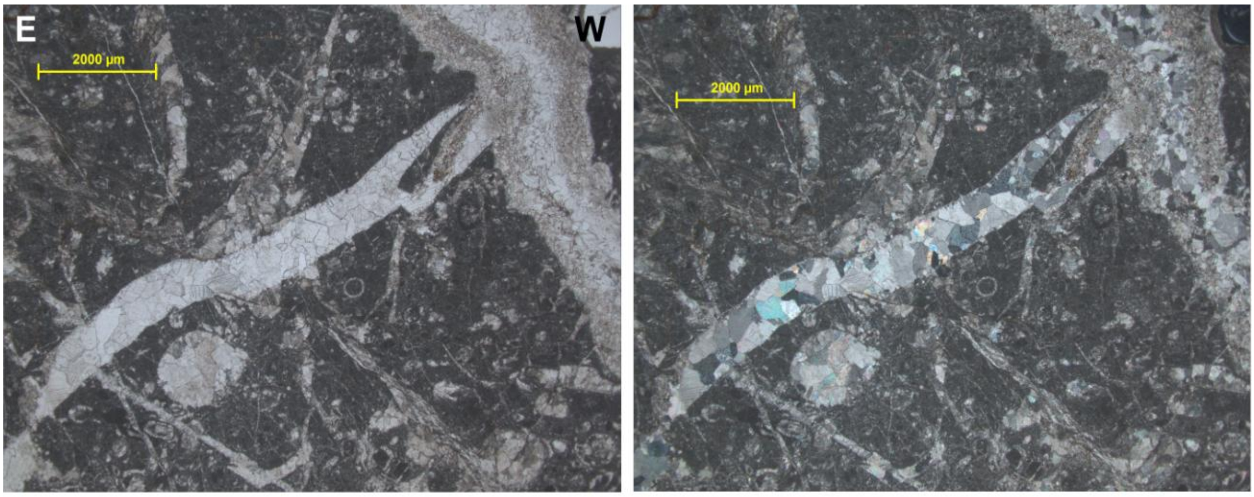

Fig. 5.13: n8: Fossil bearing Dachstein Limestone fractured under cataclastic flow with distinctive fluid interaction. Calcite vein fillings show different generations and syntaxial growth. Right picture is taken under CPL.

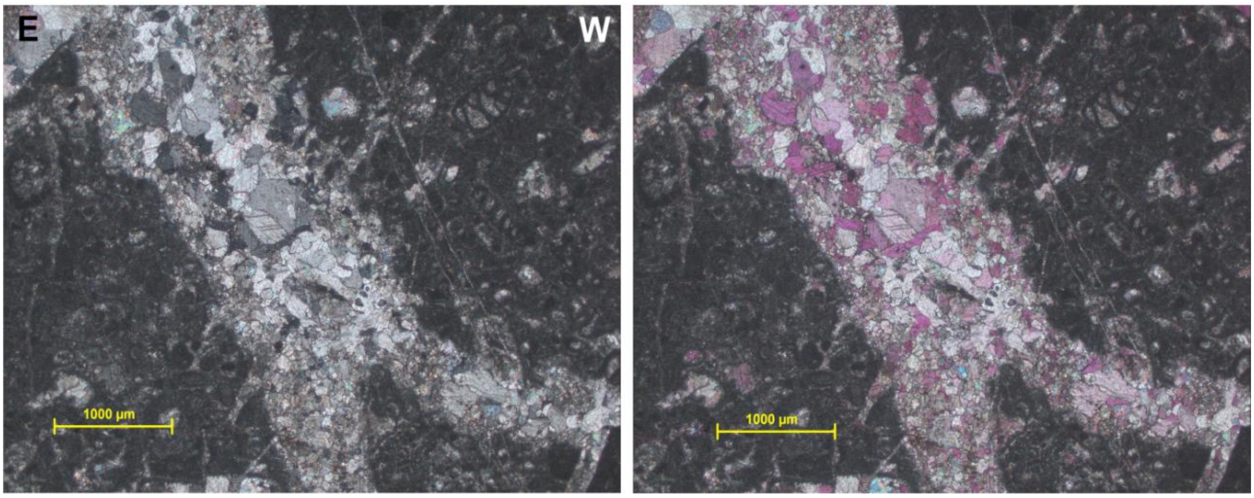

Fig. 5.14: n8: Showing a vein with recrystallised calcite in its older outer parts, whereas in the centre of the vein larger crystals of calcite with fresh deformational twinnings take place (syntaxial vein growth). The left picture is taken under CPL, the right one with inserted gypsum plate.

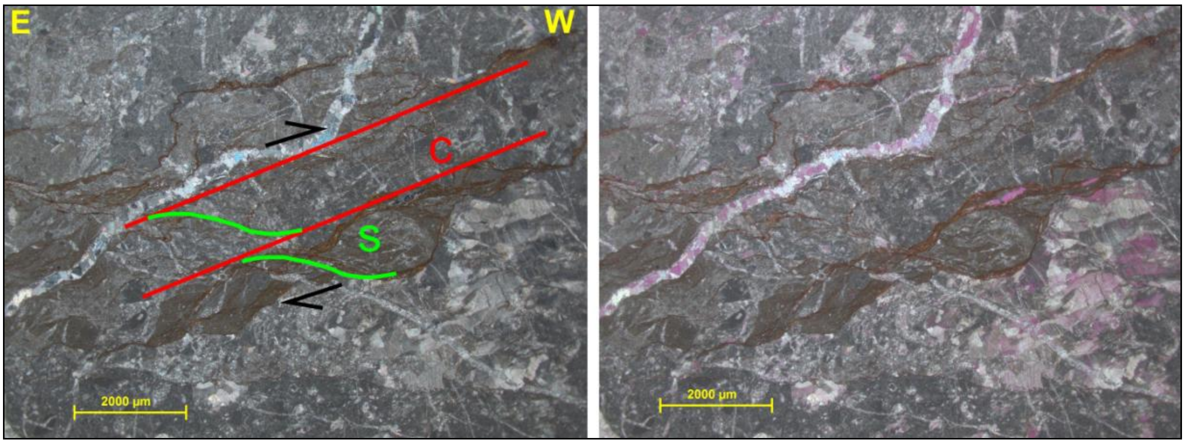

Fig. 5.15: n8: Pressure solution generates a cleavage (c) and shear bands (s) that indicate dextral shear sense with top to W movement during deformation. Left picture taken under CPL, the right one with inserted gypsum plate

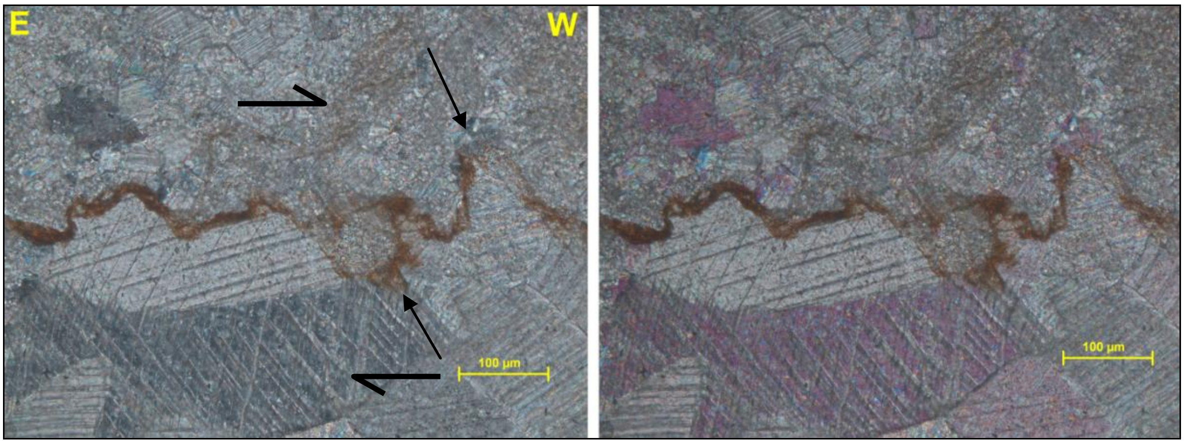

Fig. 5.16: n8: Stylolite and calcite twinning. Peaks of the stylolite face oblique to the stylolite plane against the main stress direction, indicating dextral shear sense with top to W movement as well. Left picture taken under CPL, right one with inserted gypsum plate.

5.3.3 Thin-section n9

Thin-section n9 was taken from a brownish-red coloured Dachstein Limestone in the western part of the Echernwand. This clayey fine grained carbonate is rich in fossils and shows cataclastic flow, filled veins and pressure solution interaction. Stylolites run through the whole section and produce apparent displacements at significant colour changes and veins due to the dissolution of material (**see Fig. 5.17**).

Different generations of veins are observed and cross cutting relationships are shown (**see Fig. 5.18 and 5.20**).

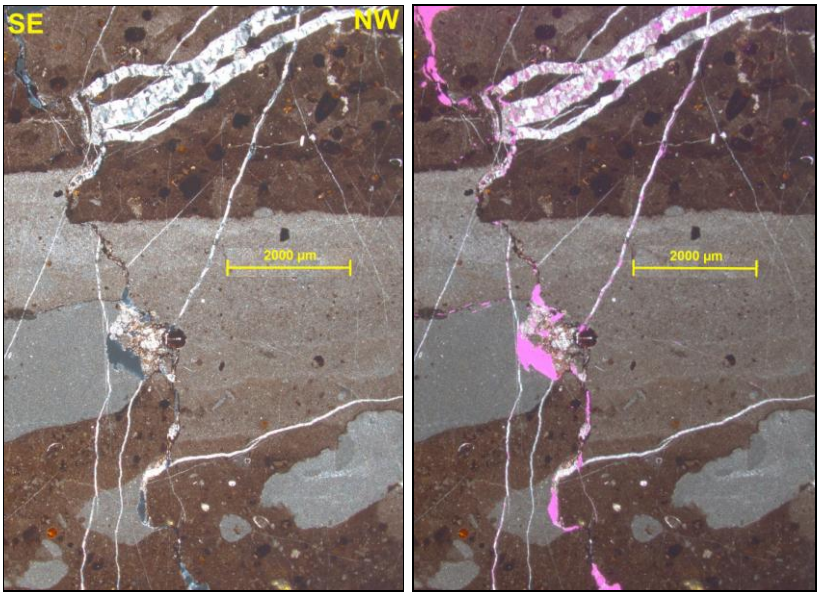

Fig. 5.17: n9: Fossil bearing cataclastic deformed limestone. Stylolite cuts through the whole section, creating an apparent displacement due to dissolution of material. The big vein on top of the picture shows fibrous calcite crystals and is cut by the younger distinctive stylolite. The left picture is taken under CPL, the right one with inserted gypsum plate.

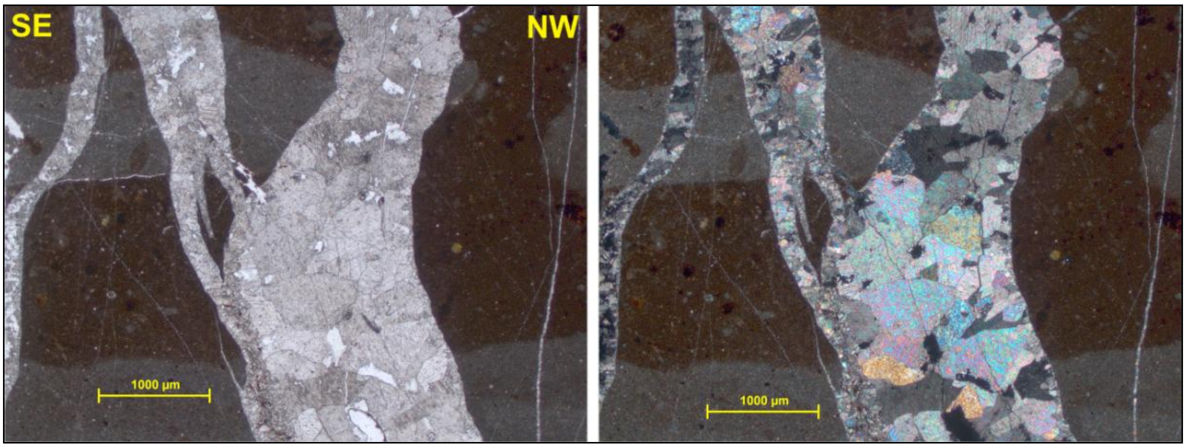

Fig. 5.18: n9: Different generations of calcite filled veins within cataclastic deformed limestone. The large vein in the centre is characterized by fine grained recrystallisation in outer parts and younger blocky crystals, partly showing deformation twinnings, in the inner part. The right picture is taken under CPL.

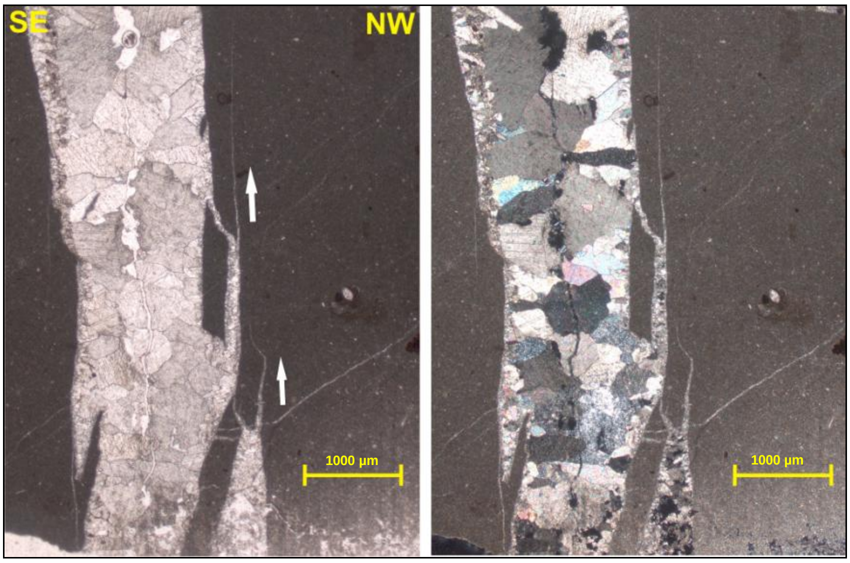

Fig. 5.19: n9: Linking of vein sets. During propagating of faults in the carbonate (marked by white arrows) the crack/vein gets linked with the already existing vein and includes "xenolites" of limestone after coincidence. The grain size of the calcite filling depends on the width of the veins. The right picture is taken under CPL.

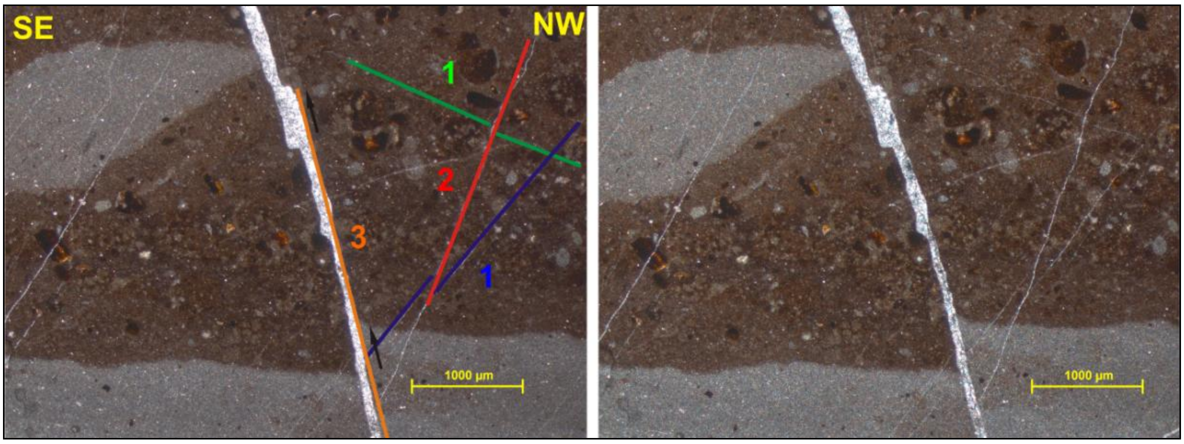

Fig. 5.20: n9: Cataclastic fine grained carbonate that shows at least 3 different generations of vein sets. The vein in the centre of the picture (Nr. 3) shows a real displacement marked by the black arrows. Right picture is taken under CPL.

5.3.4 Thin-section n15

Thin-section n15 originates from a sample of the extremely steep dipping Dachstein Limestone near the top of Hohe Sieg. The main deformation mechanisms are again cataclastic flow and pressure solution. Pressure solution cleavage cuts the components of the cataclasite linearly but also surrounds angular cataclastic fragments. Therefore pressure solution occurred during and after cataclastic flow. As seen in **Fig. 5.22** fibrous veins that are partially recrystallised to smaller grains that show unique extinction.

Furthermore apparent displacement of veins due to younger stylolites and crosscutting relationships of different vein generations are observed. Veins with larger grain size usually are younger and penetrate older veins.

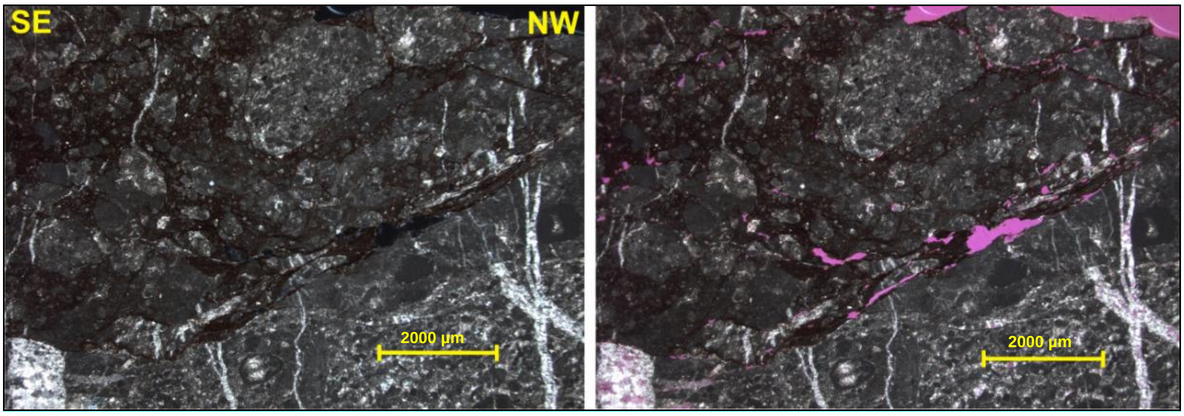

Fig. 5.21: n15: Pressure solution cleavage cuts the cataclastic fabric straight but also surrounds angular cataclastic fragments, indicating that the pressure solution process during and after cataclastic flow. Left picture is taken under CPL, the right one with inserted gypsum plate.

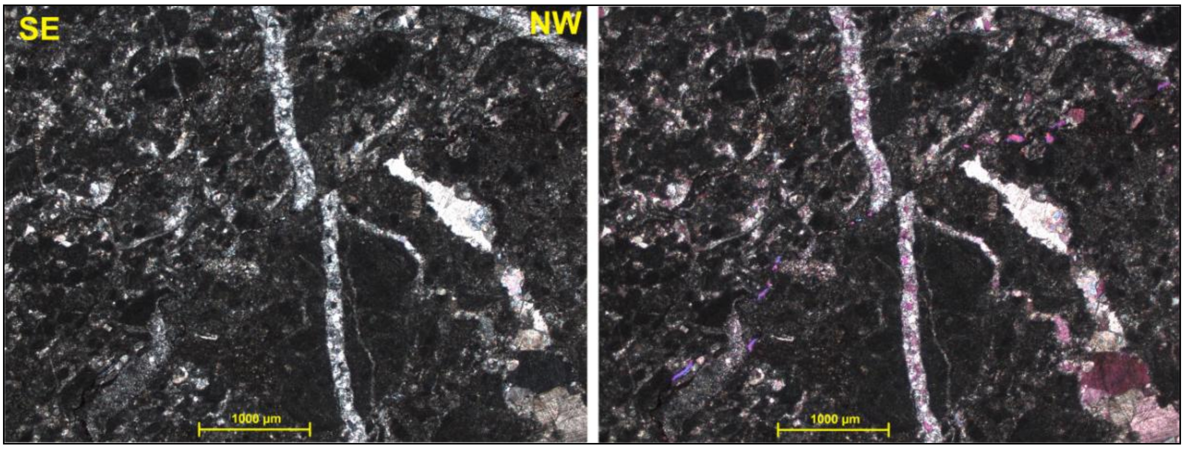

Fig 5.22: n15: Vein shows fibrous calcite crystals that are partly recrystallised. Those smaller grains show unique extinction as the original crystal did. The displacement of the vein is caused by younger pressure solution as a stylolite cuts through these older features. Left picture is taken under CPL, the right one with inserted gypsum plate.

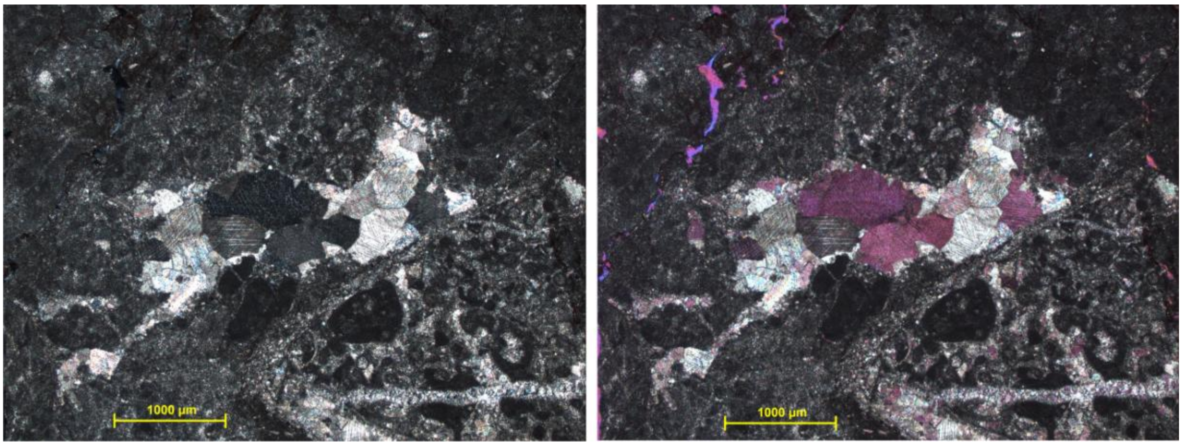

Fig. 5.23: n15: Large calcite crystals that show deformational twinning and recrystallisation, indicated by the fine grained calcite at the border of the blocky material. Left picture is taken under CPL, the right one with inserted gypsum plate.

5.4 Thin-sections of anhydrite and "*Glanzschiefer*" within the Haselgebirge

Within the Permian Haselgebirge thin-sections were cut out of samples of anhydrite and "*Glanzschiefer*" (clay slates). To create thin-sections within more salt-rich parts of the Hallstatt saltbody is rather difficult due to the high solubility of salt.

The dominant deformation processes observed within the Permian Haselgebirge are deformation twinning, dynamic recrystallisation (GBM) and pressure solution. Some of the structures observed in the thin-sections also appear at larger size and are already described in **chapter 4 Salt tectonics**. In addition to the photographs of thin-sections one picture of a mylonitic deformed anhydrite at a scale of few centimetres is shown in this chapter (**see Fig. 3.35**).

Several thin-sections are taken orientated and of course show shear sense indicators. These shear sense indicators have to be regarded with suspicion due to differences of displacement directions that are caused by local stress changes (e.g. strain shadows of big inclusions) and considerable rheology differences.

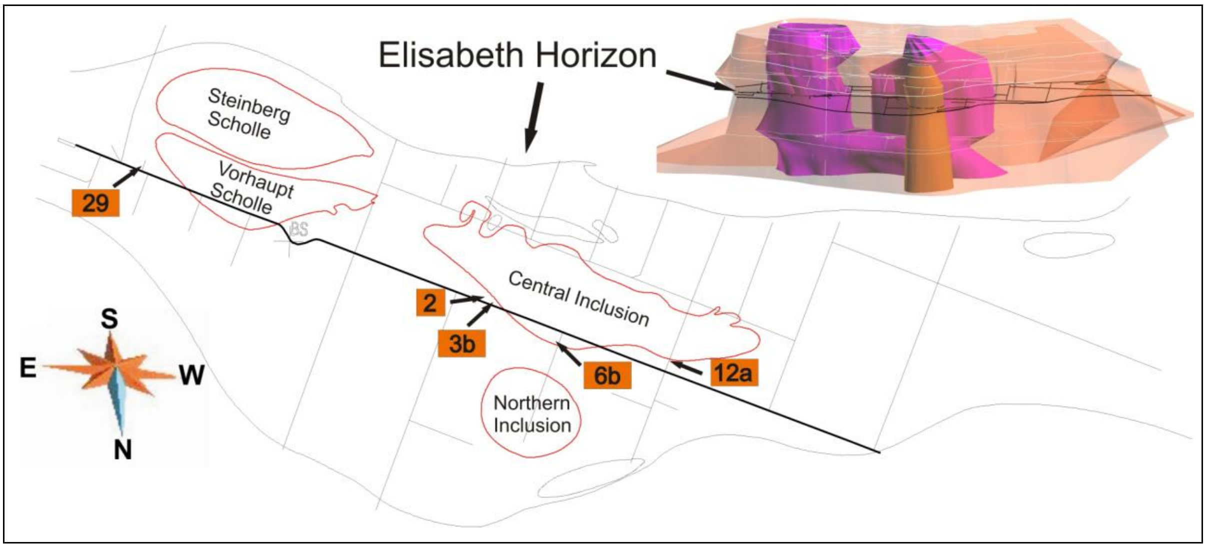

Fig. 5.24: Distribution of generated thin-section within the Hallstatt saltmine. Several samples described in this chapter were taken in the Elisabeth Horizon that is shown in top view in this figure and is marked black in the 3 times exaggerated 3D-model of the Hallstatt salt deposit at the right top.

5.4.1 Thin-section 6b

The thin-section 6b shows a "*Glanzschiefer*" from the border area of central inclusion, comprising of Hallstatt Limestone, and the Permian Haselgebirge. Deformation mechanisms of this fine grained clay-slate are cataclastic flow and displacement along shear bands. Quartz crystals enclosed in this thin-section show clear extinction and no hints of ductile deformation. Consequently the temperature conditions of this fabric reach at maximum peak of up to 280°C. The "*Glanzschiefer*" is characterized by lot of micro-slickensides along which the clayey material is sheared and polished surfaces are created that give the dark coloured slates their shiny appearance.

With exception to some relics of salt (most of it is dissolved in this material) the microstructures indicate that no ductile deformation occurred in this rock.

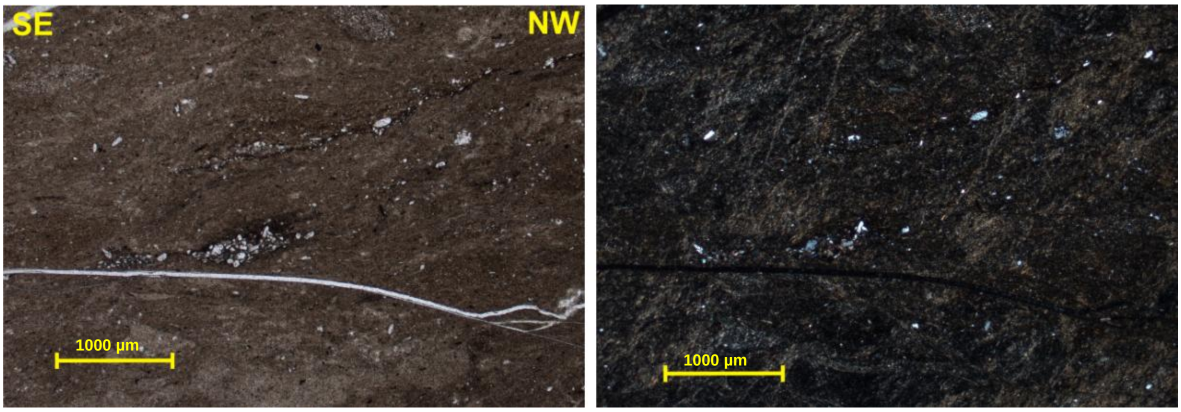

Fig. 5.25: 6b: Fine grained clay slates („*Glanzschiefer*“) showing quartz crystals that have not undergone dynamic recrystallisation. No evidences of ductile deformation in this thin-section (except relics of salt). The right picture is taken under CPL.

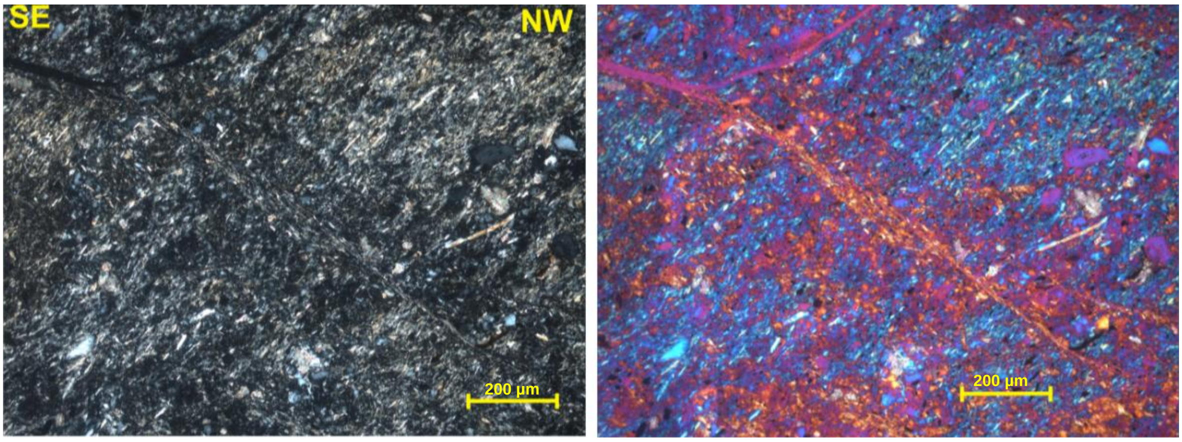

Fig. 5.26: 6b: Shear bands and cataclastic flow cause the generation of micro-slickensides that give the „*Glanzschiefer*“ its typical appearance. The phyllosilicates are adjusted in the shear band running from the left top to the right bottom of the pictures. The left picture is taken under CPL, the right one with inserted gypsum plate.

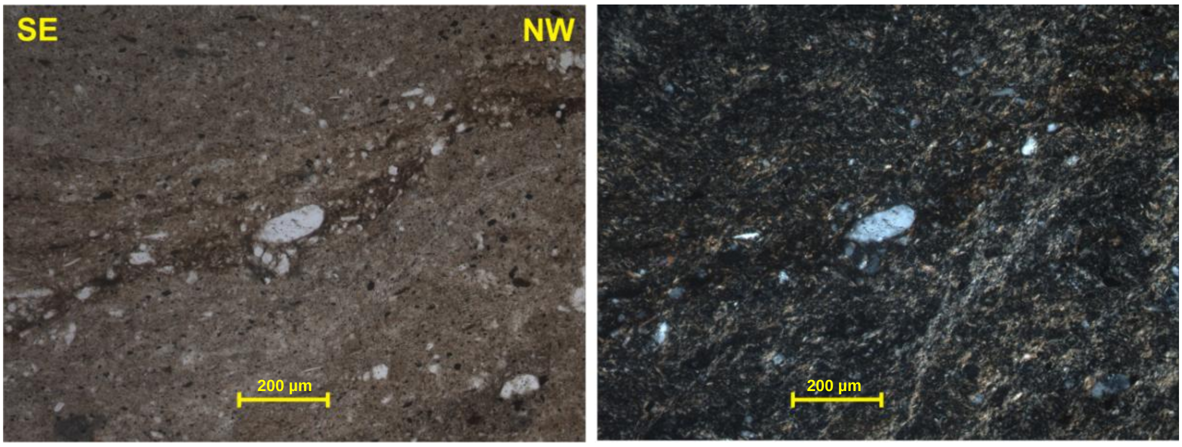

Fig. 5.27: 6b: Idiomorphic quartz crystals that show clear extinction limit the temperature condition during deformation of this rock with max. 280°C. The material is sheared under cataclastic flow. The right picture is taken under CPL.

5.4.2 Thin-section 3b

The thin-section 3b originates from so called "*Liniensalz*" near the northern boundary of the Central Inclusion. This sample shows the rheological contrast between clayey layers, which react more competent, and salt-rich portions that deform ductile. In this mylonitic fabric typical shear sense indicators like stairstepping of salt cleavage around rigid clasts, folded and rotated older generations of veins and rigid fracturing of the more competent layers or clasts within the ductile reacting matrix are observed.

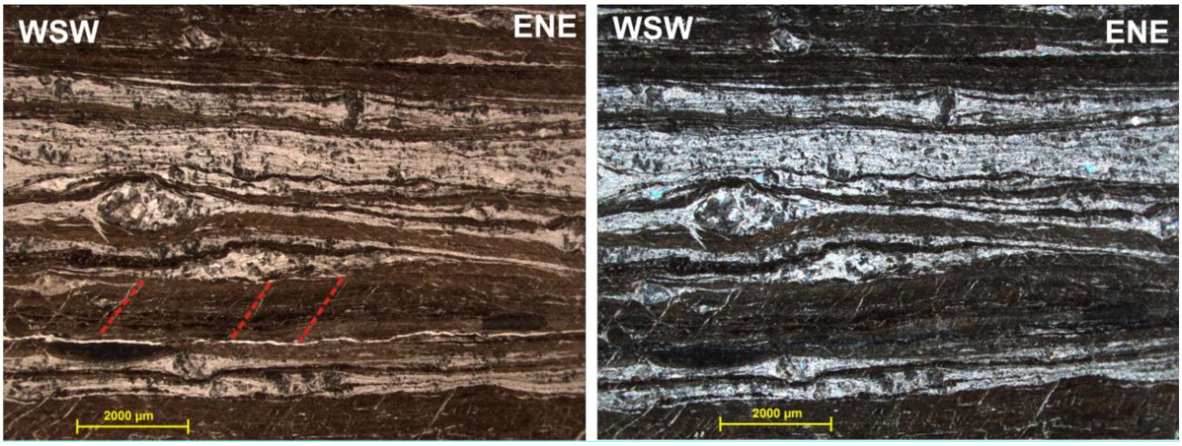

Fig. 5.28: 3b: Fracturing of competent clayey layers and ductile reacting salt rocks "flowing" around rigid clasts of clay, anhydrite or carbonate are typical features of this mylonitic fabric. The right picture is taken under CPL.

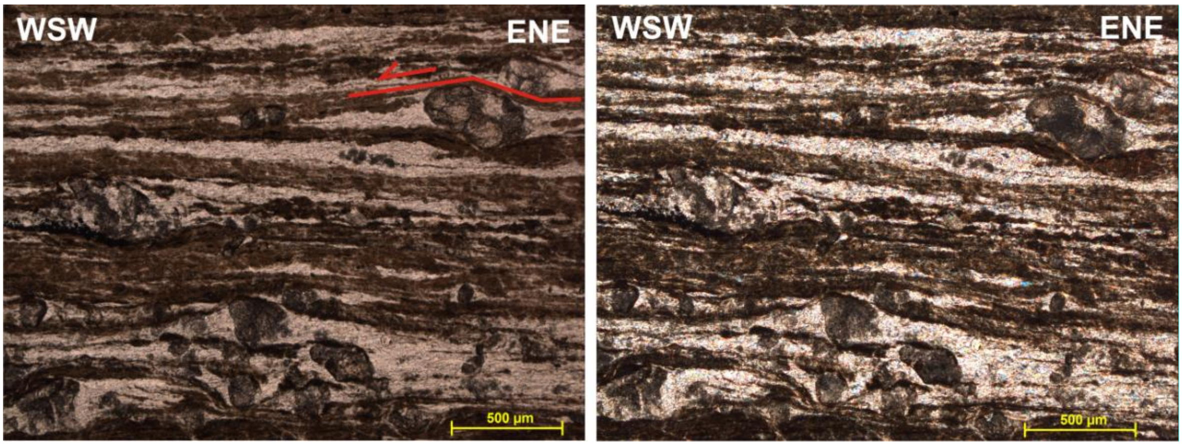

Fig. 5.29: 3b: "*Liniensalz*". The opaque clayey material enriches in layers due to pressure solution and develops a pressure solution cleavage. Clasts of carbonate, anhydrite or clay react as brittle components within the ductile deforming matrix. "Stairstepping" of rotated clasts shows top to WSW movement in this cut-out of the thin-section. The right picture is taken under CPL.

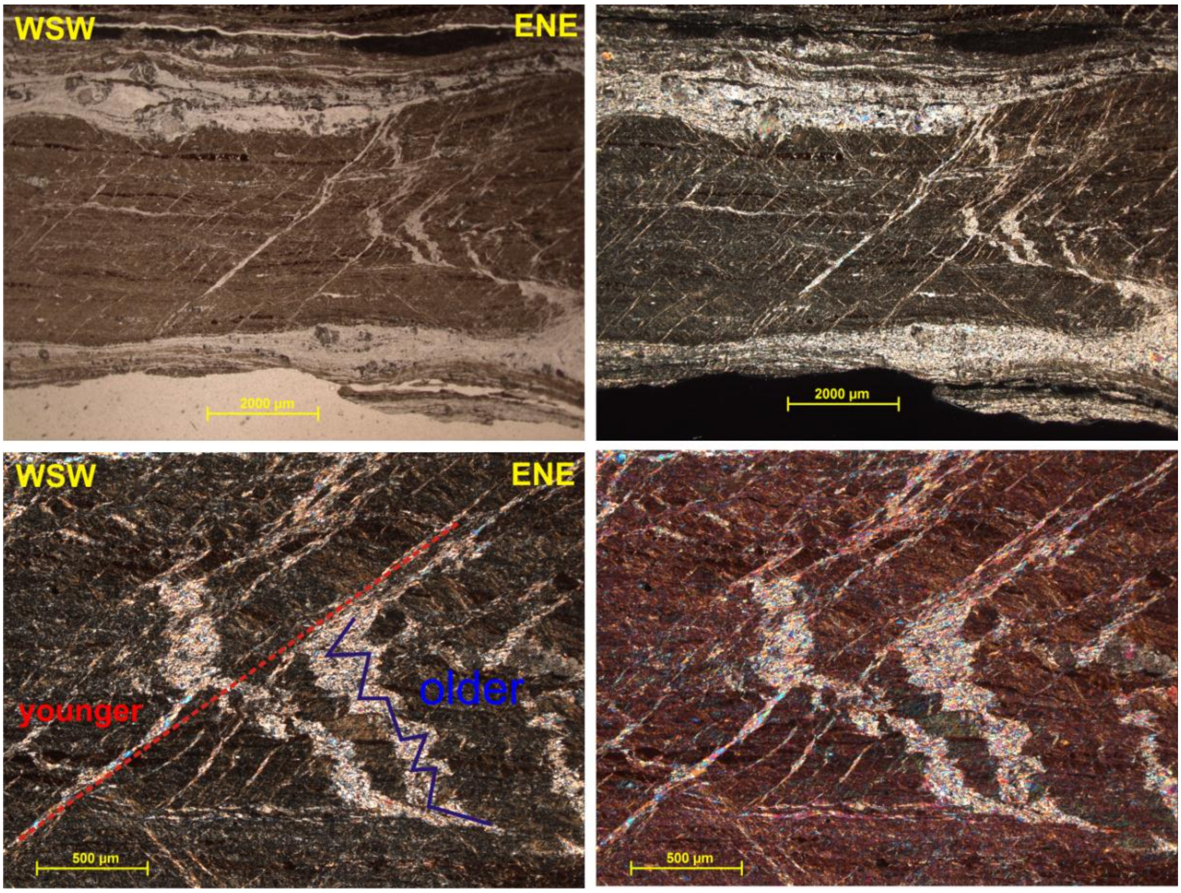

Fig. 5.30: 3b: As seen in the overview (pictures above) clayey and pure anhydrite layers react brittle and generate cracks or veins to accommodate displacement. Older generations of veins get rotated and folded by the younger ones. In the folded older veins dynamic recrystallisation of salt is observed. The upper right and lower left picture are taken under CPL. The picture at the right bottom is photographed with inserted gypsum plate.

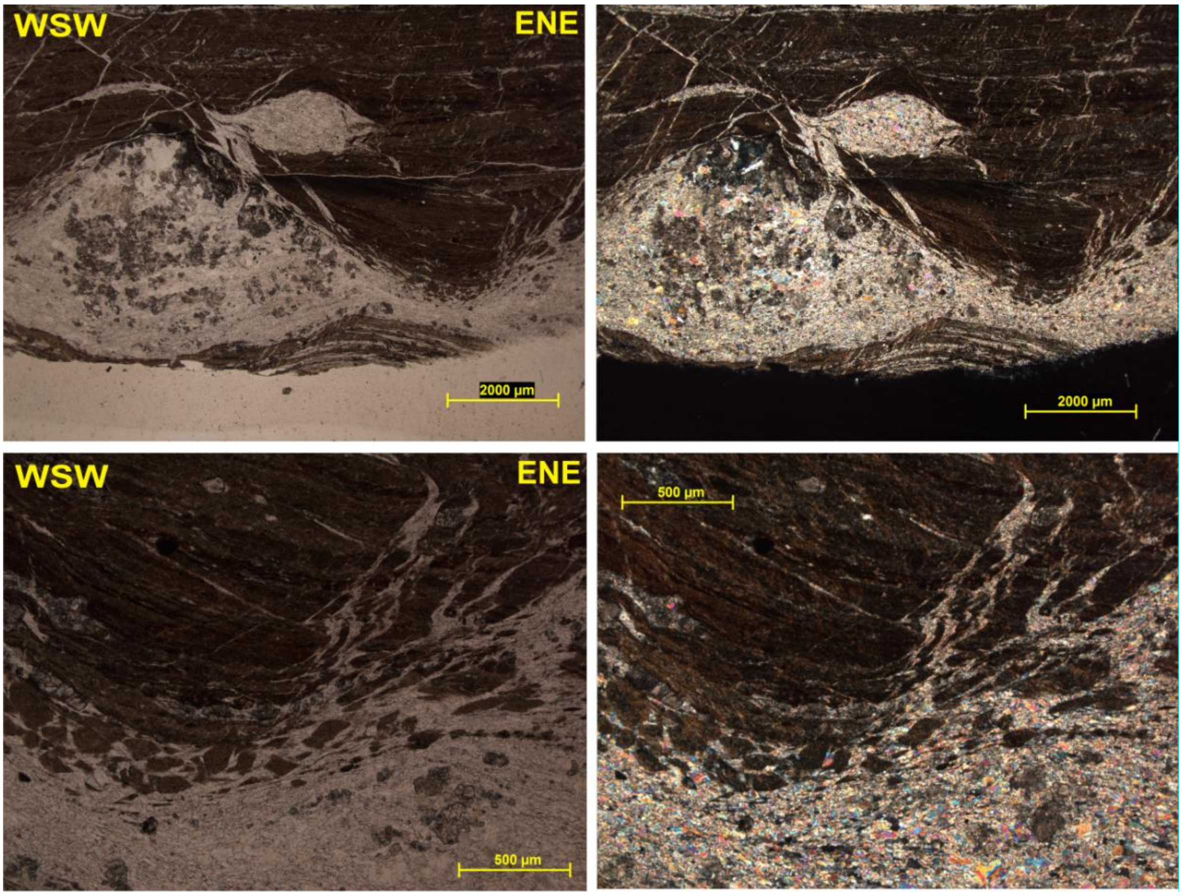

Fig. 5.31: 3b: Cataclastic deformation process of more competent brittle reacting clay-rich portions within ductile flow of salt. Components of the rigid material broke up from their host rock now “swimming” isolated in salty matrix. During further deformation such angular fragments get rotated form round clasts with different sets of wings (see chapter 4). Both right-handed pictures are taken under CPL.

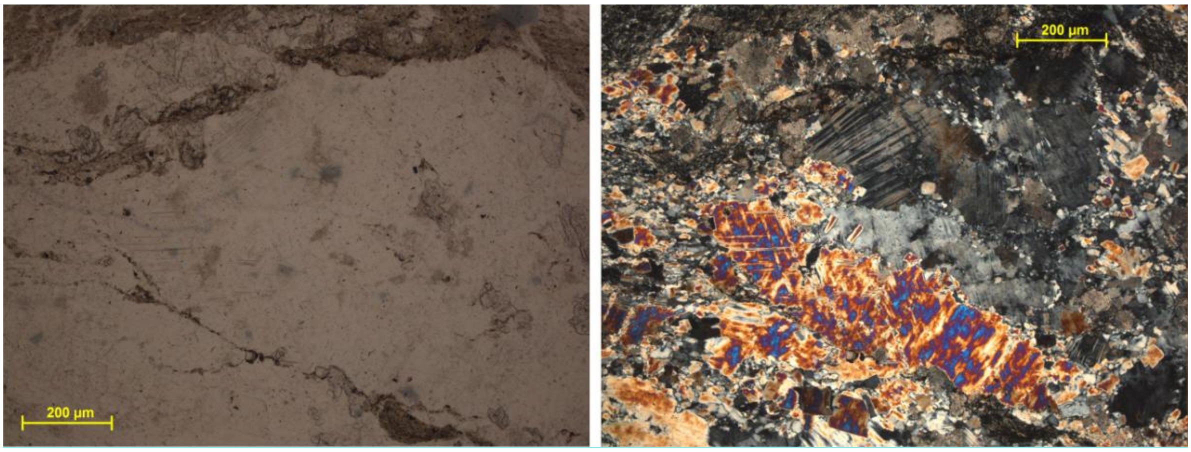

Fig: 5.32: 3b: Stylolites and pressure solution processes can be observed in the left picture. Whereas in the right picture, taken under CPL, dynamic recrystallisation (GBM, left over grains) and deformational twinning are visible.

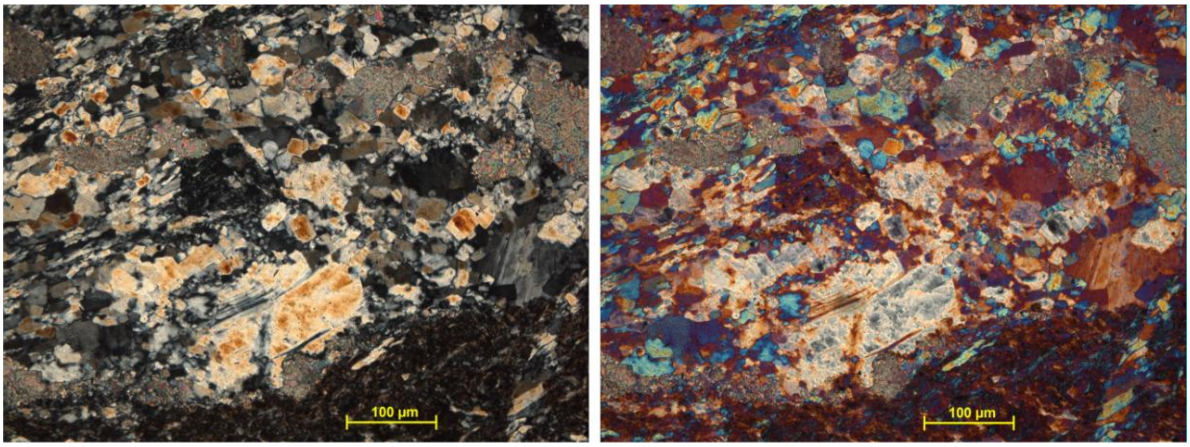

Fig: 5.33: 3b: Dynamic recrystallisation. Small grains recrystallise at borders of large ones and show undulose extinction. Left picture is taken under CPL, right one with inserted gypsum plate.

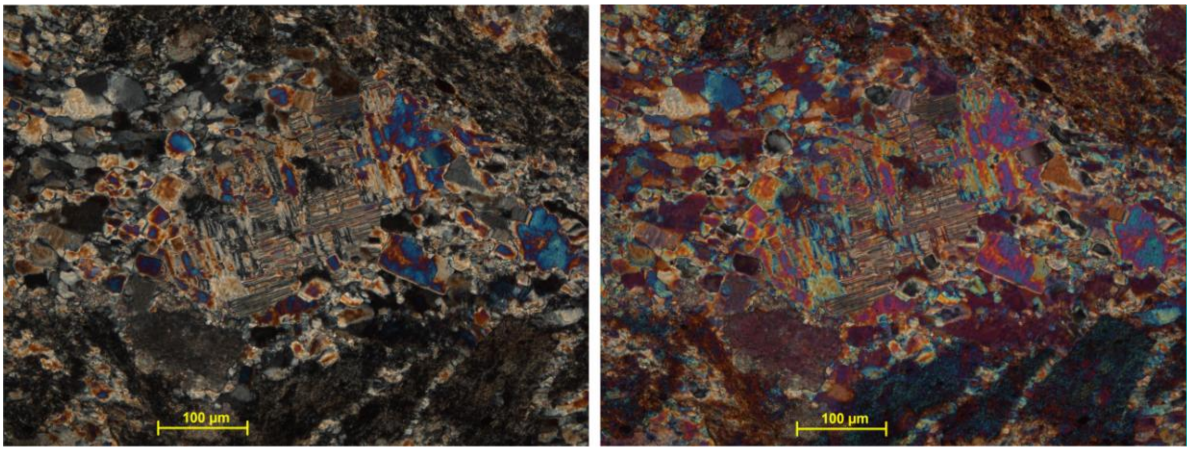

Fig: 5.34: 3b: Two generations of deformation twinning. The older one is penetrated (and partly recrystallised) by the younger distinctive process of deformational twinning. At the border of the larger grain in the centre that shows twinning dynamic recrystallisation of salt takes place. Left picture is taken under CPL, right one with inserted gypsum plate.

5.4.2.1 Photo of sample 2

The sample was taken nearby the location of thin-section 3b at a comparable lithology and it shows the same mylonitic structures as the thin-section 3b but at larger scale. “Stairstepping” and fracturing of a rigid clast within ductile deforming anhydrite are visible in sample 2 (**see Fig. 5.35**). The rigid clast that is rotated and partly fractured in this picture consists of Hallstatt Limestone. As the sample was taken at the border between Central Inclusion and Haselgebirge this clast probable originally was part of the inclusion.

The clast shows stairstepping that indicates top to NE direction. The temperature conditions are assumed to be lower than 200°C because of the brittle reacting limestone clast.

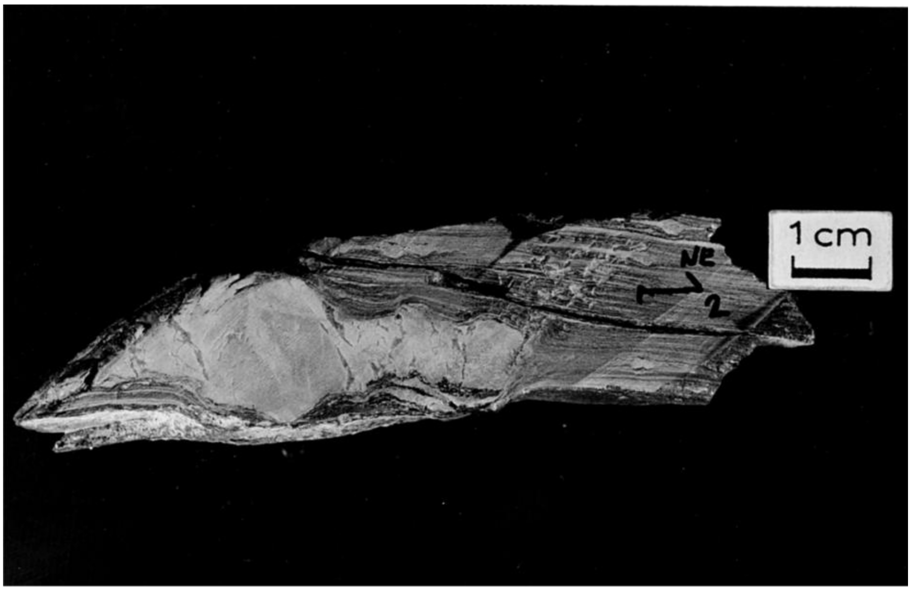

Fig. 5.35: Photo of sample 2, showing a clast of Hallstatt Limestone that is rotated and partly fractured in an anhydrite mylonite. The clast shows stairstepping that indicates top to NE direction of tectonic transport. Temperature conditions < 200°C

5.4.3 Thin-section 29

The thin-section 29 is located at the eastern part of the Hallstatt saltmine. It shows also a mylonitic fabric with pressure solution cleavage, as seen in thin-section 3b, but the salt-rich portions are not dynamically recrystallised and show static recrystallisation processes instead. In some parts of the section triple junctions of grains with 120° are frequent and larger grains with straight grain boundaries occur. The static recrystallisation indicates that deformation in this part did not last as long as in the others where clear features of dynamic recrystallisation are observed.

Various vein sets as shown in **Fig. 5.36** can be observed and different generations can be determined by cross-cutting relationships.

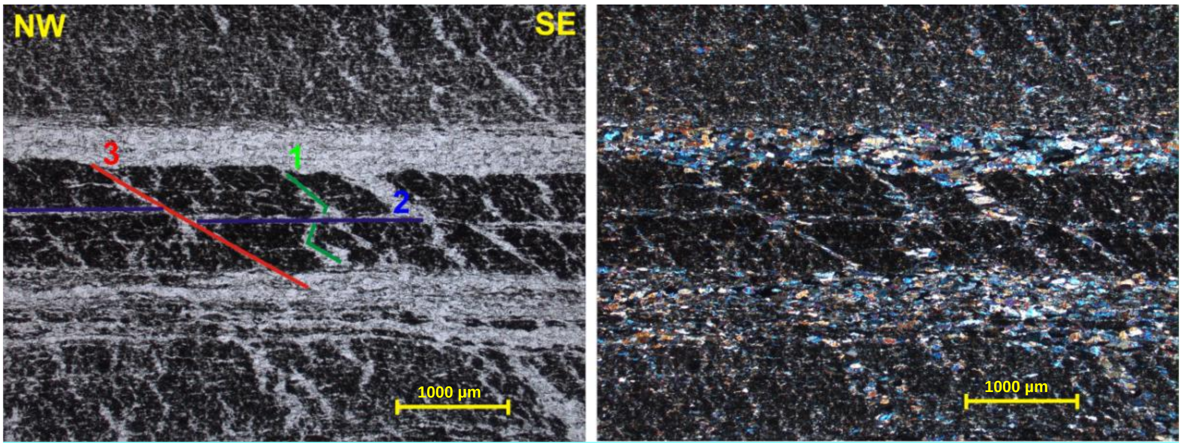

Fig. 5.36: Thin section 29 originates from a formally mylonite but salt-rich portions have already undergone static recrystallisation (shape preferred orientation?). The dark layer is more competent than the salty interlayers and so it gets fractured by veins that are infilled by evaporites. As marked in the left picture cross cutting relationships of different vein generations are observed. The right picture is taken under CPL.

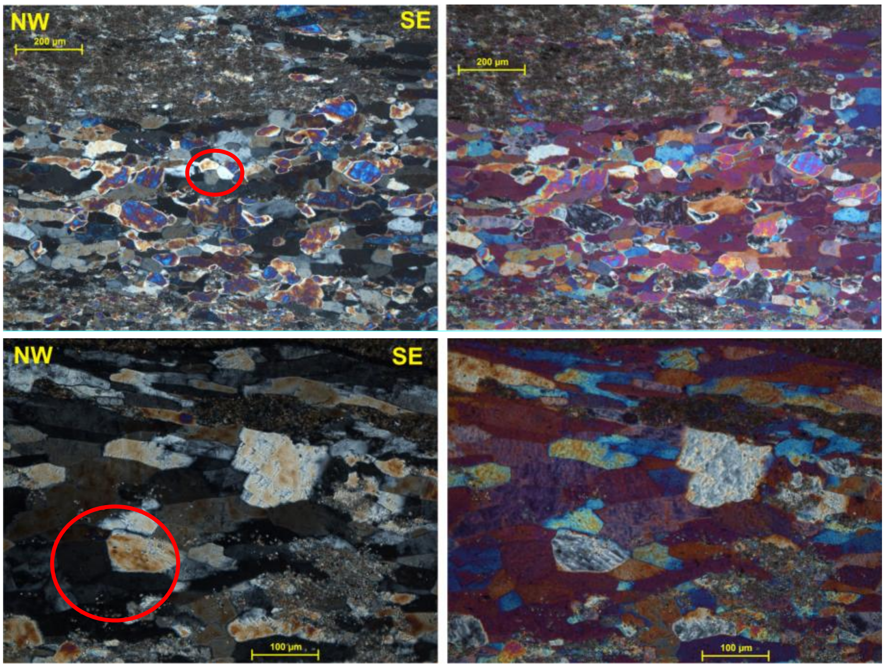

Fig 5.37: Detailed view of thin-section 29 that shows static recrystallisation of the salt layers in this thin-section. Straight grain boundaries, triple junctions at 120° (marked by the red circle) and larger grain sizes than observed in fabrics with dynamic recrystallisation (e.g. thin-section 3b) indicate static recrystallisation. Left pictures are taken under CPL, right ones with inserted gypsum plate.

5.4.4 Thin-section 12a

This thin-section shows a nearly totally recrystallised fabric. Pressure solution cleavage, deformation twinnings and grain boundary migration recrystallisation are observed. Different generations of deformation twinning occur. Older twinnings are already faded due to recrystallisation and creation of distinctive fresh deformation twinnings (**see Fig. 5.39**).

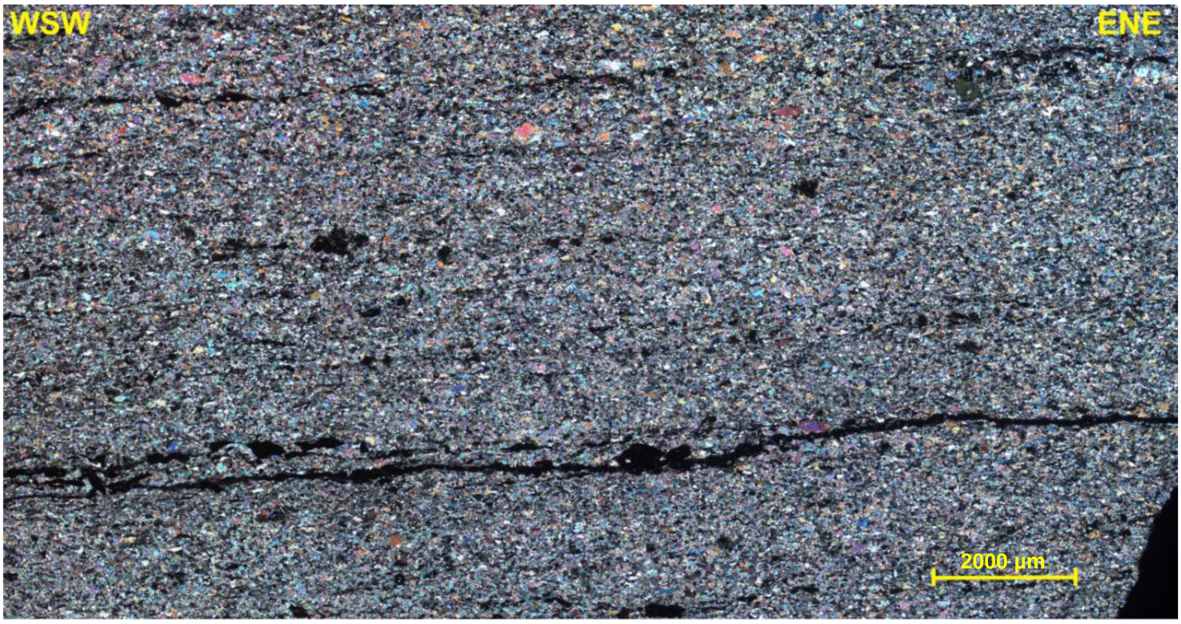

Fig. 5.38: Panoramic view of thin-section 12a, showing a recrystallised fabric of anhydrite (salt) mylonite. Grain sizes are relatively constant over the whole section, only few larger grains exist. Minor pressure solution cleavage is seen in this picture. The picture is taken under CPL.

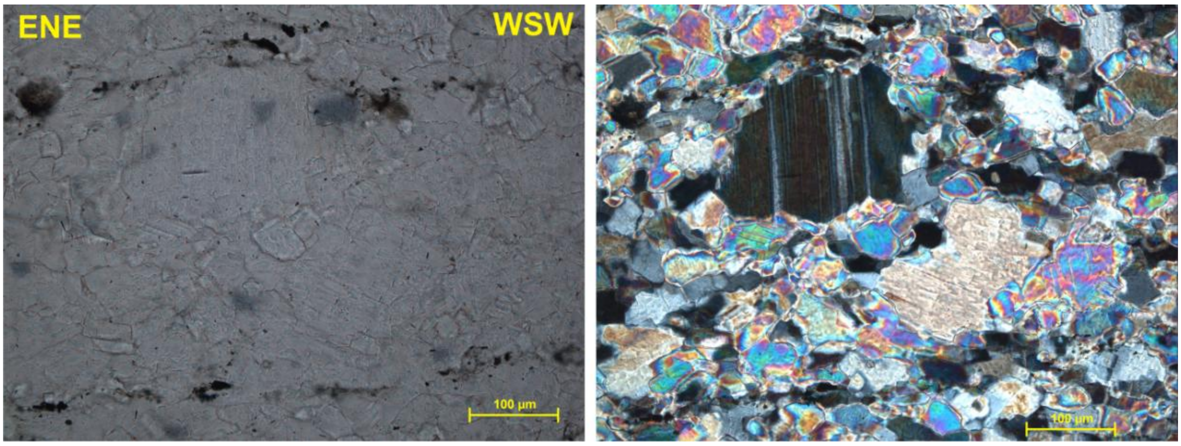

Fig. 5.39: 12a: Deformation twinning and dynamical recrystallisation of salt. The larger grains get dynamically recrystallised at their boundary. The right picture is taken under CPL.

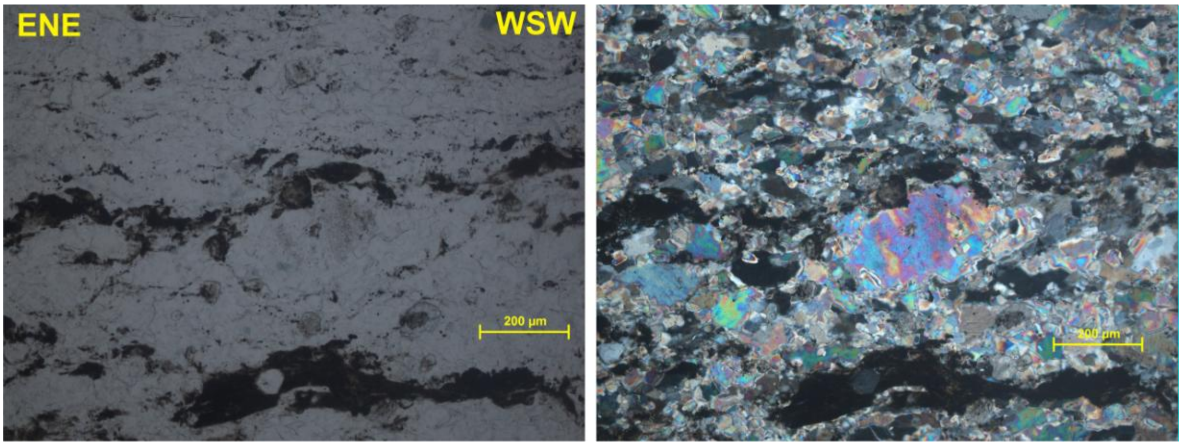

Fig. 5.40: 12a: Pressure solution cleavage and bulging. The right picture is taken under CPL.

5.5 Striated pebbles within the Haselgebirge investigated with SEM (scanning electron microscope)

5.5.1 Introduction

Within the Permian Haselgebirge some pebbles consisting mainly of shales were recognized that showed polished surfaces. To gain more information about the scratches, like size, direction and shape, the surfaces were observed and photographed under the scanning-electron-microscope (SEM). The reason for striations on the clasts of clay is assumed to be plastic deformation under high pressure. The nodular clasts are “swimming” in the weaker evaporitic-clayey matrix of the Haselgebirge. Due to the different movements of the clasts within the weaker matrix they collide with other clasts other with the big included limestone lenses (e.g. Central Inclusion) during the deformation process. As a consequence along the boundaries of such clasts striation and polishing occurred. Sometimes also partially fracturing of clasts within the ductile deforming matrix is shown by angular fragments of the clast in its wings. On the other hand some already fractured pebbles are kept together by the surrounding pressure (Hippolyte, 2001).

As described in **chapter 3** the ductile material within the core of a detachment fold is forced to pass through intense internally deformation. And also during the migration into the assumed strike slip fold – that formed the now existing saltbody – the Haselgebirge has undergone an intense deformation. The scratches and polished surfaces on the clasts are evidences of the tectonic architecture of the Permian Haselgebirge.

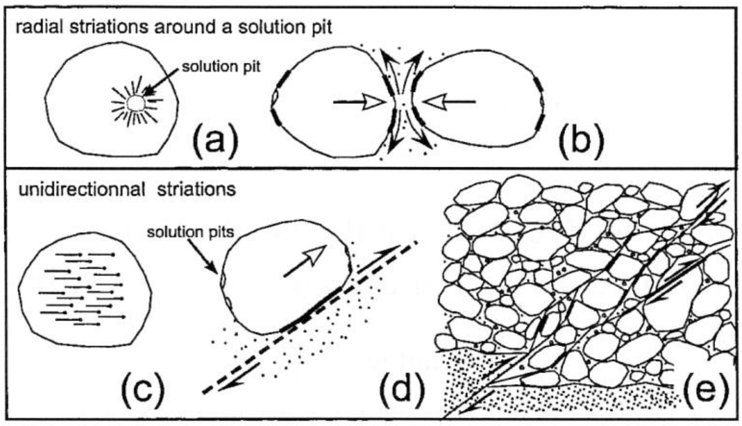

Fig.: 5.41: Samples of tectonically produced structures on clast surfaces and their development (Hippolyte, 2001).

a) Solution pits and short radial striations – are the result of pressure solution at grain contacts and indicate pure shear or oblique strain symmetries (perpendicular or oblique to the main shortening direction)

b) Divergent movement of the fine grained matrix between two colliding clasts (harder grains within the matrix may generate striations on the pebbles.

c) Parallel striations generated during shearing the conglomerate

d) Discontinuity of the matrix and clasts activate as shear plane

e) In conglomerates shear zones are cutting the whole material and striations are produced by divergent movement of adjacent clasts.

Although the samples shown in **Fig. 5.39** are drawn for conglomerates, similar movements of clasts within the weaker clayey, salty matrix are assumed to produce the observed striations.

5.5.2 EDX – energy dispersive X-ray analyses

The SEM has an EDX (Energy Dispersive X-ray analyses) linked to gain the mineralogical composition of the observed samples. The EDX measures the energy of the X-rays that are emitted by the irradiated samples. Due to the significant peaks of minerals at different energy levels the minerals can be identified. The quantitative composition can be approximately determined by the height and width of the concerning peak of a mineral in respect to the peaks of other minerals.

The main point of interest during SEM investigations was to characterize the striated pebbles and the structures on the polished surfaces. Nevertheless the EDX tool was helpful to recognize the composition of the investigated clasts. On some clasts salty crusts indicated polished and scratched surfaces in outcrop scale. With the SEM and of course the EDX these differences could be determined easily. In **Fig. 5.42** two line spectres are shown, one indicating the salt crystals on the clast, the other one showing a composition of different clay minerals.

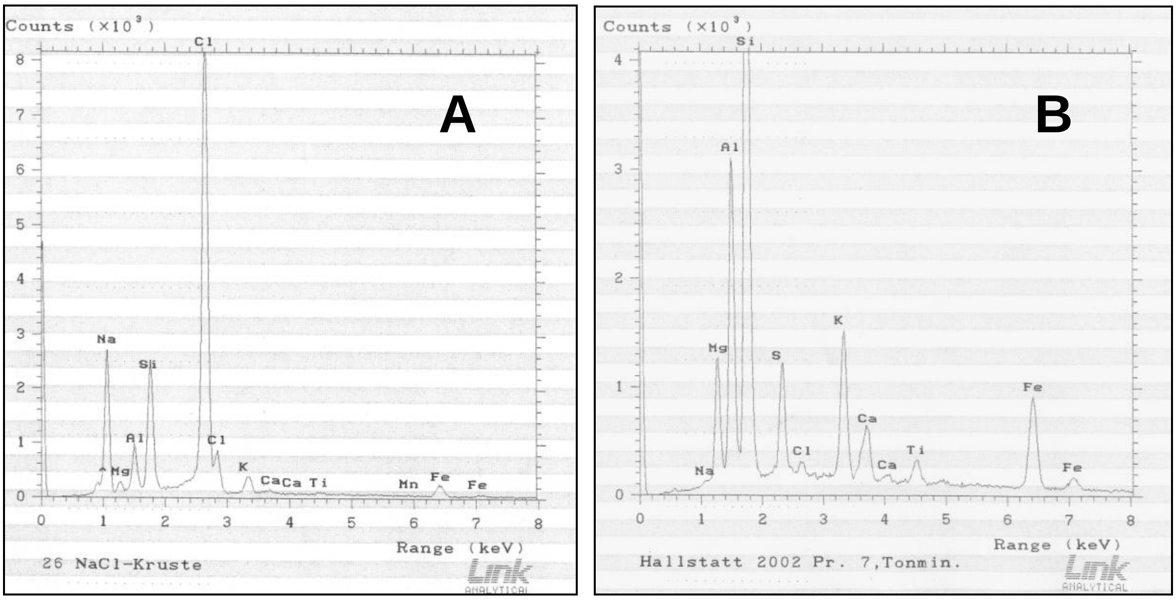

Fig. 5.42: Line spectrum of EDX analyse within the SEM.
A) Shows a typical mineralogical composition of salt (mainly halite), as the peaks of Sodium (Na) and Chloride (Cl) are much larger in respect to the other elements. The small peaks of Aluminium (Al) and Silicium (Si) indicate the clay in between the salt crystals.
B) Reflects the mineralogical composition of a clay clast at its surface. Here Al and Si are the main peaks and indicate that they capture the main part of the clast.

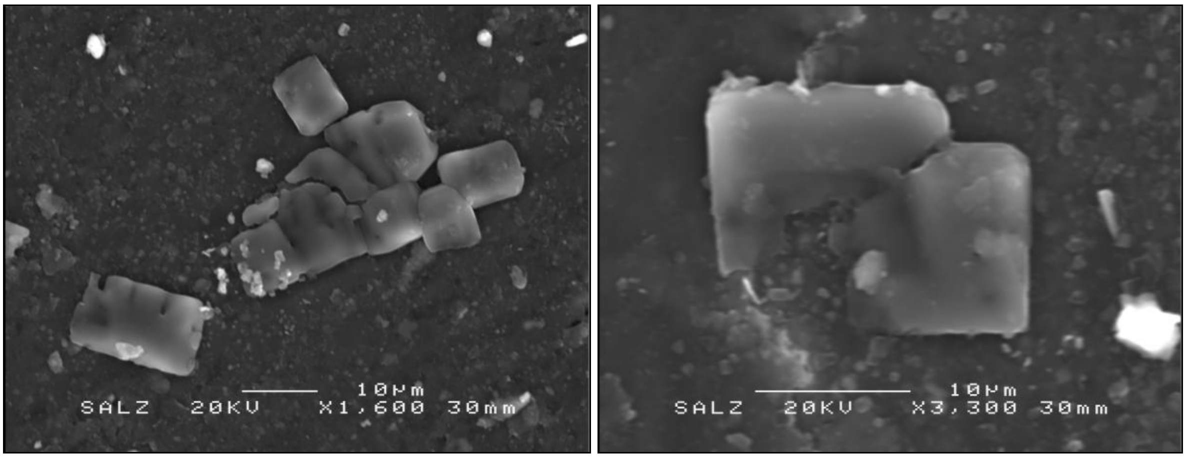

Fig. 5.43: Salt crystals on a clay pebble. First indicating a striated surface, under SEM the uneven surface was recognized as cubic crystals of halite. See also Fig.5.42 showing the EDX – spectrum of this halite cubes with sizes of up to 15µm edge length.

5.5.3 Polished and striated surfaces of clay clasts

As shown in **Fig. 5.44** already in the saltmine polished and scratched surfaces of clasts were observed. If the samples taken in the field were not immediately prepared the clast surfaces got desiccation cracks and lost their polished appearance. Therefore bigger blocks of the Haselgebirge were taken as samples and clasts were broken out of the matrix immediately before preparation and investigation under SEM.

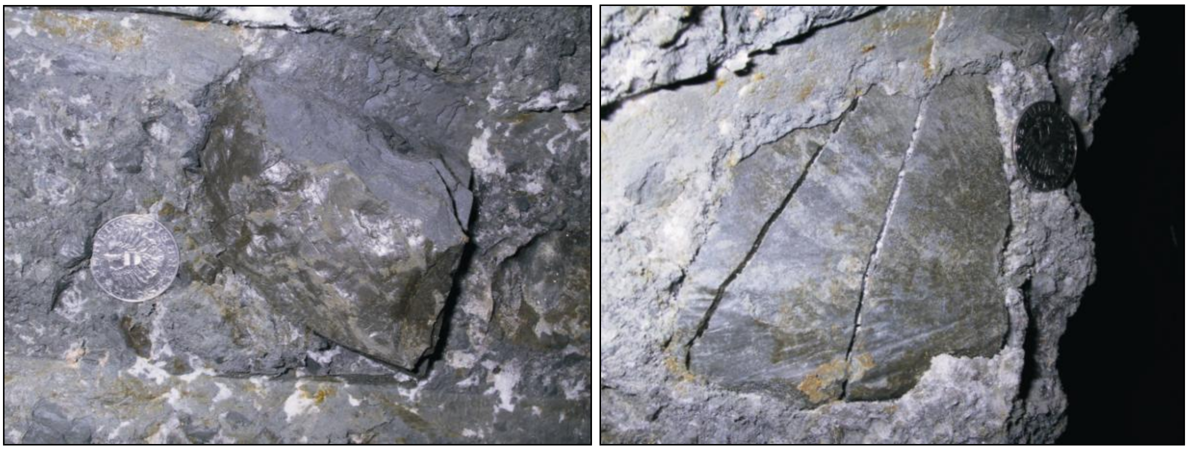

Fig. 5.44: Polished and striated surfaces of clay clasts within the polymict breccias of the Permian Haselgebirge. These structures of relatively hard components within the salty-clayey matrix result from contacts of clasts or with larger rigid components like the "Central Inclusion".

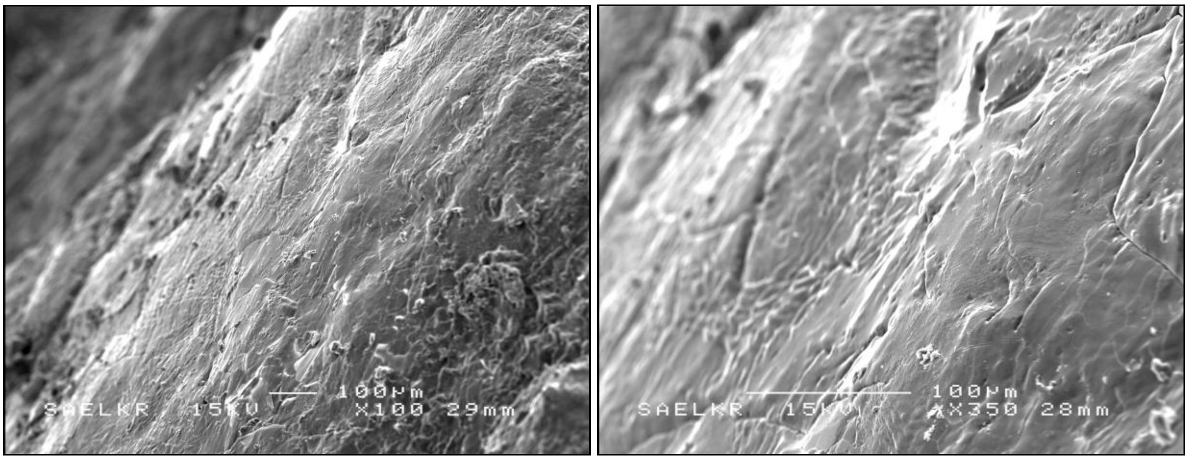

Fig. 5.45: Polished surfaces of clay pebbles observed under SEM. These surfaces don´t show a distinctive diretction of scratches. The scalebar in the pictures shows 100µm.

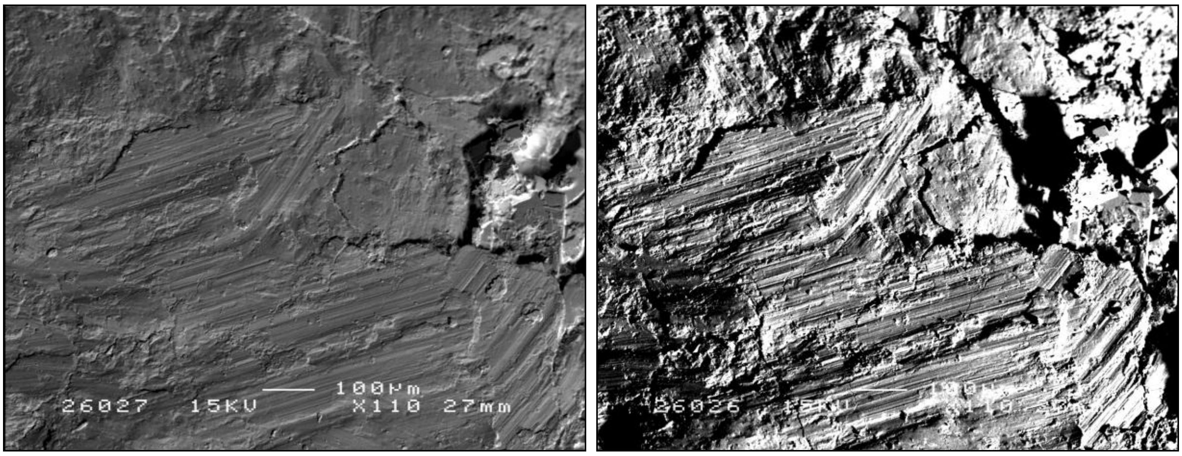

Fig. 5.46: Curved lineations on clay clast embedded in an evaporitic matrix. Both pictures show the same cutout but the left photograph was taken with the back scattered method. The curved scratches reach length of about 400µm.

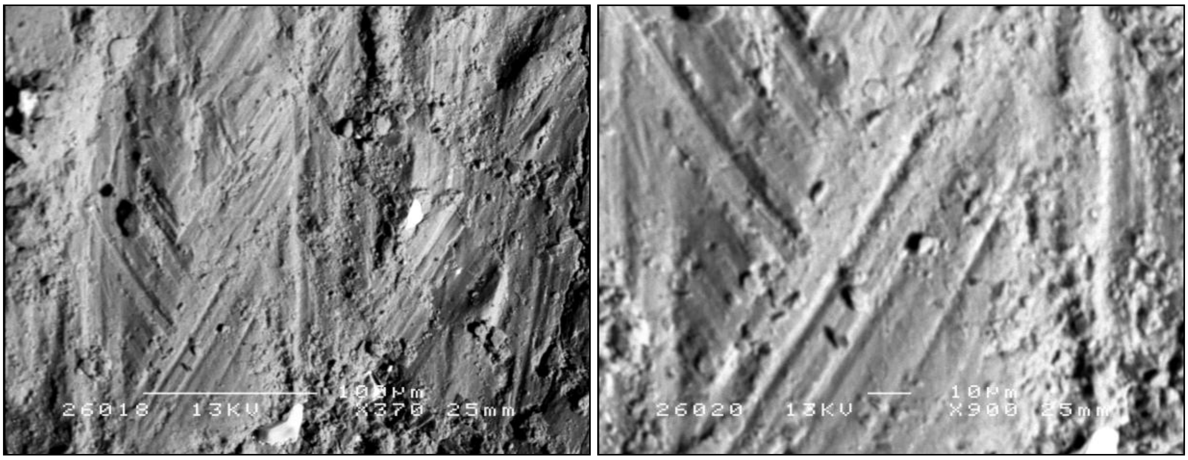

Fig. 5.47: Due to the different local stress fields within the Haselgebirge (e.g. strain shadows) and resulting different movement directions and of course due to rotation of clasts, on most striated surfaces scratches in different directions were observed.

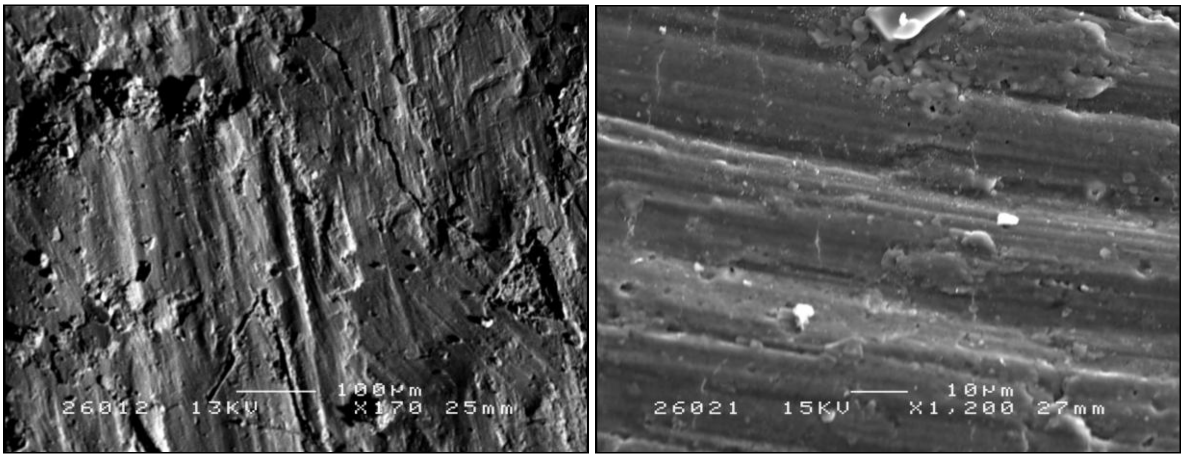

Fig. 5.48: Both pictures show relatively linear scratches. The left picture shows relatively deep scratches with more than 500µm length. Perhaps this clast collided with a bigger inclusion.

Different sizes and direction of scratches were observed on polished surfaces of clast embedded in the clayey-salty matrix of the Haselgebirge. In some cases also curved striations occurred.

Other examples of such striated and polished boulders are known from the moraine of glaciers. Rock fragments that are transported at the sediment-loaded base of the glacier cause grooves and polished structures as well on the bedrock as on the contact points of the pebbles itself.

Another geological environment where such striated pebbles are known is in impact craters. Sachs (2003) compared striated and polished clasts of tectonically developed breccias with the striated pebbles of shock metamorphism conditions like in the meteor crater of the Nördlinger Ries. In difference the impact structures show more complex features, indicating a more complex stress field than tectonically generated striations. Otherwise due to the momentary event of the impact, pressure solution can not be observed whereas in tectonically deformed breccias it is a common feature (Sachs, 2003).

In contrary to the SEM pictures of polished and striated surfaces of pebbles in impact craters, on the clasts within the Haselgebirge no fragments that caused the scratches were found.

6. Conclusion

This diploma work focused on thrust tectonics in the Hallstatt area, where the Hallstatt Nappe is tectonically juxtaposed to the Dachstein Nappe. The established deformation structures during the Alpine Orogeny are significantly affected by the geological setting. Especially the weak succession of the Permian Haselgebirge influenced fold-and-thrust geometries in the particular area within the central NCA. Field analyses at the northern slope of the Echerntal, observations within the Hallstatt saltmine and investigations of microstructures at both of them provided following conclusions.

- The Dachstein Limestone sediments at the northern slope of the Echerntal clearly display top to WNW movement. This WNW directed movement is indicated by generally ESE dipping bedding planes and thrust faults. Lineations and calcite slickenfibres on bedding plane parallel slickensides and microstructures observed in thin-sections of Dachstein Limestone from the Echernwand confirm movement towards WNW.
- The Haselgebirgs outcrop within the Erbstollen shows that at this location the Dachstein Limestone is directly overlying the evaporites. As measurements at this outcrop suggest that the evaporites where involved in the westward thrusting this is a considerable indication that the Dachstein Nappe overthrusted the Hallstatt Nappe at its southeastern boundary. Furthermore this Haselgebirgs outcrop makes up the core of a detachment fold observed in Dachstein Limestone at the northern slope of the Echerntal.
- The evaporites of the Permian Haselgebirge, in contradiction to the more brittle reacting covering carbonates, show high strain ductile deformation structures. Rotated and partly fractured rigid clasts embedded in the ductily deforming salty-clayey matrix and isoclinal folding provide evidence for the intense internal deformation of the evaporites. Microstructural investigations of thin-sections confirm the mylonitic fabric of the Hallstatt salt deposit. Furthermore the scratched and polished surfaces of clay clasts that are embedded in the salty-clayey matrix proof the intense internal deformation of the Haselgebirge.
- The saltbody of the Hallstatt saltmine is correlated with a major dextral strike-slip fault at the northern boundary of the Hallstatt Nappe. Such structures are also reproduced in analoge models (e.g. Cotton and Koyi, 2000), where the ductile material first accumulates in the core of detachment folds or similar thrust structures that accommodate shortening, but with ongoing deformation it can migrate into a transfer zone and rise up to the surface (Cotton and Koyi, 2000; Arnberger, 2006).
- The sedimentation of the limno-fluviatil to marin Gosau Group, which started in Late Turonian times, postdates the Eoalpine Orogeny peak (Wagreich and Faupl, 1994). This is also evidenced in the studied field area, where Gosau sediments are overlying the observed thrust structures discordant at several investigated outcrops. The Gosau basin is seen as a pull-apart basin along NW-striking dextral tear faults that cause subsidence of this area (Wagreich and Decker, 2001).

7. References

Ampferer, O. and W. Hammer, 1911, Geologischer Querschnitt durch die Ostalpen. Jahrbuch. geol. R.-A., v. 61, p. 531-710.

Ampferer, O., 1912a, Gedanken über die Tektonik des Wettersteingebirges. Verh, geol. R.-A., p.197-212

Ampferer, O., 1939, Im Kampfe für Reliefüberschiebung und O-W-Bewegung. Verh. Zweigst. Wien Reichsst. Bodenforsch., p. 196-205.

Andrews, L., M. and L. B. Railsback, 1997, Controls on Stylolite Development: Morphologic, Lithologic, and Temporal Evidence from Bedding-Parallel and Transverse Stylolites from the U.S. Appalachians: The Journal of Geology, v. 105, p. 59-73.

Arnberger, K., 2006, Detachment folding above the Permian Haselgebirge: palinspastic reconstruction of alpine west-directed thrusting (Plassen, Hallstatt, Upper Austria). Unpublished diploma thesis, Department of Geodynamics and Sedimentology, University of Vienna.

Bittner, A., 1890, Die Brachiopoden der alpinen Trias. Abh. geol. R.-A. v. 14, p. 1-325.

Bohadsch, J., 1782, Bericht über seine auf allerhöchsten Befehl im Jahre 1763 unternommene Reise nach dem oberösterreichischen Salzkammerbezirk. Abh. Privatges. Böhmen, v. 5, p. 91-227, Prag.

Böhm, F., 1992. "Mikrofazies und Ablagerungsmilieu des Lias und Dogger der Nordöstlichen Kalkalpen: Erlanger geol. Abh., v. 121, p. 57-217.

Buch, L. v., 1802, Geognostische Beobachtungen auf Reisen durch Deutschland und Italien. Berlin, Haude und Spencer, v.1.

Burkhard, M., 1993, Calcite twins, their geometry, appearance and significance as stress-strain markers and indicators of tectonic regime: a review. Journal of Structural Geology, v. 15, p. 351-368.

Carey, S. W., 1962, Folding: Journal of Alberta Society Petroleum Geologists, v. 10, p. 95-144.

Carter, N. L., and F. D. Hansen, 1983, Creep of rocksalt: Tectonophysics, v. 92, p. 275-333.

Cotton, T.J., and H.A. Koyi, 2000, Modelling of thrust fronts above ductile and frictional detachments: Application to structures in the Salt Range and Potwar Plateau, Pakistan: GSA Bulletin, v. 112, p. 351-363.

Dahlstrom, C. D. A., 1969, The upper detachment in concentric folding: Bull. Can. Petrol. Geol., v. 17, p. 326-346.

Dahlstrom, C. D. A., 1990, Geometric constraints derived from the law of conservation of volume and applied to evolutionary models of detachment folding. AAPG, v. 74/3, p. 336-344.

Davis, D. M., and T. Engelder, 1985, The role of salt in fold-and-thrust belts: Tectonophysics, v. 119, p. 67-88.

De Paor, D. G., 1988, Balanced Section in Thrust Belts; Part 1, Construction: AAPG Bulletin, v. 72, No. 1 (January 1988), p. 73-90.

Dixon, J. M. and R. Tirrul, 1991, Centrifuge modelling of fold-thrust structures in a tripartite stratigraphic succession: Journal of Structural Geology, v. 13, p. 3-20.

Ebner, M., D. Koehn, R. Toussaint and F. Renard, 2009, The influence of rock heterogeneity on the scaling properties of simulated and natural stylolites: Journal of Structural Geology, v 31, p.72-82.

Faupl, P., E. Pober, and M. Wagreich, 1987, Facies Development of the Gosau Group of the Eastern Parts of the Northern Calcareous Alps During the Cretaceous and the Paleogen, *in* H. W. Flügel, and P. Faupl, eds., Geodynamics of the Eastern Alps: Vienna, Franz Deuticke, p. 142-156.

Faupl, P., 1997, Historische Geologie; eine Einführung: Wien, WUV.

Faupl, P., and M. Wagreich, 2000, Late Jurassic to Eocene palaeogeography and geodynamic evolution of the Eastern Alps.: Mitteilungen der Österreichischen Geologischen Gesellschaft, v. 92, p. 79-94.

Ferrill, D. A., A. P. Morris, M. A. Evans, M. Burkhard, R. H. Groshong, Jr. and C. M. Onasch, 2004, Calcite twin morphology: a low-temperature deformation geothermometer: Journal of Structural Geology, v. 26, p. 1521-1529.

Flurl, M., 1792, Beschreibung der Gebirge von Baiern und der oberen Pfalz. München, Petrogr, Kr.

Frank, W., and W. Schlager, 2006, Jurassic strike slip versus subduction in the Eastern Alps: International Journal of Earth Sciences, v. 95, p. 431-450.

Frisch, W. and H. J. Gawlick, 2003, The nappe structure of the Northern Calcareous Alps and its disintegration during Miocene tectonic extrusion - a contribution to understanding the orogenic evolution of the Eastern Alps. International Journal of Earth Science, v. 92, p. 712-727.

Gawlick, H. J., R. Lein, F. Schlagintweit, H. Suzuki and E. Wegerer, 2001, Vortrag: Der Hallstätter Salzberg und sein geologischer Rahmen – Geschichte und Stand der Erforschung, Interpretation und neue Ergebnisse, 3.Symposium zur Geschichte der Erdwissenschaften in Österreich/ Berichte der Geologischen Bundesanstalt, Bd. 56, p. 45-49

Gawlick, H. J., and F. Schlagintweit, 2006, Berriasian drowning of the Plasssen carbonate platform at the type-locality and its bearing on the early Eoalpine orogenic dynamics in the Northern Calcareous Alps (Austria). International Journal of Earth Sciences, v. 95, p. 451-462.

Geological Survey of Austria, 1999, Geological map of Austria, 1: 2 000 000; Vienna.

Grasemann, B. and F. Fusseis, 2000, Einführung in die Strukturgeologie. Wien, Facultas.

Grasemann, B., G. Wiesmayr, C. Janda, and M. P. J. Schöpfer, 2003, Geologische Karten und Profile: Wien, Facultas.

Haas, J., et al., 1995, Significance of Late Permian - Triassic facies zones in terrane reconstruction in the Alpine - North Pannonian domain: Tectonophysics, v. 242, p. 19-40.

Habermüller, M., 2005, West-directed thrusting in the Dachstein Nappe: quantification of eo-Alpine deformation around the Echerntal valley (Hallstatt, Austria). Unpublished diploma thesis, Department of Geodynamics and Sedimentology, University of Vienna.

Hahn, F., 1912, Versuch zu einer Gliederung der austroalpinen Masse westlich der österreichischen Traun. Verh. geol. R.-A., p 337-344.

Hahn, F., 1913b, Grundzüge des Baues der nördlichen Kalkalpen zwischen Inn und Enns. Mitt. geol. Ges. Wien, v. 6, p. 238-357.

Hauer, F. v., 1848, Cephalopoden vom Rossfeld. Haidlingers Ber. Mitt. Freunde Nattw., v. 3, p. 476-480.

Haug, É., and M. Lugeon, 1904, Sur l´existence dans le Salzkammergut de quatre nappes de charriage superposes. C. R. Acad. Sci., v. 139, p. 892-894, Paris.

Hippolyte, J.-C., 2001, Palaeostress and neotectonic analyses of sheared conglomerates: Southwest Alps and Southern Apennines: Journal of Structural Geology, v. 23, p. 421-429.

Homza, T. X., and W. K. Wallace, 1995, Geometric and kinematic models for detachment folds with fixed and variable detachment depths: Journal of Structural Geology, v. 17, p. 575-588.

Huiqi, L., McClay, K. R. and D. Powell, 1992, Physical models of thrust wedges. Thrust Tectonics. K. McClay. London, Chapman & Hall, p. 71-81.

Jackson, M. P. A. and C. J. Talbot, 1989, Anatomy of mushroom-shaped diapirs: Jourmal of Structural Geology, v. 11, p. 211-230.

Jamison, W. R., 1987, Geometric analysis of fold development in overthrust terranes: Journal of Structural Geology, v. 9, p. 207-219.

Jessell, M. W., 1986, Grain boundary migration and fabric development in experimentally deformed octachloropropan. Journal of Structural geology, v. 8, p. 527-542

Jessel, M. W., 1987, Grain-boundary migration microstructures in a naturally deformed quartzite: Journal of Structural Geology, v. 9, p. 1007-1014.

Jordan, P., 1994, Evaporite als Abscherhorizonte, Beitraege zur Geologischen Karte der Schweiz = Materiaux pour la Carte Geologique de la Suisse = Materiali per la Carta Geologica della Svizzera, vol.164, 79 pp., 1994.

Klaus, W., 1953, Mikrosporen-Stratigraphie der ostalpinen Salzberge: Verh. Geol. B.-A., v. 3, p. 161-175.

Klaus, W., 1955, Alpine Salz Sporendiagenese: Z. dt. geol. Ges, v. 105.

Kober, L., 1909, Über die Tektonik der südlichen Vorlagen des Schneebergs und der Rax. Mitt. geol. Ges. Wien, v. 2, p. 493-511.

Kober, L., 1911a, Untersuchungen über den Aufbau der Voralpen am Rande des Wiener Beckens. Mitt. geol. Ges. Wien, v. 4, p. 63-116.

Kober, L., 1911b, Der Aufbau der östlichen Nordalpen. Sitzber. Akad. Wiss. Wien, v. 120, p. 1115-1124.

Kober, L., 1912a, Über Bau und Entstehung der Ostalpen. Mitt. geol. Ges. Wien, v. 5, 368-481.

Kober, L., 1912b, Der Deckenbau der östlichen Nordalpen.: Denkschr. Akad. Wiss. Wien, math.-natw. Kl., v. 88, p. 345-396.

Kober, L., 1923, Bau und Entstehung der Alpen.: Berlin, Borntraeger.

Kober, L., 1950, Der Hallstätter Salzberg und der Hallstätter Erbstollen: Berg- und Hüttenmännische Monatshefte, v. 95, p. 165-171.

Koyi, H. A., 1998, The shaping of salt diapirs: Journal of Structural Geology, v. 20, p. 321-338.

Kozur, H., 1991, The evolution of the Meliata - Hallstatt ocean and its significance for the early evolution of the Eastern Alps and Western Carpathians: Paläogeography, Paläoclimatology, Paläoecology, v. 87, p. 109-135.

Krystyn, L., 1971, Stratigraphie, Fauna und Fazies der Klaus-Schichten (Aalenium-Oxford) in den östlichen Nordalpen: Verh. geol. B.-A., v. 3, p. 486-509.

Lein, R., 1987, Evolution of the Northern Calcareous Alps during Triassic times, Geodynamics of the Eastern Alps: Wien, Deuticke, p. 85-102.

Lilienbach, L. V., 1830, Ein Durchschnitt aus den Alpen, mit Hindeutungen auf die Karpathen. Leonhard Jb. Mineral, Geognosie,1, Heidelberg.

Linzer, H. G., L. Ratschbacher, and W. Frisch, 1995, Transpressional collision structures in the upper crust: the fold-thrust belt of the Northern Calcareous Alps: Tectonophysics, v. 242, p. 41-61.

Lobitzer, H. and G. W. Mandl, 2008, A brief history of geological research of the Dachstein-Hallstatt-Salzkammergut region: Berichte Geol. B.-A., v. 76 (ISSN 1017-8880).

Mandl, G. W., 1982, Jurassische Gleittectonic im Bereich der Hallstätter Zone zwischen Bad Ischl und Bad Aussee (Salzkammergut, Österreich): Mitt. Ges. Geol. Bergbaustud. Österr., v. 28, p. 55-76.

Mandl, G. W., 1984a, Zur Trias des Hallstätter Faziesraumes - ein Modell am Beispiel des Salzkammerguts: Mitt. Ges. Geol. Bergbaustud. Österr., v. 30/31, p. 133-166.

Mandl, G. W., 2000, The Alpine sector of the Tethyan Shelf; examples of Triassic to Jurassic sedimentation and deformation from the Northern Calcareous Alps: Mitteilungen der Oesterreichischen Geologischen Gesellschaft, vol.92, no.1999, pp.61-77, 2000.

Mandl, G. W., O. Ganss, F. Kümel, and E. Spengler, 1998, Geologische Karte der Dachsteinregion: Geol. B.-A. und Umweltbundesamt.

Marshak, S., and N. Woodward, 1988, Introduction to cross-section balancing:, Basic Methods of Structural Geology, Prentice Hall, Englewood, p. 303-314.

McClay, K., 1992, Glossary of thrust tectonics terms: Thrust Tectonics, Chapman & Hall, p. 419-433.

Medwenitsch, W., 1949, Die Geologie der Hallstätterzone von Ischl - Aussee: Mitt. Ges. Geol. Bergbaustud. Wien, v. 2, p. 1-27.

Medwenitsch, W., 1958, Die Geologie der Salzlagerstätten Bad Ischl und Alt Aussee (Salzkammergut). Mitt. geol. Ges. Wien, v. 50, 133-200.

Mitra, S., and J. S. Namson, 1989, Equal-area balancing: American Journal of Science, vol.289, no.5, pp.563-599, May 1989.

Mojsisovics, E. v., 1873, Das Gebirge um Hallstatt. Eine geologisch-paläontologische Studie aus den Alpen. 1. Tl. Die Moluskenfaunen der Zlammbach- und Hallstätter Schichten. Abh.k.k.Geol.Reichanst., v.6, p1-174.

Mojsisovics, E. v., 1882, Die Cephalopoden der Mediteranen Triasprovinz. Abh.k.k.Geol.Reichsanst., v.10, p.1-322.

Mojsisovics, E. v., 1893, Die Cephalopoden der Hallstaetter Kalke.: Abh.k.k.Geol.Reichsanst., v.6, p.1-835.

Mojsisovics, E. v., 1902, Die Cephalopoden der Hallstätter Kalke. Abh.k.k.Geol.Reichsanst., v.6, p.177-356.

Morlot, A. v., 1847, Erläuterungen zur geologischen Übersichtskarte der nordöstlichen Alpen. Ein Entwurf zur vorzunehmenden Bearbeitung der physikalischen Geographie und Geologie ihres Gebietes. VIII, Wien (Braumüller und Seidel).

Oberhauser, R., 1980, Der Geologische Aufbau Österreichs: Wien, Springer Verlag.

Passchier, C. W., and C. Simpson, 1986, Porphyroclast systems as kinematic indicators: Journal of Structural Geology, v. 8, p. 831-843.

Passchier, C. W., and R. A. J. Trouw, 1996, Microtectonics: Berlin, Springer Verlag.

Passchier, C. W. and R. A. J. Trouw, 2005, Microtectonics: Berlin, Springer Verlag.

Piller, W. E., H. Egger, et al., 2004, Die stratigraphische Tabelle von Österreich 2004 (sedimentäre Schichtfolgen): Österreichische stratigraphische Kommission und Kommission für die paläontologische und stratigraphische Erforschung Österreichs.

Plöchinger, B., 1982, Geologische Karte der Republik Österreich 1:50000; Blatt 95, Sankt Wolfgang: Wien, Geol. B.-A.

Plöchinger, B., 1995, Tectonics of the Northern Calcareous Alps: a Review: Memorie di Scienze Geologiche, v. 47, p. 73-86.

Poblet, J., and K. McClay, 1996, Geometry and kinematics of single-layer detachment folds: AAPG Bulletin, v. 80, p. 1085-1109.

Ramberg, H., 1981, Gravity, deformation and the earth´s crust in theory, experiments and geological application (2nd ed.): Academic Press, London.

Ramsay, J. G., and M. I. Huber, 1983, The Techniques of Modern Structural Geology: Strain analysis, v. 1, Academic Press Inc. Ltd, London.

Ratschbacher, L., 1991, Lateral extrusion in the Eastern Alps: Tectonics, v. 10, p. 257-271.

Reis, O. M., 1910, Erläuterungen zur Geologischen Karte des Wettersteingebirges: Geogn. Jahresh., v. 23, p. 61-114.

Sachs, O. 2003, Der Diapir von Penacerrada (Spanien): Unpublished diploma thesis, Department of Geodynamics and Sedimentology, University of München

Schäffer, G., 1976, Einführung zur Geologischen Karte der Republik Österreich, Blatt 96, Bad Ischl. Arbeitstagg. Geol. B.-A. 1976. Wien, Geol. B.-A., p. 6-26.

Schäffer, G., 1982, Geologische Karte der Republik Österreich 1:50000; Blatt 96, Bad Ischl: Wien, Geol. B.-A.

Schauberger, O., and W. Medwenitsch, 1951, Der Hallstätter Erbstollen (Salzberg Hallstatt), Verh. Geol. B.-A.: Geologischer Führer zu Exkursionen anlässlich der Hundertjahrfeier der Geologischen Bundesanstalt: Wien, p. 51-63.

Schauberger, O., 1955, Die Genese des alpinen Haselgebirges.: Z. dt. geol. Ges, v. 105, p. 736-751.

Schauberger, O., 1986, Bau und Bildung der Salzlagerstätten des ostalpinen Salinars. Building and structure of the salt deposits of the East-Alpine Salinar: Archiv für Lagerstättenforschung der Geologischen Bundesanstalt, vol.7, p.217-254.

Sedgwick, A., and R. I. Murchison, 1831, A sketch of the structure of the eastern Alps: Geol. Soc. London, v. 3, p. 301-420, London.

Sinha-Roy, S., 2007, Kinetics of differentiated stylolite formation: Current Science, v. 82, p. 1038-1046.

Spötl, C., 1987, Eine klastisch-evaporitische Oberperm-Entwicklung im Hallstätter Salzberg (Salzkammergut, Österreich). A clastic-evaporite Upper Permian in the Hallstätter salt; Salzkammergut, Austria: Mitteilungen der Österreichischen Geologischen Gesellschaft, vol. 80, p. 115-142.

Spötl, C., 1988, Sedimentologisch-fazielle Analyse tektonischer Evaporitserien; eine Fallstudie am Beispiel des Alpinen Haselgebirges (Permoskyth, Nördliche Kalkalpen). Geologisch-Paläontologische Mitteilungen Innsbruck, v. 15, p. 59-56.

Spötl, C., 1989, The Alpine Haselgebirge Formation, Northern Calcareous Alps (Austria): Permo-Scythian evaporites in an alpine thrust system: Sedimentary Geology, v. 65, p. 113-125.

Spötl, C., and E. Pak, 1996, A Strontium and sulfur isotopic study of Permo-Triassic evaporites in the Northern Calcareous Alps: Chemical Geology, v. 131, p. 219-234.

Spötl, C., and C. Hasenhüttl, 1998, Thermal history of the evaporitic Haselgebirge melange in the Northern Calcareous Alps (Austria): Geologische Rundschau, v. 87, p. 449-460.

Suppe, J., 1983b, Geometry and kinematics of fault-bend folding: American Journal of Science, v. 283, p. 684-721.

Suppe, J., 1985, Principles of Structural Geology, Prentice Hall, New Jersey.

Suppe, J., and D. A. Medwedeff, 1990, Geometry and kinematics of fault-propagation folding: Eclogae geol. Helv., v. 83, p. 409-454.

Tollmann, A., 1976a, Analyse des klassischen nordalpinen Mesozoikums. - Monographie der nördlichen Kalkalpen., v. 2: Wien, Deuticke.

Tollmann, A, 1981, Oberjurassische Gleittektonik als Hauptformungsprozeß der Hallstätter Region. Mitt. österr. geol. Ges., v. 74, p. 167-195.

Tollmann, A., 1985, Geologie von Österreich, v. 2: Wien, Deuticke.

Tollmann, A., 1987, The Alpidic evolution of the Eastern Alps, *in* H. W. Flügel, and P. Faupl, eds., Geodynamics of the Eastern Alps: Vienna, Franz Deuticke, p. 361-379.

van der Pluijm, B. A. and S. Marshak, 2004, Earth Structure - an Introduction to Structural Geology and Tectonics. WCM/McGraw-Hill.

Wagreich, M., and K. Decker, 2001, Sedimentary tectonics and subsidence modelling of the Upper Cretaceous Gosau basin (Northern Calcareous Alps, Austria): International Journal of Earth Sciences, v. 90, p. 714-726.

Wagreich, M., and P. Faupl, 1994, Palaeogeography and geodynamic evolution of the Gosau Group of the Northern Calcareous Alps (Late Cretaceous, Eastern Alps, Austria): Palaeogeography, Palaeoclimatology, Palaeoecology, v. 110, p. 235-254.

Wilkerson, M. S., and C. L. Dicken, 2001, Quick-look techniques for evaluating two-dimensional cross sections in detached contradictional settings: AAPG Bulletin, v. 85, p. 1759-1770.

Wilkerson, M. S., J- M. Wilson, J. Poblet and M. P. Fischer, 2004, DETACH: an Excel spreadsheet to simulate 2-D cross sections of detachment folds: Computers & Geosciences, v. 30, p. 1069-1077.

CURRICULUM VITAE

Wien, Oktober 2009

Personalien:

Name:	Nikolaus Schmid
Geburtsort:	Eggenburg
Geburtsdatum:	21.01.1978
Familienstand:	verheiratet, 3 Kinder
Hauptwohnsitz:	3910 Zwettl, Großglobnitz 123
Nebenwohnsitz:	1180 Wien, Herbeckstr. 7/14
Tel.:	0650/3533178
Email:	a9605532@unet.univie.ac.at

Schulbildung:

Volksschule:	1984- 1986 Kirchberg/Walde 1986- 1988 Großglobnitz, 3910 Zwettl
Mittelschule:	1988- 1996 BG Zwettl

Studium:

seit 10/1996 Studium der Geologie an der Universität Wien
voraussichtliches Ende: November 2009
seit Wintersemester 1997 Studium der Sportwissenschaften

Zivildienst:

03.02.2003- 31.01.2004; Caritas Wohnhaus für Menschen mit geistiger Behinderung, 3910 Zwettl (vorübergehende Beurlaubung von der Universität Wien)

Karenz:

01.10.2004 – 30.09.2005 &
01.01.2008 – 30.06.2008

Kenntnisse und besondere Interessen:

Fremdsprachen: Englisch (verhandlungsfähig)
Latein (Maturaniveau)
Alt-Griechisch (Maturaniveau)

EDV: MS-Office2000; Windows 98/2000/NTprofessional/XP;
GIS Programme (ArcView/GIS);
Grafiksoftware (CorelDraw, Photoshop, GeoDIN, GoCAD, AutoCAD, Surpac);
Strukturgeologie (TectonicsFP, Mathematica, 2DMove);

Führerschein: B

Bes. Interessen: Strukturgeologie, Salztektonik, Hydrogeologie, technische Geologie
Diplomarbeitsthema: „Detachment folding and salt tectonics in the Permian Haselgebirge (Hallstatt, Northern Calcareous Alps)“
Betreuer: Prof. Bernhard Grasemann

Studienbegleitende Lehrtätigkeiten:

2001	Tutor für Geologische Kartenkunde
2005	Tutor für Gesteinsbetimmungsübungen auf der TU Wien
2006	Tutor für Kartierungsübung im Gelände

Geländepraxis:

Juli 2000	Geologische Kartierung im Hochgebirge
Juni 2001	Geologische Kartierung im Gelände
Juni 2002	Sprödtektonische Strukturanalysen
Februar 2002	Bergbaukartierung im Salzbergbau Sondershausen
September 2002	Strukturgeologisches Geländepraktikum
Febr. 2002 & 2003	Kartierung im Hallstätter Salzbergwerk im Rahmen der Diplomarbeit
Aug. 2002 & 2004	Geländekartierung in Hallstatt (Echerntal, Solinger Kogel, Plassen) im Rahmen der Diplomarbeit
Juni 2006 – September 2008	Aufnahme von Schürfen, Bohrkernen und geologische Kartierung in Steinbrüchen im Rahmen der Arbeit im Ingenieurbüro Weixelberger

Geologische Praktika:

Sommer 1999 & 2000	Mitarbeit an einem Hydrogeologischen Projekt in Oberösterreich unter Prof. Hermann Häusler
November 2005	Mitarbeit am Brenner Basis Tunnel Projekt (anfertigen von Ortsbrust-bildern) unter Prof. Kurt Decker

Arbeit:

06.06.2006 – 30.09.2008	Angestellter bei Weixelberger, Ingenieurbüro für Geologie
seit 01.10.2008	Angestellter bei der Fa. Bitustein Straßenbaustoffe GesmbH